

Diss. ETH No. 13665

# **METABOLIC ENGINEERING OF YEAST**

A dissertation submitted to the  
SWISS FEDERAL INSTITUTE OF TECHNOLOGY ZÜRICH  
for the degree of  
Doctor of Natural Sciences

Presented by  
Zeynep Petek Çakar  
M.Sc. Chem. Eng., Bogaziçi University, Istanbul  
born August 23, 1972  
citizen of Turkey

Accepted on the recommendation of  
Prof. Dr. Bernard Witholt, examiner  
Prof. Dr. Theo Wallimann, co-examiner  
Dr. Uwe Sauer, co-examiner  
Prof. Dr. Markus Aebi, chairman

Zürich, 2000

## Acknowledgements

I wish to express my gratitudes to my supervisor, Prof. Dr. James E. Bailey, for giving me the chance to do a Ph.D. in his group and for his support throughout this study. I would also like to thank Prof. Dr. Bernard Witholt for accepting to be my examiner, and the time he devoted to reading and commenting on my thesis. Many thanks also go to Prof. Dr. Markus Aebi, the chairman of the examination committee.

I am indebted to Prof. Dr. Theo Wallimann, my co-examiner, for his continuous support throughout my Ph.D. study. I am also thankful to Drs. Uwe Schlattner and Martin Stolz for many fruitful discussions and for introducing me with cell biological techniques. It was a pleasure to collaborate with the Wallimann Group.

I would also like to thank Dr. Uwe Sauer, my co-examiner and group leader, for the direct and excellent supervision, stimulating discussions and the rapid correction of my thesis.

I am grateful to Ms. Miriam Bryant for her significant contributions to my scientific English. May she rest in peace.

Many thanks also go to PD. Dr. Pauli Kallio, as well as Max Haueter and Helena Zuber for their efforts especially during the last few months regarding the administrative issues of my Ph.D.

Thank you all former and current IBTECH-members (I apologize for not listing all your names here) for the friendly and motivating working atmosphere and your help.

Thank you my good friends for all your (E-)mails, calls, visits and support from here, back home, and the U.S..

Thank you my dear yeasts, for showing me how complex life really is and making also me 'multistress-resistant' during my Ph.D.

Merci vielmal und ade ETH-Zürich, it was nice to be a Ph.D. student here.

Finally, to my family goes my eternal gratitude for their everlasting love, support, and patience. Sevgili ailem, sizin sevginiz, sonsuz desteginiz ve bana olan derin güven ve inanciniz sayesinde bu noktaya kadar gelebildim. Bu nedenle doktora tezimi, herseyimi borçlu olduğum aileme ithaf ediyorum.

**I would like to dedicate this thesis to my family whom I owe everything.**

**Table of Contents**

Preface	Summary/Zusammenfassung	4
Chapter 1	General Introduction	9
Chapter 2	Improving Yeast Energy Metabolism by Overexpression of Creatine Kinase?	23
Chapter 3	Intracellular Carbon Fluxes in the Yeasts <i>Saccharomyces cerevisiae</i> and <i>Pichia stipitis</i>	43
Chapter 4	Metabolic Engineering of Yeast: the Perils of Auxotrophic Hosts	69
Chapter 5	Vacuolar Morphology and Cell Cycle Distribution are Modified by Leucine Limitation in Auxotrophic <i>Saccharomyces cerevisiae</i>	83
Chapter 6	Directed Evolution of Multiple-Stress Resistant <i>Saccharomyces cerevisiae</i>	103
Chapter 7	General Conclusions	126
Curriculum Vitae		130

**Preface**

**Summary/Zusammenfassung**

## SUMMARY

The aim of this thesis was to provide insights into cellular properties that are relevant for metabolic engineering of yeast: intracellular carbon fluxes, side effects of using auxotrophic markers, and susceptibility of multiple stress resistance to evolutionary engineering. For this purpose, several new methodologies were adapted for application to yeast, and the reported results as well as the methods themselves can be used to increase the efficiency of metabolic engineering in yeast.

First, we describe a metabolic engineering strategy that aims at improving yeast energy metabolism by overexpression of creatine kinases, key enzymes of energy metabolism in higher eukaryotes. Despite a previous report that creatine kinase-overexpressing *Saccharomyces cerevisiae* takes up creatine and form phosphocreatine, our *in vivo*  $^{31}\text{P}$ -NMR and inhibitor data reveal that such cells do not form phosphocreatine, presumably for lack of creatine uptake. Thus, installing a functional creatine kinase system in yeast requires further metabolic engineering of either intracellular creatine biosynthesis or creatine uptake.

Second, we adapt a new methodology for metabolic flux analysis in yeast for the first time. This method is based on the combination of classical metabolic flux balancing and NMR tracing of  $^{13}\text{C}$ -labeled amino acids. The wealth of available data also allowed to include compartmentalization in the model and, contrary to previous attempts, to actually conclude on the localization of certain metabolite pools. This flux model, along with the generated data, were used to gain insights into the metabolic differences between the yeasts *Pichia* and *Saccharomyces*. Most prominently, the results reveal significantly higher fluxes through the pentose phosphate pathway in *Pichia*. A possible explanation for these differences is the presence of a transhydrogenase or transhydrogenase-like activity in *Pichia* and its absence in *Saccharomyces*. Furthermore, our results suggest transaldolase and transketolase, possibly in combination with transhydrogenase as a target for metabolic engineering of xylose utilization for fuel ethanol production in *S. cerevisiae*.

Third, we show that auxotrophic yeast mutants may have physiological alterations and sensitivities that are not generally recognized. Analyzing yeast morphology by advanced high pressure freezing-freeze substitution and transmission electron microscopy, we show the interrelation of vacuolar morphology, cell cycle, and amino acid availability in auxotrophic *S. cerevisiae* strains. These techniques for sample preparation, so far, have been barely successful in yeast. The results present a note of caution that auxotrophic host-related physiological effects may complicate interpretation of morphological, cell cycle, and metabolic engineering studies.

Fourth, we describe directed evolution of multiple-stress resistant *S. cerevisiae*. Specifically, various batch and chemostat selection strategies were compared for their suitability of selecting multiple-stress resistant mutants. These results revealed that

transient stress challenges in chemostat yielded mutants with up to 10-fold improved oxidative, freezing and ethanol stress survival, compared to the wild-type. Selection in batch culture, in contrast, yielded more specialized mutants with highly improved (up to 150-fold) resistances to oxidative and freezing stresses. These results suggest a combination of selection in batch and transient stress challenges in a chemostat as most appropriate for obtaining further improved multiple-stress resistant *S. cerevisiae*.

## ZUSAMMENFASSUNG

Das Ziel dieser Doktorarbeit war die Untersuchung zellulärer Eigenschaften, die für das 'Metabolic Engineering' von Hefe bedeutsam sind: intrazelluläre Kohlenstoffflüsse, Nebeneffekte auxotropher Marker und die Möglichkeit, Mutanten zu isolieren, die gegen mehrere Stressbedingungen resistent sind. Zu diesem Zweck wurden diverse neue Methoden für die Anwendung in Hefe adaptiert. Sowohl die Methoden als auch die erzielten Ergebnisse ermöglichen die Verbesserung zukünftiger 'Metabolic Engineering' Strategien.

Zunächst beschreiben wir eine 'Metabolic Engineering' Strategie zur Verbesserung des Energiemetabolismus der Hefe durch Ueberexpression von Kreatinkinasen, wichtiger Enzyme des Energiemetabolismus in höheren Eukaryonten. Trotz früherer Berichte, dass Kreatinkinase-exprimierende *Saccharomyces cerevisiae* Kreatin aufnehmen und Phosphokreatin bilden können, zeigen unsere *in vivo* <sup>31</sup>P-NMR und Inhibitor-daten, dass solche Zellen kein Phosphokreatin bilden, wahrscheinlich wegen eines fehlenden Transportsystems. Zur Etablierung eines funktionellen Kreatinkinasesystems sind daher weitere Veränderungen der Hefe notwendig. Diese sollten entweder die intrazelluläre Biosynthese von Kreatin oder dessen Transport ermöglichen.

Im zweiten Teil modifizieren wir eine neue Methode zur Abschätzung der intrazellulären Kohlenstoffflüsse für die erstmalige Anwendung in Hefe. Diese Methode basiert auf der Kombination von klassischen Flussbilanzierungen und NMR Analyse von <sup>13</sup>C markierten Aminosäuren. Die ermittelten, umfangreichen Daten ermöglichen auch die Berücksichtigung der Kompartimentalisierung der Hefezelle in unserem Modell und, anders als in bisherigen Modellen, die Gewinnung von Informationen über die Lokalisierung von bestimmten Metabolitenpools. Modell und Analyse erlaubten uns einen tieferen Einblick in die metabolischen Unterschiede zwischen den Hefen *Saccharomyces* und *Pichia* zu erhalten. Die Ergebnisse zeigen insbesondere deutlich höhere Kohlenstoffflüsse durch den Pentose Phosphat Weg von *Pichia*. Eine mögliche Erklärung für diesen Unterschied ist die Präsenz einer Transhydrogenase oder Transhydrogenase-ähnlichen Aktivität in *Pichia* und deren Abwesenheit in *Saccharomyces*. Weiterhin erlauben unsere Ergebnisse den Schluss, dass die Reaktionen der Transaldolase und Transketolase, möglicherweise in Kombination mit der Transhydrogenase, in *S. cerevisiae* stärker exprimiert werden müssen, um Alkohol aus Xylose zu produzieren.

Drittens zeigen wir, dass auxotrophe Hefe Mutanten häufig unbeachtete physiologische Veränderungen zeigen. Durch morphologische Analysen mit 'Advanced High Pressure Freezing-Freeze Substitution' und Transmissions Elektronenmikroskopie, konnten wir zeigen, dass die Vakuolenmorphologie, der Zellzyklus und die Aminosäureverfügbarkeit in auxotrophen Hefestämmen in einem Zusammenhang stehen. Diese Technik zur Probenvorbereitung konnte bisher noch nicht erfolgreich in Hefe

angewendet werden. Unsere Ergebnisse zeigen, dass physiologische Effekte von auxotrophen Mutationen mit morphologischen, Zellzyklus- und 'Metabolic Engineering' Experimenten interferieren.

Viertens beschreiben wir eine Strategie zur Selektion von *S. cerevisiae* Mutanten, die gegen mehrere Stressbedingungen resistent sind. Zu diesem Zweck wurden diverse Batch und Chemostat Selektionsverfahren auf ihre Tauglichkeit hin untersucht. Die Ergebnisse zeigen, dass Chemostaten mit kurzzeitigen Stressbedingungen auf Mutanten selektionierten, die bis zu 10-fach erhöhte Resistenz gegenüber oxidativem, Gefrier- und Alkoholstress als der Elternstamm zeigen. Batchverfahren dagegen selektionierten Mutanten mit bis zu 150-fach höherer Resistenz gegenüber oxidativem und Gefrierstress. Die Ergebnisse erlauben den Schluss, dass Mutanten mit Mehrfachstressresistenzen am Besten durch eine Kombination von Selektionsverfahren in Batch und Chemostat mit kurzzeitigen Stressbedingungen zu erhalten sind.



**Chapter 1**

**General Introduction**

## **METABOLIC ENGINEERING**

Living cells have evolved in natural settings and are generally not optimized for objectives relevant to biotechnology. Thus, development and improvement of biotechnological processes often necessitates substantial restructuring of cellular metabolism. Improvement of cellular functions by recombinant DNA technology has been termed *metabolic engineering* (Bailey, 1991). The classical approach of metabolic engineering follows a rational, deductive strategy, which is usually based on knowledge of the metabolic system of interest and a proposed, more or less defined genetic manipulation towards a desired objective. However, this endeavor has often been hampered by the need for extensive information on the target metabolic system. In contrast to this *constructive* metabolic engineering, the term *inverse* metabolic engineering has recently been introduced to describe an alternative approach (Bailey et al., 1996). In this approach, the elucidation of a metabolic engineering strategy proceeds through three distinct phases: first, identification of a desired phenotype; second, determination of factors that confer that phenotype; and third, transferring the basis of that phenotype to the organism of choice. The obvious potential advantage is based on the initiation of the optimization process with a known, desirable phenotype. A prime example of inverse metabolic engineering is the successful improvement of energetic efficiency of microaerobic respiration by heterologous expression of a bacterial hemoglobin (Khosla and Bailey, 1988; Khosla et al., 1990). This example addresses a key problem in microbial fermentation processes, the influence of cellular energetics on biotechnological product formation (Stouthamer and van Verseveld, 1987).

## **ENGINEERING YEAST ENERGY METABOLISM**

The yeast *Saccharomyces cerevisiae* is one of the most important biotechnological microorganisms and therefore also a prime target for metabolic engineering. The worldwide baker's yeast (*S. cerevisiae*) industry produces more than 2 million tons of yeast per year. It is currently expanding at about 4% per year owing to the increasing population, industrialization and dietary changes (Trivedi, 1986). Wide application of *S. cerevisiae* in traditional biotechnologies like baking, brewing, distiller's fermentations and wine making, emphasizes the industrial importance of this organism (Attfield, 1997). Since the early 1980s, *S. cerevisiae* has also been used for the large-scale production of intracellular and extracellular proteins of human, animal, and plant origin (Romanos et al., 1992). The yeast expression systems for heterologous protein production as well as the external conditions are usually optimized to obtain a high yield of the heterologous protein of interest. A typical example is proinsulin production by *S. cerevisiae*, where host cell properties and external pH were found to have an effect on proinsulin production (Kozlov et al., 1995). Additionally, *S. cerevisiae* is a traditional microorganism used for ethanol

fermentation. The increasing demand for ethanol as a substitute for gasoline requires the development of lower-cost feedstocks like lignocellulosic ones, which are sufficient to substitute for corn starch (Hacking et al., 1986). Genetic engineering of *S. cerevisiae* for pentose utilization is an important research target for this purpose. The familiarity and experience of the corn processing industry with yeast fermentations and the potential robustness of the organism makes *S. cerevisiae* most attractive to the corn processing industry (Bothast et al., 1999).

When yeasts are used in these biotechnological processes, however, they have to endure various environmental stresses like nutrient limitation, elevated temperatures and oxidation. Since they respond to these stresses by signal transduction, transcriptional and post-translational control, protein-targeting to organelles and activation of repair functions, which are all energy-requiring cellular activities, they have higher energy requirements under stress conditions (Attfield, 1997). As a consequence, cells must use ATP to expel protons via plasma membrane H<sup>+</sup>-ATPase activity. Cell survival might therefore be determined by the balance between maintenance of intracellular ATP levels for repair, growth and ATP expenditure for pH homeostasis.

The heterologous expression of the bacterial hemoglobin (VHb) in *S. cerevisiae* is a successful example of metabolic engineering to improve yeast energetics. Upon growth on acetaldehyde, there has been a 3-fold increase in the final cell density of the VHb-expressing *S. cerevisiae* compared to its control (Chen et al., 1994).

Another potentially relevant target for improving energy metabolism is creatine kinase (CK), a key enzyme in energy metabolism of excitable cells and tissues of vertebrate species, that appears to play a complex, multifaceted role in energy homeostasis (Wallimann et al., 1992). As a main function, it catalyzes the reversible phosphorylation from ATP to phosphocreatine (PCr), which serves as an energy-storage metabolite. Thus, the readily accessible phosphorylation potential of PCr can be used to regenerate ATP, by functioning as a temporal energy buffer. The CK system also functions as an energy transport system by connecting sites of energy production with sites of energy utilization and thus maintains a high intracellular ATP-to-ADP ratio. Additionally, as the CK reaction in the direction of ATP synthesis utilizes one proton, it serves as a pH-buffering function, thus counteracting the intracellular acidification. Therefore, the installation of a CK-PCr circuit in yeast seems to have potential to be beneficial to energy metabolism, either by improving overall efficiency, or by the 'energy buffer' function during transient stress conditions. Transient stress conditions occur very commonly in industrial fed-batch cultivations of *S. cerevisiae*. A typical example is short-term glucose fluctuations during large-scale fed-batch cultivations (Neubauer et al., 1995a). Since these short-term stresses influence cellular physiology and growth, their reduction is crucial for the process

performance (Neubauer et al., 1995b). The investigation of the CK-PCr circuit in yeast are reported in **Chapter 2**.

## **METABOLIC ENGINEERING OF YEAST CENTRAL CARBON METABOLISM**

### **Studies on Xylose Utilization and Pentose Phosphate Pathway**

In addition to yeast energy metabolism, central carbon metabolism is also an important target for metabolic engineering, because it will eventually limit production, once the biosynthetic branches are optimized. Several groups have been working on the improvement of yeast central carbon metabolism for the production of various compounds. Some efforts are directed towards introduction of features from other yeasts, mostly utilization of certain sugars. It is known, for example, that the yeast *Pichia stipitis* can grow on pentoses like xylose. *S. cerevisiae*, however, cannot utilize xylose (Walfridsson et al., 1995). However, for the production of fuel ethanol from lower-cost feedstocks, which are the lignocellulosic ones, utilization of pentose sugars like xylose is necessary. Although *P. stipitis* can grow on xylose, it cannot produce ethanol. Xylose is derived from the hemicellulose component of lignocelluloses (Bothast et al., 1999). For the purpose of xylose utilization, *S. cerevisiae* was metabolically engineered by cloning the *P. stipitis* genes *XYL1* and *XYL2* encoding xylose reductase and xylitol dehydrogenase. These two enzymes catalyze the initial steps in xylose utilization, which do not exist in wild type *S. cerevisiae*. Additionally, the *S. cerevisiae* *TKL1* and *TAL1* genes encoding transketolase and transaldolase were overexpressed, to improve pentose phosphate pathway utilization. The results showed that *XYL1*- and *XYL2*-expressing *S. cerevisiae* that co-overexpresses *TAL1* had considerably enhanced growth on xylose compared to a strain expressing only *XYL1* and *XYL2*. From these data, it was concluded that the insufficient transaldolase levels cause the inefficient utilization of pentose phosphate pathway in *S. cerevisiae* (Walfridsson et al., 1995). Some aspects of this problem are discussed in **Chapter 3**.

### **Studies on Glycolysis**

As the central pathway of carbon metabolism, glycolysis is the prime route to the most important yeast product, ethanol. There have been several attempts to metabolically engineer yeast glycolysis by modifying various enzymes, especially those known as 'rate limiting'. A typical example is overexpression of eight different enzymes of glycolysis and alcoholic fermentation in *S. cerevisiae* including hexokinase, phosphofructokinase and pyruvate kinase, which catalyze irreversible reactions (Schaaff et al., 1989). However, this overexpression had no effect on ethanol production rate. Additionally, simultaneous increases in the activities of enzyme pairs like pyruvate kinase and phosphofructokinase, or pyruvate decarboxylase and alcohol dehydrogenase, did not

increase the ethanol formation rate, either (Schaaff et al., 1989). In a former study, however, a higher yield of ethanol was found in mutants overexpressing both pyruvate decarboxylase and alcohol dehydrogenase (Sharma and Tauro, 1986). But these two results are not comparable, since the latter was based on stationary phase-cells that were grown anaerobically. It was concluded that the control of fluxes or metabolite concentrations was generally shared among all enzymes, and only under specific conditions certain enzymes assume a higher control than the others (Schaaff et al., 1989).

A later study of glycolysis mutants of *S. cerevisiae* revealed that in these mutants, induction of pyruvate decarboxylase is correlated with the concentrations of three-carbon glycolytic metabolites (Boles and Zimmermann, 1993). Characterization of some glycolytic enzymes was also done in *S. cerevisiae* like the glucose-repressed pyruvate kinase (Pyk2p), which was shown to be catalytically insensitive to fructose-1,6-bisphosphate, and may be used under conditions of very low glycolytic flux (Boles et al., 1997). In a different study, the energetic aspects of glucose metabolism were investigated in a pyruvate-dehydrogenase-negative mutant of *S. cerevisiae*. It was found that, during aerobic glucose-limited growth of *S. cerevisiae* at low growth rates, the pyruvate dehydrogenase complex accounts for the major part of the pyruvate flux (Pronk et al., 1994).

### **Studies on Byproduct Formation**

Pyruvate decarboxylase is a key enzyme for the production of low-molecular-weight byproducts (ethanol, acetate) in biomass-directed applications of *S. cerevisiae* (Flikweert et al., 1999). Pyruvate is the branch point between respiration and fermentation. For respiration, pyruvate must be oxidatively decarboxylated to acetyl coenzyme A, a reaction catalyzed by the mitochondrial pyruvate dehydrogenase complex. Alcoholic fermentation, however, requires pyruvate decarboxylation to acetaldehyde by the cytosolic pyruvate decarboxylase. In order to reduce byproduct formation in industrial fermentations, pyruvate-decarboxylase deficient mutants were constructed and their physiology was investigated extensively. These studies showed that the mitochondrial pyruvate dehydrogenase complex cannot function as the sole carbon source of acetyl-CoA during growth of *S. cerevisiae* on glucose, neither in glucose-limited chemostats nor in batch cultures (Flikweert et al., 1996). In a similar study, the metabolic responses of pyruvate-decarboxylase-negative *S. cerevisiae* to glucose excess was investigated. It was concluded that reoxidation of cytosolic NADH via pyruvate decarboxylase and alcohol dehydrogenase is a prerequisite for high glycolytic fluxes in *S. cerevisiae* (Flikweert et al., 1997). In a more detailed analysis of steady-state and transient-state growth and metabolite production in a *S. cerevisiae* strain with reduced pyruvate decarboxylase activity, it was found that inactivation of PDC2 gene, which encodes a positive regulator of pyruvate decarboxylase synthesis, is not a viable option for reducing byproduct

formation in industrial fermentations. This conclusion resulted from the observation that the pyruvate-decarboxylase deficient mutants had low maximum growth rates ( $\mu_{\max}$ ) in glucose-limited chemostat cultures, showing that the respiro-fermentative metabolism in wild-type cultures is not only caused by the competition of respiration and fermentation for pyruvate (Flikweert et al., 1999).

There are also pyruvate decarboxylase overexpression studies, which, in contrast to pyruvate-decarboxylase deficient mutant studies, aimed at increasing the glycolytic flux to ethanol. These studies showed that pyruvate decarboxylase overproduction influenced flux distribution at the pyruvate branch point by affecting the competition for pyruvate between pyruvate decarboxylase and the mitochondrial pyruvate dehydrogenase complex. In chemostat cultures, it was observed that the dilution rate at which aerobic fermentation started decreased from  $0.30 \text{ h}^{-1}$  in the reference strains to  $0.23 \text{ h}^{-1}$  in the pyruvate decarboxylase-overproducing strain (van Hoek et al., 1998). Additionally, it was shown that pyruvate decarboxylase by itself does not control the specific growth rate of *S. cerevisiae* on glucose, as previously concluded (Schaaff et al., 1989).

## **METABOLIC FLUX ANALYSIS**

From the above, it becomes clear that engineering of central carbon metabolism, although important, is difficult to do. In many cases, consequences of metabolic engineering may have already affected the intracellular reaction rates, i. e. the metabolic fluxes, but these effects have apparently not influenced the physiological phenotype. Hence, it would be desirable to have an analytical tool that would allow to monitor such intracellular flux responses. Ideally, it could also provide valuable information for choosing a subsequent target for metabolic engineering.

Stoichiometric flux balancing is a common way to perform flux analysis. In this method, extracellular metabolite concentrations are measured, and the fluxes through the primary metabolic pathways are determined by means of stoichiometric balance equations of metabolites (Vallino and Stephanopoulos, 1990). However, in most of the systems, there are more unknown fluxes than balancing equations, which makes these systems underdetermined. Under these conditions, extra equations like flux ratios would be necessary, to make the system determined and therefore solvable. In the absence of such equations, several assumptions have to be made, which might be questionable from a biological point of view, such as the assumption that cells maximize their ATP production.

An alternative way of determining metabolic fluxes is the use of isotopic-tracer experiments. Certain flux ratios are determined at some branch points by tracing the metabolic fate of carbon-labelled substrates and nuclear magnetic resonance (NMR) technology is applied to biological systems for this purpose. It has been widely applied to

estimate metabolite concentrations in whole cells, cell extracts and growth media (Gadian, 1982). Biosynthetically directed fractional  $^{13}\text{C}$ -labeling of the common proteinogenic amino acids is a relatively new technique for peptides and proteins to obtain  $^1\text{H}$  resonance assignments (Szyperski et al., 1992). It can also be used to monitor the flux of metabolites within the key metabolic pathways like glycolysis, pentose phosphate pathway, citric acid cycle and  $\text{C}_1$  metabolism (Szyperski, 1995). The method is based on isotopic imprinting of amino acids by their precursors, which enables the direct determination of the active central carbon pathways and the ratios of their fluxes from two-dimensional (2D) NMR analysis of hydrolyzed cell protein (Szyperski, 1998). This method is referred to as METAFoR (**metabolic flux ratio**) analysis, which can complement the stoichiometric flux balancing approach by providing extra equations or constraints to make the system determined (Sauer et al., 1999). This combined approach of using METAFoR and stoichiometric flux analysis has successfully been applied to determine the flux distributions in riboflavin-producing *Bacillus subtilis* (Sauer et al., 1997).

Previous studies involving yeast flux analysis relied mainly on stoichiometric flux balancing without independent labeling data (see, for example, Jin et al., 1997; Nissen et al., 1997). Additionally, most of the yeast flux studies did not take compartmentalization into account, in order to simplify their models (Vanrolleghem et al., 1996; Jin et al., 1997).

Under these circumstances, stoichiometric flux balancing combined with METAFoR analysis for *S. cerevisiae* in a network which considers compartmentalization would give more realistic and reliable view of the metabolic flux distribution in this eukaryotic organism. Additionally, using this combined approach, a comparison of metabolic flux distributions between *P. stipitis* and *S. cerevisiae* may also reveal intracellular flux differences between these two organisms which cause the different utilization of pentoses. This could help to identify new metabolic engineering strategies for improving *S. cerevisiae*'s pentose phosphate pathway utilization. These aspects and the application of this method to yeasts are discussed in **Chapter 3**.

### **POTENTIAL PERILS OF METABOLIC ENGINEERING IN YEAST**

Metabolic engineering has been successfully applied to various bioprocesses. However, the metabolic consequences of the genetic change are usually much different from the expected ones (Bailey, 1991). Limitations in our knowledge of metabolic networks are one reason for these unexpected responses. These responses are called secondary responses to metabolic engineering (Bailey, 1996). The fact that any network considered for metabolic engineering purposes is a subnetwork of a much more complex global metabolic network is one of the main causes of these secondary responses. Additionally,

the cells' own control mechanisms, misfolding, aggregation, degradation or incorrect localization of foreign proteins are other possibilities of secondary responses, which often result in failure of metabolic engineering attempts (Bailey et al., 1996).

Similar problems are also encountered in yeasts. A typical example is the common use of auxotrophic host systems with dominant selection markers like *URA3*, *LEU2*, *TRP1* or *HIS3*. Such auxotrophic mutants may have physiological alterations and sensitivities, which might complicate the interpretation of the effects of an introduced genetic change. Although expected by some, these effects have never been reported and they obscure several published data. In **Chapter 4**, such complications are described, quantified and their impact on fundamental and biotechnological research is discussed.

In addition to these physiological sensitivities, auxotrophic markers may also have morphological alterations and sensitivities which are interrelated with physiological alterations as well as changes in cell cycle distribution, due to different levels of auxotrophic amino acid supply. These aspects are discussed in **Chapter 5**.

## **DIRECTED EVOLUTION AND SELECTION FOR MULTIPLE-STRESS RESISTANT YEASTS**

Some of the above-mentioned problems of rational metabolic engineering may be overcome by the alternative approach of inverse metabolic engineering (Bailey et al., 1996). In this approach, the desired phenotype is identified or constructed first. Random mutation and selection is the most traditional approach in order to obtain a desired phenotype. Chemostat selection, where strains adapt to continuous cultivation conditions with nutrient limitation, is an alternative way for strain development (Helling et al., 1987; Weikert et al., 1997). Here the cells compete for the limiting nutrient and in response, such populations evolve by adaptation. Such selection strategies are also named 'directed evolution'.

The successful application of directed evolution as an inverse metabolic engineering approach depends on the availability of an enabling technology for the identification of a genetic basis for the selected, desirable phenotypes. To characterize the mutants at the protein level, two dimensional gel electrophoresis (2DE) is a high-resolution method, which allows the separation of thousands of proteins (Wilkins et al., 1996). Alternatively, a recent technology with high-density oligonucleotide arrays allows monitoring of global gene expression levels (Wodicka et al., 1997). In this approach, mRNA levels are determined by hybridization of complete mRNA populations to sets of arrays containing hundreds of thousands of chemically synthesized oligonucleotides (Wodicka et al., 1997). By means of this technology, mutants with the desired phenotype(s) can be characterized and by comparison with their ancestors it may be possible to identify the relevant genes. For biotechnological purposes, this would mean



that certain strain improvements could be done very efficiently by selecting for industrially relevant characteristics of the organisms of interest and subsequent transfer of the desired property. Until recently, improved strains were either obtained by random mutation and selection procedures or via rational metabolic engineering. In the first approach, they were usually characterized physiologically or morphologically. In the latter one, site-directed mutagenesis was usually applied, which was not very efficient, since multiple genes or gene families are usually involved in the expression of a phenotype. Therefore, deleting or overexpressing one or few genes is usually not sufficient to achieve a desired, often complex phenotype.

During growth in large-scale bioreactors, yeast cells are faced with several stresses like oxidative stress, temperature changes, organic acids, alcohols and nutrient limitation. Additionally, during storage and in frozen dough technology, yeasts are also exposed to freezing stress. Thus, it would be desirable to obtain yeast cells that are resistant to multiple stresses (Singer and Lindquist, 1998).

In **Chapter 6**, directed evolution is used to improve *S. cerevisiae*'s multiple-stress resistance. Additionally, various chemostat and batch selection strategies employed for obtaining multiple-stress resistant yeast strains are compared in that Chapter, to provide guidance for further selection schemes. Successfully selected mutants were subjected to global transcript analysis to identify the relevant mutations.

## **AIM AND SCOPE OF THIS THESIS**

In this thesis, several new technologies were applied to yeast and yeast metabolic engineering. The aim of this thesis was to improve the general understanding of various aspects of yeast carbon and energy metabolism, physiology, morphology and genetics, with a particular emphasis on metabolic engineering. In light of the reported results, future metabolic engineering of yeast can be done more efficiently in certain cases and some pitfalls may be avoided.

To be more precise, the most important new technologies successfully applied to yeast throughout this study are listed below. Firstly, the novel and elaborate high pressure freezing-freeze substitution techniques for transmission electron microscopy were applied to yeast for the first time, revealing important morphological differentiations in the vacuoles of auxotrophic revertants, compared to the wild-type strains. This was previously not known, and supported our data on physiological differences between auxotrophic mutants and their corresponding wild-type strains.

The first application of a new flux analysis technology to yeast was also done in this study by combining the traditional metabolic flux balancing approach with NMR-tracing of  $^{13}\text{C}$ -labeled proteinogenic amino acids, the so-called METAFoR analysis. Additionally, the compartmentalization in yeast was taken into account in our flux model,

an aspect that was neglected in many former yeast flux studies. This model and the generated data were used to understand the differences between the metabolism of *Pichia* and *Saccharomyces* yeasts, especially regarding pentose phosphate pathway utilization.

Additionally, the state-of-the-art DNA array technology was applied for the first time to analyze mutants from a directed evolution selection. This directed evolution study plays also a pioneering role, because no previous data were available on obtaining multiple-stress resistant yeasts.

Following the general introduction given here in **Chapter 1**, metabolic engineering of yeast energy metabolism by overexpression of creatine kinase is described in **Chapter 2**. Investigation of the metabolic fluxes in *S. cerevisiae* and *P. stipitis* is demonstrated in **Chapter 3**. **Chapters 4** and **5** focus on problems related to the application of rational metabolic engineering in *S. cerevisiae*, emphasizing the physiological, morphological, and cell cycle-level alterations in auxotrophic yeast expression systems. **Chapter 6** introduces directed evolution as an inverse metabolic engineering approach, which was successfully used for the selection of multiple-stress resistant *S. cerevisiae* mutants in batch and chemostat cultures. A summary of the main results as well as future prospects are given as general conclusions in **Chapter 7**.

## REFERENCES

- Attfield, P. V. 1997. Stress tolerance: the key to effective strains of industrial baker's yeast. *Nature Biotechnol.* **15**: 1351-1357.
- Bailey, J. E. 1991. Toward a science of metabolic engineering. *Science* **252**: 1668-1675.
- Bailey, J. E., Sburlati, A., Hatzimanikatis, V., Lee, K., Renner, W. A., Tsai, P. S. 1996. Inverse metabolic engineering: a strategy for directed genetic engineering of useful phenotypes. *Biotechnol. Bioeng.* **52**: 109-121.
- Boles, E., Zimmermann, F. K. 1993. Induction of pyruvate decarboxylase in glycolysis mutants of *Saccharomyces cerevisiae* correlates with the concentrations of three-carbon glycolytic metabolites. *Arch. Microbiol.* **160**: 324-328.
- Boles, E., Schulte, F., Miosga, T., Freidel, K., Schluter, E., Zimmermann, F. K., Hollenberg, C. P., Heinisch, J. J. 1997. Characterization of a glucose-repressed pyruvate kinase (Pyk2p) in *Saccharomyces cerevisiae* that is catalytically insensitive to fructose-1,6-bisphosphate. *J. Bacteriol.* **179**: 2987-2993.
- Bothast, R. J., Nichols, N. N., Dien, B. S. 1999. Fermentations with new recombinant organisms. *Biotechnol. Prog.* **15**: 867-875.
- Chen, W., Hughes, D. E., Bailey, J. E. 1994. Intracellular expression of *Vitreoscilla* hemoglobin alters the genetic metabolism of *Saccharomyces cerevisiae*. *Biotechnol. Prog.* **10**: 308-313.
- Flikweert, M. T., Van Der Zanden, L., Janssen, W. M., Steensma, H. Y., Van Dijken, J. P., Pronk, J. T. 1996. Pyruvate decarboxylase: an indispensable enzyme for growth of *Saccharomyces cerevisiae* on glucose. *Yeast* **12**: 247-257.
- Flikweert, M. T., van Dijken, J. P., Pronk, J. T. 1997. Metabolic responses of pyruvate decarboxylase-negative *Saccharomyces cerevisiae* to glucose excess. *Appl. Environ. Microbiol.* **63**: 3399-3404.
- Flikweert, M. T., Kuyper, M., van Maris, A. J., Kötter, P., van Dijken, J. P., Pronk, J. T. 1999. Steady-state and transient state analysis of growth and metabolite production in a *Saccharomyces cerevisiae* strain with reduced pyruvate-decarboxylase activity. *Biotechnol. Bioengin.* **66**: 42-50.
- Gadian, D. G. 1982. Nuclear magnetic resonance and its applications to living systems. Oxford University Press, Oxford.
- Hacking, A. J. 1986. Economic aspects of biotechnology, Cambridge University Press, Cambridge, U.K., pp. 74-92.
- Helling, R. B., Vargas, C. N., Adams, J. 1987. Evolution of *Escherichia coli* during growth in a constant environment. *Genetics* **116**: 349-358.
- Jin, S., Ye, K., Shimizu, K. 1997. Metabolic flux distributions in recombinant *Saccharomyces cerevisiae* during foreign protein production. *J. Biotechnol.* **54**: 161-174.

- Khosla, C., Bailey, J. E., 1988. Heterologous expression of a bacterial haemoglobin improves the growth properties of recombinant *Escherichia coli*. *Nature* **331**: 633-635.
- Khosla, C., Curtis, J. E., De Modena, J., Rinas, U., Bailey, J. E. 1990. Expression of intracellular hemoglobin improves protein synthesis in oxygen-limited *Escherichia coli*. *Bio/Technol.* **8**: 849-853.
- Kozlov, D. G., Prahl, N., Efremov, B. D., Peters, L., Wambut, R., Karpychev, I. V., Eldarov, M. A., Benevolensky, S. V. 1995. Host cell properties and external pH affect proinsulin production by *Saccharomyces* yeasts. *Yeast* **11**: 713-724.
- Neubauer, P., Ahman, M., Tornkvist, M., Larsson, G., Enfors, S. O. 1995a. Response of guanosine tetraphosphate to glucose fluctuations in fed-batch cultivations of *Escherichia coli*. *J. Biotechnol.* **43**: 195-204.
- Neubauer, P., Haggstrom, L., Enfors, S. O. 1995b. Influence of substrate oscillations on acetate formation and growth-yield in *Escherichia coli* glucose-limited fed-batch cultivations. *Biotechnol. Bioengin.* **47**: 139-146.
- Nissen, T. L., Schulze, U., Nielsen, J., Villadsen, J. 1997. Flux distributions in anaerobic, glucose-limited continuous cultures of *Saccharomyces cerevisiae*. *Microbiol.* **143**: 203-218.
- Pronk, J. T., Wenzel, T. J., Luttik, M. A., Klaassen, C. C., Scheffers, W. A., Steensma, H. Y., van Dijken, J. P. 1994. Energetic aspects of glucose metabolism in a pyruvate-dehydrogenase-negative mutant of *Saccharomyces cerevisiae*. *Microbiol.* **140**: 601-610.
- Romanos, M. A., Scorer, C. A., Clare, J. J. 1992. Foreign gene expression in yeast: a review. *Yeast* **8**: 423-488.
- Sauer, U., Hatzimanikatis, V., Bailey, J. E., Hochuli, M., Szyperski, T., Wüthrich, K. 1997. Metabolic fluxes in riboflavin-producing *Bacillus subtilis*. *Nature Biotechnol.* **15**: 448-452.
- Sauer, U., Lasko, D. R., Fiaux, J., Hochuli, M., Glaser, R., Szyperski, T., Wüthrich, K., Bailey, J. E. 1999. Metabolic flux ratio (METAFor) analysis of genetic and environmental modulations of *Escherichia coli* central carbon metabolism. *J. Bacteriol.* **181**: 6679-6688.
- Schaaff, I., Heinisch, J., Zimmermann, F. K., 1989. Overproduction of glycolytic enzymes in yeast. *Yeast* **5**: 285-290.
- Sharma, S., Tauro, P. 1986. Control of ethanol production by yeast: role of pyruvate decarboxylase and alcohol dehydrogenase. *Biotech. Lett.* **8**: 735-738.
- Singer, M. A., Lindquist, S. 1998. Thermotolerance in *Saccharomyces cerevisiae*: the Yin and Yang of trehalose. *Trends Biotechnol.* **16**: 460-468.

- Stouthamer, A. H., van Verseveld, H. W. 1987. Microbial energetics should be considered in manipulating metabolism for biotechnological purposes. *Trends-Biotechnol.* **5**: 149-155.
- Szyperski, T., Neri, D., Leiting, B., Otting, G., Wüthrich, K. 1992. Support of <sup>1</sup>H-NMR assignments in proteins by biosynthetically directed fractional <sup>13</sup>C-labeling. *J. Biomol. NMR* **2**: 323-334.
- Szyperski, T. 1995. Biosynthetically directed fractional <sup>13</sup>C-labelling of proteinogenic amino acids. An efficient analytical tool to investigate intermediary metabolism. *Eur. J. Biochem.* **232**: 433-448.
- Szyperski, T. 1998. <sup>13</sup>C-NMR, MS and metabolic flux balancing in biotechnological research. *Q. Rev. Biophys.* **31**: 41-106.
- Trivedi, N. B. 1986. Bakers' yeast. *CRC Crit. Rev. Biotechnol.* **4**: 75-109.
- Vallino, J. J., Stephanopoulos, G. 1990. Flux determinations in cellular bioreaction networks: application to lysine fermentations. In *Frontiers in Bioprocessing* (eds. S. K. Sikdar, M. Bier, P. Todd), pp. 205-219, CRC Press, Boca Raton.
- van Hoek, P., Flikweert, M. T., van der Aart, Q. J., Steensma, H. Y., van Dijken, J. P., Pronk, J. T. 1998. Effects of pyruvate decarboxylase overproduction on flux distribution at the pyruvate branch point in *Saccharomyces cerevisiae*. *Appl. Environ. Microbiol.* **64**: 2133-2140.
- Vanrolleghem, P. A., de Jong-Gubbels, P., van Gulik, W. M., Pronk, J. T., van Dijken, J. P., Heijnen, S. 1996. Validation of a metabolic network for *Saccharomyces cerevisiae* using mixed substrate studies. *Biotechnol. Prog.* **12**: 434-448.
- Walfridsson, M., Hallborn, J., Penttila, M., Keranen, S., Hahn-Hagerdal, B. 1995. Xylose-metabolizing *Saccharomyces cerevisiae* strains overexpressing the TKL1 and TAL1 genes encoding the pentose phosphate pathway enzymes transketolase and transaldolase. *Appl. Environ. Microbiol.* **61**: 4184-4190.
- Wallimann, T., Wyss, M., Brdiczka, D., Nicolay, K., Eppenberger, H. M. 1992. Intracellular compartmentation, structure and function of creatine kinase isoenzymes in tissues with high and fluctuating energy demands: the 'phosphocreatine circuit' for cellular energy homeostasis. *Biochem. J.* **281**: 21-40.
- Weikert, C., Sauer, U., Bailey, J. E. 1997. Use of a glycerol-limited, long-term chemostat for isolation of *Escherichia coli* mutants with improved physiological properties. *Microbiol.* **143**: 1567-1574.
- Wilkins, M. R., Pasquali, C., Appel, R. D., Ou, K., Golaz, O., Sanchez, J. C., Yan, J. X., Gooley, A. A., Hughes, G., Smith, I. H., Williams, K. L., Hochstrasser, D. F. 1996. From proteins to proteomes: large scale protein identification by two-dimensional electrophoresis and amino acid analysis. *Nature Biotechnol.* **14**: 61-65.

Wodicka, L., Dong, H., Mittmann, M., Ho, M.-H., Lockhart, D. J. 1997. Genome-wide expression monitoring in *Saccharomyces cerevisiae*. Nature Biotechnol. **15**: 1359-1367.

**Chapter 2**

**Improving  
Yeast Energy Metabolism  
by Overexpression of Creatine Kinase?**

## SUMMARY

As a key enzyme of energy metabolism in excitable cells and tissues of vertebrate species, creatine kinase plays a complex role in energy homeostasis. It increases the efficiency of cellular energetics and connects sites of energy production with sites of energy utilization. The cytosolic brain-type (B-CK) and the mitochondrial (Mi<sub>b</sub>-CK) isoforms of chicken creatine kinase were functionally expressed in *Saccharomyces cerevisiae*, which normally does not contain this enzyme. Growth physiological analysis showed that neither B-CK nor Mi<sub>b</sub>-CK expression had any effect on yeast growth and/or byproduct formation. Additionally, the potential effects of co-overexpression of B-CK on heterologous protein production were investigated in yeast. For this purpose, a set of constitutive and galactose-inducible vectors encoding the bovine pancreatic trypsin inhibitor (BPTI) gene were transformed into both B-CK-expressing hosts and their controls, which did not express B-CK. The results revealed that, in high-level expression systems, where BPTI production was induced by galactose, B-CK co-overexpression did not have any effect on BPTI production. Despite a previous report that recombinant *S. cerevisiae* cells expressing rabbit muscle type creatine kinase can form phosphocreatine (PCr) upon incubation with creatine, our *in vivo* <sup>31</sup>P-NMR analysis of intracellular PCr indicated that the substrate of CK, which is PCr, is not available intracellularly in yeast. Therefore, in its existing form, the CK system is not functioning in *S. cerevisiae*. In this respect, the up to 3-fold increase in the secreted BPTI concentration upon co-overexpression of B-CK in constitutive BPTI expression systems is a secondary effect, and is not related to CK-activity. Thus, the installation of a functional creatine kinase system in yeast requires further metabolic engineering of either intracellular creatine biosynthesis or creatine uptake.



## INTRODUCTION

Accessible chemical energy is crucial for most basic cell functions, and is an absolute requirement for many metabolic processes that are relevant to biotechnology. Excitable cells and tissues of vertebrate species, with large bursts of energy utilization (e.g., skeletal muscle fibers and neurons), exploit an energy buffering and transport system based on creatine kinase (CK) (Wallimann et al., 1992). As its main function, CK catalyzes the reversible transfer of the phosphoryl group from ATP to phosphocreatine (PCr), which serves as an energy-storage metabolite. Thus, the readily accessible phosphorylation potential of PCr can be used to regenerate ATP by functioning as an immediate temporal energy buffer on a sub-second time scale.

There are several additional functions of CK-PCr system that have potential for a positive contribution to applied bioprocesses (Wallimann et al., 1992; Wallimann, 1994):

- 1) There is accumulating evidence for an 'energy carrier' function that connects energy producing and consuming sites via subcellular compartmentalized CK isoenzymes.
- 2) By functional coupling of CK to ATP-consuming processes it provides appropriate local ATP-to-ADP ratios at subcellular sites. This is especially important for the energetically demanding  $\text{Ca}^{++}$ -pump ATPase, as shown by the significantly altered  $\text{Ca}^{++}$  response in muscles of a M-CK/Mi-CK double knockout mouse (Steeghs et al., 1997).
- 3) By stabilization of the intracellular ATP-to-ADP ratio, which is a key regulator in many fundamental metabolic processes, overshoot responses can be avoided.
- 4) As the CK reaction in the direction of ATP synthesis utilizes one proton, it serves a pH buffering function, thus counteracting the intracellular acidification.
- 5) The release of inorganic phosphate ( $\text{P}_i$ ) is also a metabolic function of the CK-PCr system. Since net PCr hydrolysis is the major  $\text{P}_i$  source, and since  $\text{P}_i$  is necessary for glycolysis and glycogenolysis, CK has an indirect regulatory effect in muscles which depend on glycogenolysis.

The CK system, which evolved in higher organisms to optimize the link between energy production and utilization, does not exist in prokaryotes or lower eukaryotic microorganisms (Stryer, 1988). However, the possibility that the CK system could, if artificially introduced, show beneficial effects on energy metabolism of mitochondria-carrying microorganisms, has generated our interest. The fact that the presence of the CK-PCr system in a cell can improve the efficiency of ATP hydrolysis and thus the energy metabolism during transient periods as well as on a sustained level may also be true for yeast. Such an energetic benefit may be exploited for biotechnological processes that impose heavy energetic demands on cultivated cells. Firstly, the 'energy buffer' function of CK-PCr system could have beneficial effects on yeast cells which undergo various

transient stress conditions during industrial bioprocesses like aerobic fed-batch, the method employed to produce baker's yeast, in which molasses are used as the sugar source. The fed-batch process requires the addition of incremental amounts of a sugar source and supplementation with nitrogen and phosphate sources, as well as some vitamins and minerals. It is limited by the aeration capacity of the fermenter system. The accumulation of some molass components like organic acids, aldehydes, ketones and SO<sub>2</sub> during the fed-batch process also cause stressful conditions as growth inhibitors (Attfield, 1997). Secondly, even a few per cent increase in the overall energetic efficiency by linking cytosolic and mitochondrial sites of energy utilization and generation, would improve yeast energy metabolism significantly.

In this study, the cytosolic brain type (B-CK) and the mitochondrial (Mi<sub>b</sub>-CK) isoforms of creatine kinase from chicken have been functionally expressed in *Saccharomyces cerevisiae*, which is an important host for many traditional biotechnological applications and also for heterologous protein production, because of its advantages of rapid growth and ease of genetic manipulation, as well as its ability to post-translationally modify proteins. Additionally, the fact that wild-type *S. cerevisiae* does not have the CK system could help to better understand the complex mechanism of this system. In a previous study, the muscle isoform of rabbit CK (M-CK) was successfully expressed in *S. cerevisiae* and the functionality of the system was verified by the detection of PCr with *in vivo* <sup>31</sup>P-NMR upon feeding the cells with creatine, the substrate of the CK reaction (Brindle et al., 1990). This also suggests that *S. cerevisiae* would be an ideal host for this study. Here we investigate the effects of CK overexpression on growth physiology and recombinant protein production in *S. cerevisiae*.

## MATERIALS AND METHODS

### Strains and Plasmids

Genetic constructions of CK vectors were performed using *Escherichia coli* strain BMH 71-18 and *S. cerevisiae* strain PJ17-6A (*MAT $\alpha$* , *trp1-1*, *ura3-1*, *ade2-1*, *lys2-1*, *met4-1*, *can1-100*, *gal10-1*, *his5-2*, *leu2-1*) (James and Hall, 1990). All physiological analyses were conducted with the *S. cerevisiae* strains CBS7752 (*MAT $\alpha$* , *ura3-52*, *leu2-3/112*, *trp1*), Centraalbureau voor Schimmelcultures (Delft, the Netherlands) and INVSC1 (*MAT $\alpha$* , *ura3-52*, *his3- $\Delta$ 1*, *leu2-3/112*, *trp1-289*), Invitrogen BV (Leek, the Netherlands). The constitutive yeast expression vectors pAAH5 (Ammerer, 1983) and YEP24 (Botstein et al., 1979), which are *S. cerevisiae*-*E. coli* shuttle vectors, were used for B-CK and Mi<sub>b</sub>-CK-expressing constructs, respectively. For secreted BPTI expression, three different yeast-*E. coli* shuttle vectors all carrying the BPTI gene together with the URA3 and Amp<sup>R</sup> selection markers were employed, which were kindly provided by Prof. Dane Wittrup (Dept. of Chemical Engineering, Univ. of Illinois, Urbana, USA): pEB311U, with the constitutive *GPD* promoter, episomal; pCB216U, with the galactose-inducible *GALI*-promoter, centromeric; and pEB316U, with the galactose-inducible *GALI*-promoter, episomal.

### DNA Manipulations

A constitutive expression plasmid for the cytosolic brain-type isoform of creatine kinase (B-CK) was constructed using standard cloning protocols (Maniatis et al., 1982). The original chicken cDNA encoding the B-CK gene was a generous gift from Prof. J. C. Perriard, Institute of Cell Biology, ETH Zürich, Switzerland. In chicken, two distinct B-CK isoforms exist (B<sub>a</sub>- and B<sub>b</sub>-CK), which are formed by alternative splicing of a unique B-CK gene (Wirz et al., 1990) and each subspecies dimerizes in a tissue-specific manner (Quest et al., 1990). In this study, we have expressed the B<sub>b</sub>-CK sub-type isoform in yeast, and in the text we refer to this enzyme as B-CK. Using site-directed mutagenesis, a *Hind*III site was created 17 bp upstream of the ATG start codon of the B-CK-coding sequence (Furter-Graves, personal communication). This construction allowed cloning of the B-CK gene as a *Hind*III fragment into the unique *Hind*III site of the yeast expression vector pAAH5 (Furter-Graves, personal communication). In the resulting plasmid, FG12, the B-CK gene is expressed under the control of the constitutive *ADHI* promoter and terminator. For the construction of Mi-CK vector, the Mi-CK gene was fused with the *S. cerevisiae* cytochrome *c*<sub>1</sub> presequence for mitochondrial targeting (Hossle et al., 1988). The fused sequences were inserted into the *ADHI* expression cassette for constitutive expression from YEP24 containing the *URA3* selection marker. The resulting plasmid was called FG8, and correct processing was verified by N-terminal sequencing of the purified Mi-CK from transformed yeast. The so-called 'double construct', co-expressing B-CK and Mi-CK, was created by co-transforming *S. cerevisiae* with both B-

CK and Mi-CK vectors. For transformation of yeast cells, electroporation was used as reported previously with minor modifications (Becker et al., 1990). Transformants were selected by means of the LEU-marker on the plasmids pAAH5 and FG12, and the URA-marker on YEP24, FG8, and the BPTI-expressing plasmids.

### **Growth Media and Culture Conditions**

For cultivations during the genetic constructions, LB-medium (10 g/L tryptone, 5 g/L yeast extract, and 10 g/L NaCl) was used for *E. coli*, and YPD-medium (10 g/L yeast extract, 20 g/L peptone, and 20 g/L dextrose) for *S. cerevisiae*. For selection in *E. coli*, ampicillin was added to a final concentration of 100 µg/mL. For physiological experiments, yeast minimal medium (YMM), containing 6.7 g/L yeast nitrogen base without amino acids (Difco) and 1% (w/v) glucose was used.

BPTI production was investigated in YMM with either 1% (w/v) glucose, or 2% (w/v) galactose, or 2% (w/v) raffinose as the carbon source. For constitutive BPTI expression, cultures were grown in glucose-containing YMM for 96 hours. For inducible BPTI expression, cells were harvested by centrifugation at 3500 rpm for 10 min in a benchtop centrifuge (GS-6R, Beckman) after 48 h cultivation in glucose- or raffinose-containing YMM. The supernatants were discarded and the cells were resuspended in galactose-containing YMM to induce expression of BPTI for the next 96 h (Parekh and Wittrup, 1997, with slight modifications). According to the host strain's requirement, filter-sterilized tryptophan, uracil, and/or histidine were added to a final concentration of 20 mg/L each. Leucine was supplied to a final concentration of 240 mg/L.

For creatine supplementation of the growth medium, filter-sterilized creatine was added to a final concentration of 15 mM. In the case of cyclocreatine experiments, filter-sterilized cyclocreatine was added to a final concentration of 10 mM. Cultivations were performed aerobically using a rotary shaker at 30°C and 200 rpm, in 500 mL baffled shake flasks containing 100 mL medium.

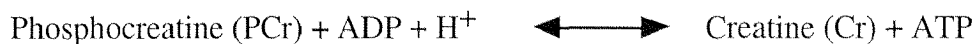
### **Analytical Methods**

Growth was monitored spectrophotometrically by measuring the optical density of cultures at 600 nm ( $OD_{600}$ ). For determination of cellular dry weight (cdw), Eppendorf tubes were dried at 80°C for 48 h, cooled in a desiccator for 30 min and weighed. Two mL aliquots of culture broth were centrifuged in these Eppendorf tubes at 3500 rpm for 10 min in a benchtop centrifuge. The resulting cell pellets were washed twice with 2 mL deionized water and dried at 80°C for 24 h. They were then placed in a desiccator for 30 min and weighed afterwards. Total soluble protein content was determined using the method of Bradford (1976) with bovine serum albumin (BSA) as the standard. To verify mitochondrial targeting of Mi-CK, SDS-PAGE analysis was performed as described previously (Laemmli, 1970).

### **Creatine Kinase Activity Determination**

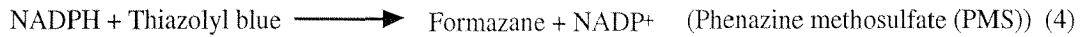
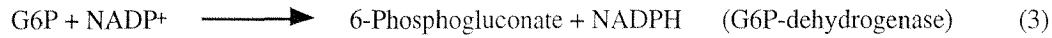
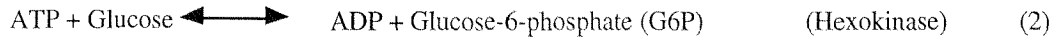
For determination of CK activity, lysates were prepared according to a protocol adapted from Beggs (1978). 250 mL cultures were centrifuged at 3500 rpm for 10 min in a benchtop centrifuge (GS-6R, Beckman). The resulting pellets were washed in deionized water, centrifuged at 3500 rpm for 5 min, resuspended in 5 mL freshly-prepared SEM buffer (1 M sorbitol, 25 mM EDTA, 50 mM  $\beta$ -mercaptoethanol, pH 8.0), and incubated at 30°C for 10 min. The suspension was then centrifuged at the previous settings, washed with 5 mL of 1 M sorbitol, centrifuged again, resuspended in 5.0 mL SCE buffer (1 M sorbitol, 0.1 M sodium citrate, 0.01 mM EDTA, pH 5.8) with 25 U of lyticase (Sigma), and incubated at 30°C for 30 min under moderate shaking. Phenylmethylsulfonylfluoride was then added to a final concentration of 0.1 mM, and the cell suspension was sonified on ice for 2 min at 60% output (Branson Sonifier-250). The resulting lysates were analysed for creatine kinase activity using either quantitative pH-stat analysis (Millner-White et al., 1971; Wallimann et al., 1984) or qualitative cellulose polyacetate gel electrophoresis (Wyss et al., 1990).

pH-stat analysis takes advantage of the stoichiometric proton consumption of the reverse reaction catalyzed by CK:



By monitoring the rate of proton consumption in the reaction mixture, it is thus possible to determine CK activity. The reaction mixtures for pH-stat consisted of 2.5 mL pH-stat buffer (75 mM KCl, 10 mM MgCl<sub>2</sub>, 0.1 mM EGTA, and 1 mM  $\beta$ -mercaptoethanol), 0.3 mL 0.1 M PCr, 120  $\mu$ L 0.1 M ADP, 50-100  $\mu$ L 20 mM NaOH (for initial-pH adjustments), and 20  $\mu$ L cell lysate. The reactions were started at pH 7.0 and room temperature. Control blanks were measured in the absence of PCr or ADP. CK activity was normalized to the determined total soluble protein concentration.

Cellulose polyacetate electrophoresis was performed for qualitative detection of CK isoenzyme activity (Wyss et al., 1990). In this procedure, protein separation is based on charge and size, as well as distribution differences in stationary phase (cellulose-polyacetate-membrane matrix) and mobile phase (running buffer). In contrast to SDS-polyacrylamide gel electrophoresis, this method separates the proteins in their native form and thus also allows separation of CK isoforms. CK can then be visualized on the cellulose polyacetate membrane by activity staining via the overlay gel technique, which is an adaptation of a previously described procedure (Dawson et al., 1967, Smith, 1968). This activity staining procedure is based on the following set of reactions that are initiated by CK:



In the last reaction, thiazolyl blue is hydrolyzed to formazane, which is violet and barely soluble in water. This reaction is catalyzed by PMS, a reducible dye which serves as an artificial electron acceptor for NADPH. PMS is colorless in its reduced form. In this study, cellulose polyacetate electrophoresis was performed at room temperature and 150 V for 1 h. The location of the B-CK isoenzyme was determined by incubating the cellulose polyacetate strip on top of an agarose overlay activity gel containing the above substrates and enzymes except CK, at 37°C for 30 min. The exact location of CK activity was then visualized as violet bands on the cellulose polyacetate strip and in the agarose matrix.

### Determination of BPTI Activity

BPTI activity was determined as modified from Wunderer and Fritz (1983) and Berman Marks et al. (1986). Culture supernatants of 0.5 mL volume were incubated for 30 min in the presence of 2.5 mL buffer (15 mM CaCl<sub>2</sub>, 0.2 M triethanolamine, pH 7.8) and 0-25 µg of bovine trypsin (L-(tosylamido 2-phenyl) ethyl chloromethyl ketone treated, dissolved in 15 mM HCl) (Fluka) at 30°C in a cuvette holder (Peltier temperature programmer, PTP-6, Ero Electronic). The reaction was initiated by adding 150 µL of 24 mg/mL of L-BAPA dissolved in DMSO (Fluka). The cuvette contents were mixed well and the increase in absorbance at 405 nm was recorded for 8 min using a Lambda 2 UV/VIS spectrometer (Perkin Elmer). The activity data were used to calculate the amount of BPTI present in the culture supernatant, because BPTI activity is equal to the difference between the added and detected trypsin activities, due to the irreversibility of BPTI-trypsin binding (Parekh and Wittrup, 1997).

## RESULTS

### Functional CK Expression in *S. cerevisiae*

The constructed constitutive B-CK-expression plasmid FG12 and Mi-CK-expression plasmid FG8 were transferred into *S. cerevisiae* CBS7752 and INVSC1 via electroporation. These strains were chosen because they carry only small numbers of auxotrophic mutations. Additionally, the empty expression vectors pAAH5 and YEP24 were transformed into the same hosts as a control for B-CK and Mi-CK expression studies. For combined overexpression, the two vectors carrying B-CK and Mi-CK were co-transformed into CBS7752 and INVSC1. Correct targeting of Mi-CK to the mitochondria was verified by SDS-PAGE analysis, where the short Mi-CK band was observed (data not shown). This indicates that the signal sequence was cleaved from Mi-CK, which, in turn, indicates correct targeting into mitochondria.

To verify whether the transformants functionally expressed B-CK and/or Mi-CK, pH-stat analysis and cellulose polyacetate gel electrophoresis were performed. Using pH-stat analysis, no activity was detected in cell lysates derived from the control strains. B-CK-expressing cells, however, were found to exhibit CK activity in the range of 5.5-8.5 U per mg of total soluble protein. In the case of Mi-CK-expressing cells, CK activity was in the range of 2.5-4.0 U per mg of total soluble protein. The double construct showed the highest CK activity, which was in the range of 7.0-10.0 U per mg of total soluble protein. Cellulose polyacetate gel electrophoresis qualitatively confirmed these results (Figure 1). CK activity of B-CK-expressing cells was detected at the same relative position as purified chicken B<sub>b</sub>-CK, clearly demonstrating expression of enzymatically active B-CK from the recombinant vector FG12. As expected, no activity could be detected in the cell lysates of the control strains, implying that the observed activity in B-CK-expressing cells resulted from heterologous CK expression and is not present in wild-type *S. cerevisiae*. Similarly, CK activity in Mi-CK-expressing cells was also detected using cellulose polyacetate gel electrophoresis (data not shown), demonstrating that also Mi-CK was functionally expressed.

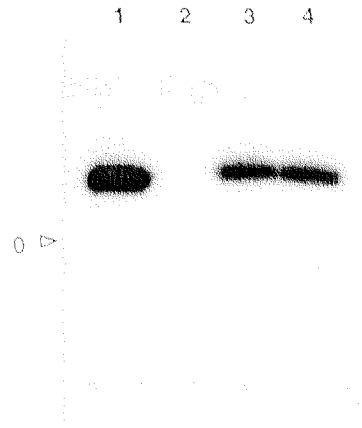


**Figure 1.** B-CK activity determination after cellulose polyacetate gel electrophoresis of crude cell extracts from: purified chicken B<sub>β</sub>-CK (lane 1); the pAAH5-carrying control strain (CBS7752) (lane 2); the FG12-carrying strains CBS7752 and INVSC1 (lanes 3 and 4); respectively. 0 denotes the position for sample application.

### **Growth Physiology of B-CK- and/or Mi-CK-Overexpressing *S. cerevisiae***

To investigate whether the CK-overexpression had any appreciable effect on growth physiology of *S. cerevisiae* CBS7752 and INVSC1, transformants expressing the Mi-CK and B-CK genes exclusively or in combination were studied. YEP24- and/or pAAH5-transformants of the strains, which contain the empty vectors without any CK-insert, were used as the control.

However, when cells were grown aerobically in YMM containing 1% (w/v) glucose as the sole carbon source, no significant difference was observed in their growth rate, metabolite formation (data not shown), or final OD<sub>600</sub> (Figure 2). Cellular dry weight determination results were also consistent with OD<sub>600</sub> values (data not shown). Furthermore, these results indicate that CBS7752 transformants cannot attain final cell densities as high as those of INVSC1 transformants, a phenomenon that is investigated and discussed in Chapter 4.



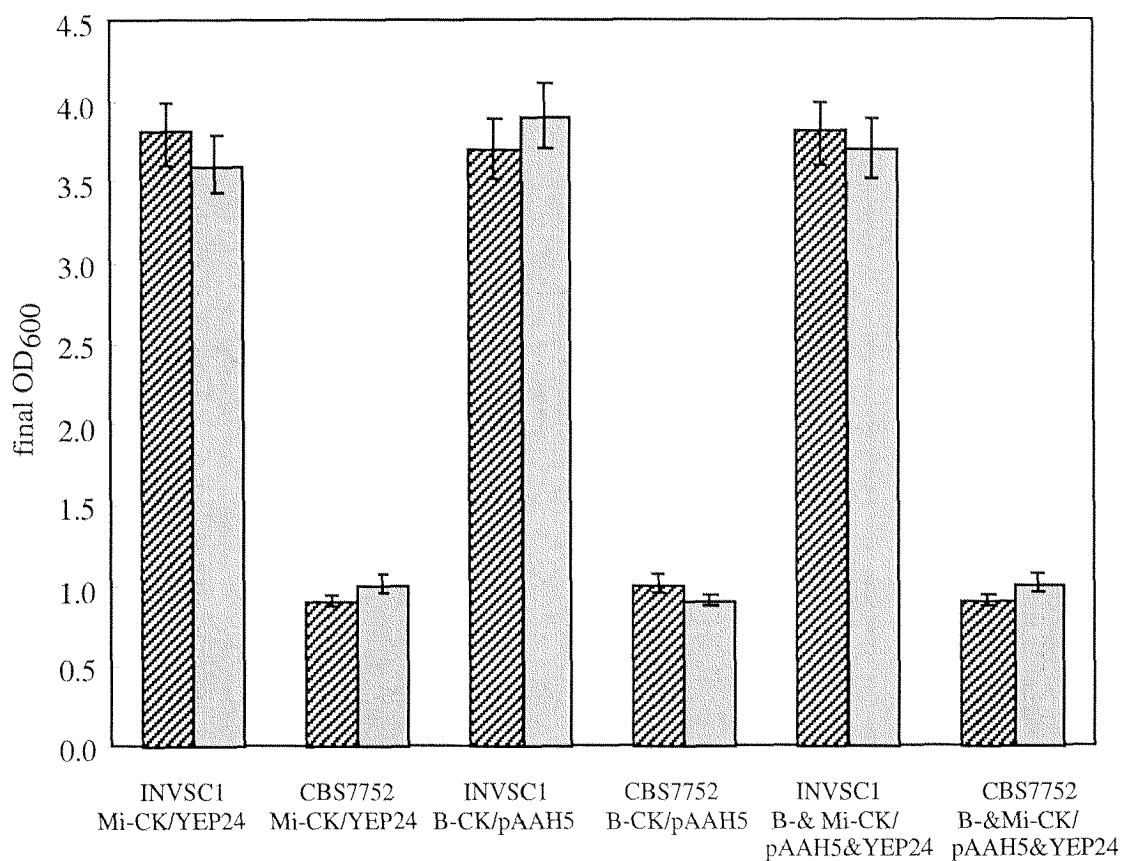


**Figure 2.** Final OD<sub>600</sub> of *S. cerevisiae* INVSC1 and CBS7752 transformants with various CK-expression constructs and the control vectors YEP24 and pAAH5, grown in a minimal medium with 1% (w/v) glucose.

### Increased Constitutive Expression of Recombinant BPTI Upon Co-Overexpression of B-CK

Because protein formation is a very energy-requiring process (Gancedo, 1992), we investigated the potential effects of B-CK co-overexpression on recombinant protein production in *S. cerevisiae*. For this purpose, the B-CK-expressing cells and their controls were transformed with the expression vector carrying the gene for secreted BPTI. This vector, pEB311U, is characterized by the constitutive expression promoter *GPD* and has a low level of secreted BPTI production (D. Wittrup, personal communication). With both host strains, the B-CK-expressing constructs reproducibly had up to 3-fold higher BPTI concentrations in the culture supernatants, compared to their corresponding controls (Table 1).

**Table 1.** Final OD<sub>600</sub> and secreted BPTI concentrations of *S. cerevisiae* CBS7752 and INVSC1 carrying pEB311U and either the B-CK vector or its control. Cells were grown aerobically for 92 h in 15 mM creatine-containing YMM with 1% (w/v) glucose as the carbon source. Data are the average of duplicate experiments.

strain	final OD <sub>600</sub>	secreted BPTI concentration (µg/mL supernatant)
CBS7752:pEB311U:control	0.86	1.05
CBS7752:pEB311U:B-CK	1.04	2.15
INVSC1:pEB311U:control	3.87	3.72
INVSC1:pEB311U:B-CK	3.57	10.79

### Effects of B-CK Co-Overexpression on Galactose-Inducible Expression of Recombinant BPTI.

To further investigate this beneficial effect of B-CK at high BPTI expression levels, two galactose-inducible BPTI expression systems, the centromeric pCB216U and the episomal pEB316U were employed. Initially, the B-CK-expressing *S. cerevisiae* CBS7752:FG12 strain and its control were transformed with both vectors. However, transformants grown for 48 h in glucose-containing YMM and subsequently for 96 h in galactose-containing YMM, all in the presence of 15 mM creatine, accumulated low BPTI levels, ranging between 0.2-0.8 µg/mL supernatant. Growth studies of CBS7752 in YMM supplemented with 2% (w/v) galactose as the sole carbon source revealed that CBS7752 was unable to grow on galactose (data not shown), most likely because of a so far unknown mutation. Therefore, INVSC1 which grew well on galactose was chosen as the host.

The results of the galactose-inducible BPTI expression studies are summarized in Table 2. As expected, the episomal, galactose-inducible BPTI expression system pCB316U conferred the highest secreted BPTI concentration. However, co-overexpression of B-CK apparently did not have a positive effect on the final secreted BPTI concentration. In the case of the centromeric, galactose-inducible expression system pCB216U, the cells co-overexpressing B-CK had even lower secreted BPTI concentrations compared to their control (Table 2). These results needed to be verified, since glucose is a strong inhibitor of galactose-inducible expression systems. Even traces of glucose, which might have remained after transfer to the galactose medium, could have caused these results. For this purpose, the same set of strains was grown first for 48 h in YMM containing 15 mM creatine and 2% (w/v) raffinose, which does not exert repression. The cells were then transferred, as before, to the 2% (w/v) galactose-

containing YMM with 15 mM creatine for further growth for 96 h. The results demonstrated that indeed glucose repression had hampered high BPTI expression in the previous experiments, since the secreted BPTI levels of all cells were between 10-100% higher in raffinose-experiments (Table 3). However, the B-CK co-overexpression clearly had a negative effect in both cases.

**Table 2.** Final OD<sub>600</sub> and secreted BPTI concentrations of *S. cerevisiae* INVSC1:FG12 (B-CK) or INVSC1:pAAH5 (control), co-transformed with the galactose-inducible BPTI expression systems pCB216U (centromeric) or pCB316U (episomal). Cultures were first grown aerobically for 48 h in 15 mM creatine-containing YMM with 1% (w/v) glucose as the carbon source. They were then grown in 2% (w/v) galactose and 15 mM creatine-containing YMM for another 96 h. Data are the average of duplicate experiments.

vector system	final OD <sub>600</sub>	secreted BPTI concentration (µg/mL supernatant)
pCB216U: control	3.36	9.81
pCB216U: B-CK	4.71	2.93
pCB316U: control	3.83	21.90
pCB316U: B-CK	4.31	20.16

**Table 3.** Final OD<sub>600</sub> and secreted BPTI concentrations of *S. cerevisiae* INVSC1, co-transformed with the galactose-inducible BPTI expression systems pCB216U (centromeric) or pCB316U (episomal). Cells were first grown aerobically for 48 h in 15 mM creatine-containing YMM with 2% (w/v) raffinose as the carbon source. They were then grown in 2% (w/v) galactose and 15 mM creatine-containing YMM for another 96 h. Data are the average of duplicate experiments.

vector system	final OD <sub>600</sub>	secreted BPTI concentration ( $\mu\text{g/mL}$ supernatant)
pCB216U: control	3.11	12.61
pCB216U: B-CK	3.44	3.25
pCB316U: control	3.12	50.00
pCB316U: B-CK	2.80	39.62

### **CK-Inhibition Studies Using Cyclocreatine and *in vivo* <sup>31</sup>P-NMR Analysis Question the Functionality of the CK system in *S. cerevisiae***

In order to verify that any effects we had observed in yeast cells co-overexpressing CK were indeed related to CK-activity, we have tested the functionality of the CK-system in these constructs using two different approaches. As a first approach, CK-inhibition studies were done with cyclocreatine, a Cr analog. It was expected that, when CK-co-overexpressing yeast cells were grown in the presence of the CK-inhibitor cyclocreatine, their physiology should be negatively affected because of the CK-inhibition. For this purpose, B-CK, Mi-CK and their corresponding controls were grown with and without 10 mM cyclocreatine and 15 mM creatine in YMM containing 1% (w/v) glucose as the sole carbon source (Figure 3). These data showed that presence or absence of creatine and cyclocreatine in the growth medium of B-CK-expressing *S. cerevisiae* strains CBS7752 and INVSC1 did not have any effect on their growth physiology in terms of the final OD<sub>600</sub>. The same conclusion was also derived in the case of the Mi-CK constructs and corresponding controls of the two strains (data not shown).

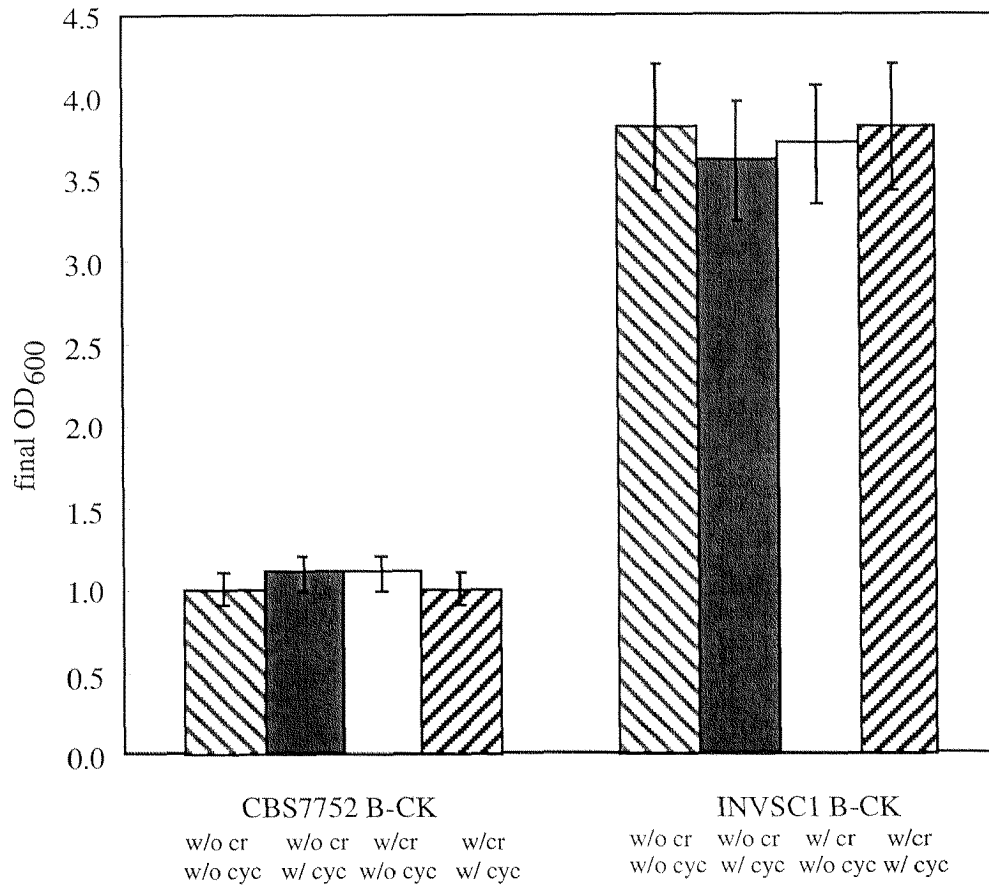


**Figure 3.** Comparison of final OD<sub>600</sub> of *S. cerevisiae* CBS7752- and INVSC1-transformants expressing B-CK. The bars in each set represent cells grown (from left to right) without creatine and cyclocreatine; without creatine with cyclocreatine; with creatine without cyclocreatine, and with creatine and cyclocreatine, respectively.

Secondly, we attempted to verify whether the CK reaction occurs *in vivo* in our *S. cerevisiae* CK-transformants, as was previously suggested for another *S. cerevisiae* strain (Brindle et al., 1990). For this purpose, *in vivo* NMR analysis was performed. Yeast cells were grown in 15 mM creatine-containing medium and their extracts were analyzed using *in vivo* <sup>31</sup>P-NMR analysis. For a functional CK system, one would expect the intracellular presence of PCr, which is amenable to *in vivo* <sup>31</sup>P-NMR. However, the <sup>31</sup>P-NMR data clearly showed that there was no PCr peak in any of the extracts from our CK-transformants (Figure 4).

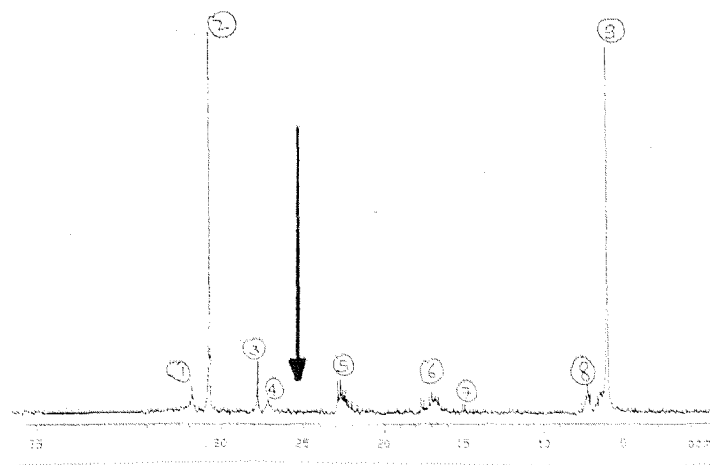


**Figure 4.**  $^{31}\text{P}$ -NMR spectra of *S. cerevisiae* CBS7752 expressing B-CK. The peaks are: 1) sugar phosphates, 2) inorganic phosphates, 3) glycerophosphorylcholine, 4) unidentified, but not PCr, 5) terminal P in ADP and ATP and polyphosphates, 6)  $\alpha$ -P in ATP and ADP, also in NAD(P)H, 7) UDPG, 8)  $\beta$ -P in ATP, 9) internal P of polyphosphates. The arrow indicates the expected position of the PCr peak.

## DISCUSSION

In this study, we aimed at improving growth characteristics and heterologous protein production by installing the heterologous CK-system in *S. cerevisiae*. In addition to a great deal of scientific information accumulated on CK, this work was based on the premise that a functional CK system could be installed in yeast. There was already strong evidence from a previous study that this is indeed feasible (Brindle et al., 1990). In that study, it had been shown that recombinant rabbit muscle-type creatine kinase enzyme was functioning in *S. cerevisiae* (Brindle et al., 1990). This statement was based on the detection of a phosphocreatine peak by *in vivo*  $^{31}\text{P}$ -NMR analysis upon perfusion of the immobilized yeast cells with creatine, the substrate of the CK reaction, in the presence or absence of 1 mM  $\text{P}_i$ . However, our *in vivo*  $^{31}\text{P}$ -NMR and HPLC studies with B-CK yeasts grown in the presence of 15 mM creatine showed that no phosphocreatine was detectable inside the cells (Klaas Nicolay, personal communication). Furthermore, in a B-CK inhibition study using 10 mM of the inhibitor cyclocreatine, the B-CK-expressing cells had even higher final  $\text{OD}_{600}$  values than the controls, when they were grown in the presence of cyclocreatine (data not shown). These results clearly show that the effects related to heterologous protein production were secondary and probably unrelated to CK activity. Furthermore, they indicate that either creatine and cyclocreatine cannot be taken up, because yeast does not have a special transporter system, or that intracellular creatine is rapidly degraded. Both cases would interfere severely with installing the CK-system in yeast and could explain our results.

B-CK co-overexpression had a negative effect on the galactose-inducible BPTI expression system. This can be explained by ‘protein burden’, which specifies the effects of the synthesis of an extra protein on host cell function and metabolism (Bailey, 1993; Snoep et al., 1995). Despite the fact that the CK system was not functional in our cells, the positive secondary effect we have observed in constitutive expression of recombinant secreted BPTI upon co-overexpression of B-CK is significant and reproducible. Specifically, we found 3-fold improvement in secreted BPTI levels by co-overexpression of B-CK, compared to the control without B-CK. The concentration of the secreted BPTI in the constitutive expression system was low, in the range of 1-5  $\mu\text{g}$  secreted BPTI/mL. Thus, the secondary effect may only be important in a low expression system. Alternatively, the secondary effect may exist only in cells grown on glucose, but not in galactose-containing media. The latter hypothesis is supported by the fact that galactose metabolism of yeast is known to be very different from glucose metabolism, mainly because of catabolite repression (Gancedo, 1992).

To summarize, further metabolic engineering attempts are necessary to install a functional creatine kinase system in yeast. These could be either in the direction of intracellular creatine bioynthesis or creatine uptake.

**ACKNOWLEDGEMENTS**

We thank Rolf Furter and Elizabeth Furter-Graves for construction of plasmid FG12, Dane Wittrup for providing us with the BPTI expression vectors, and Klaas Nicolay for *in vivo*  $^{31}\text{P}$ -NMR measurements.



**REFERENCES**

- Ammerer, G. 1983. Expression of genes in yeast using the *ADCI* promoter. *Meth. Enzymol.* **101**: 192-211.
- Attfield, P. V. 1997. Stress tolerance: the key to effective strains of industrial baker's yeast. *Nature Biotechnol.* **15**: 1351-1357.
- Bailey, J. E. 1993. Host-vector interactions in *Escherichia coli*. *Adv. Biochem. Eng. Biotechnol.* **48**: 29-52.
- Becker, D. M., Guarante, L. 1990. High efficiency transformation of yeast by electroporation. *Meth. Enzymol.* **194**: 182.
- Beggs, J. D. 1978. Transformation of yeast by a replicating hybrid plasmid. *Nature* **275**: 104-109.
- Berman Marks, C., Vasser, M., Ng, P., Henzel, W., Anderson, S. 1986. Production of native, correctly folded bovine pancreatic trypsin inhibitor by *Escherichia coli*. *J. Biol. Chem.* **261**: 7115-7118.
- Botstein, D., Falco, S. C., Stewart, S. E., Brennan, M., Scherer, S., Stinchcomb, D. T., Struhl, K., Davis, R. W. 1979. Sterile host yeasts (shy): a eukaryotic system of biological containment for recombinant DNA experiments. *Gene* **8**: 17-24.
- Bradford, M. M. 1976. A rapid and sensitive method for the quantitation of microgram quantities of protein utilizing the principle of protein-dye binding. *Anal. Biochem.* **72**: 248-254.
- Brindle, K., Braddock, P., Fulton, S. 1990. <sup>31</sup>P NMR measurements of the ADP concentration in yeast cells genetically modified to express creatine kinase. *Biochemistry* **29**: 3295-3302.
- Dawson, D. M., Eppenberger, H. M., Kaplan, N. O. 1967. The comparative enzymology of creatine kinases: II. Physical and chemical properties. *J. Biol. Chem.* **242**: 210-217.
- Gancedo, J. M. 1992. Carbon catabolite repression in yeast. *Eur. J. Biochem.* **206**: 297-313.
- Hossle, J. P., Schlegel, J., Wegmann, G., Wyss, M., Böhlen, P., Eppenberger, H. M., Wallimann, T., Perriard, J.-C. 1988. Distinct tissue specific mitochondrial creatine kinases from chicken brain and striated muscle with a conserved CK framework. *Biochem. Biophys. Res. Commun.* **151**: 408-416.
- James, P., Hall, B. D. 1990. *ret1-1*, a yeast mutant affecting transcription termination by RNA polymerase III. *Genetics* **125**: 293-303.
- Laemmli, L. K. 1970. Cleavage of structural proteins during the assembly of the head of bacteriophage T4. *Nature* **227**: 680-685.
- Maniatis, T., Fritsch, E. F., Sambrook, J. 1982. *Molecular cloning: a laboratory manual*, Cold Spring Harbor Laboratory, New York.

- Millner-White, E. J., Watts, D. C. 1971. Inhibition of adenosine 5'-triphosphate-creatine phosphotransferase by substrate-anion complexes. *Biochem. J.* **122**: 727-740.
- Parekh, R. N., Wittrup, K. D. 1997. Expression level tuning for optimal heterologous protein secretion in *Saccharomyces cerevisiae*. *Biotechnol. Prog.* **13**: 117-122.
- Quest, A. F. G., Eppenberger, H. M., Wallimann, T. 1990. Two different B-type creatine kinase subunits dimerize in a tissue-specific manner. *FEBS Lett.* **262**: 299-304.
- Smith, I. (ed.) 1968. *Chromatographic and electrophoretic techniques*: **2**, Interscience, New York.
- Snoep, J. L., Yomano, L. P., Westerhoff, H. V., Ingram, L. O. 1995. Protein burden in *Zymomonas mobilis*: negative flux and growth control due to overproduction of glycolytic enzymes. *Microbiol.* **141**: 2329-2337.
- Stryer, L. 1988. *Biochemistry*, Third Edition, W. H. Freeman and Company, New York.
- Steeghs, K., Benders, A., Oerlemans, F., de Haan, A., Heerschap, A., Ruitenbeek, W., Jost, C., van Deursen, J., Perryman, B., Pette, D., Bruckwilder, M., Koudijs, J., Jap, P., Veerkamp, J., Wieringa, B. 1997. Altered Ca<sup>2+</sup> responses in muscles with combined mitochondrial and cytosolic creatine kinase deficiencies. *Cell* **89**: 93-103.
- Wallimann, T., Schlösser, T., Eppenberger, H. M. 1984. Function of M-line-bound creatine kinase as intramyofibrillar ATP regenerator at the receiving end of the phosphorylcreatine shuttle in muscle. *J. Biol. Chem.* **259**: 5238-5246.
- Wallimann, T., Wyss, M., Brdiczka, D., Nicolay, K., Eppenberger, H. M. 1992. Intracellular compartmentation, structure and function of creatine kinase isoenzymes in tissues with high and fluctuating energy demands: the 'phosphocreatine circuit' for cellular energy homeostasis. *Biochem. J.* **281**: 151-170.
- Wallimann, T. 1994. Dissecting the role of creatine kinase. *Curr. Biol.* **4**: 42-46.
- Wirz, T., Brändle, U., Soldati, T., Hossle, J. P., Perriard, J-C. 1990. A unique chicken B-creatine kinase gene gives rise to two B-creatine kinase isoproteins with distinct N termini by alternative splicing. *J. Biol. Chem.* **265**: 11656-11666.
- Wunderer, G., Fritz, H. 1983. Biochemistry and applications of aprotinin the kallikrein inhibitor from bovine organs. *Drug Research* **33**:4.
- Wyss, M., Schlegel, J., James, P., Eppenberger, H. M., Wallimann, T. 1990. The mitochondrial creatine kinase from chicken brain. *J. Biol. Chem.* **265**: 15900-15908.

**Chapter 3****Intracellular Carbon Fluxes in the Yeasts  
*Saccharomyces cerevisiae* and *Pichia stipitis***

## SUMMARY

In this study, we applied for the first time metabolic flux ratio (METAFoR) analysis by NMR, and used it in combination with stoichiometric flux balancing for flux analysis in the yeasts *Saccharomyces cerevisiae* and *Pichia stipitis*. Unlike many former yeast flux studies, we had sufficient information to also include compartmentalization in the model and to significantly reduce the number of assumptions that are necessary to solve the equations. The flux analyses of three glucose-limited chemostats with wild-type *S. cerevisiae* and *P. stipitis* strains revealed that *S. cerevisiae* has low fluxes through pentose phosphate pathway, which, according to our analyses, seems to be related to the lack of a transhydrogenase activity. *P. stipitis*, in turn, has significantly higher fluxes through the pentose phosphate pathway, which may be one explanation why it is such an efficient utilizer of xylose. The lower fluxes through the pentose phosphate pathway in *S. cerevisiae* are possibly caused by the absence of a transhydrogenase reaction in this yeast. These results point to a new target for metabolic engineering of efficient xylose utilization for bioethanol production.

## INTRODUCTION

Metabolic engineering of central carbon metabolism is complicated and elaborate. A major problem is that metabolic engineering attempts may influence certain intracellular reaction rates, the metabolic fluxes, but not necessarily affect the physiological phenotype. Thus, an analytical tool is required to monitor intracellular flux changes, possibly to guide further metabolic engineering targets. There are various analytical methods to gain information about the intracellular flux distribution, commonly referred to as metabolic flux analysis.

The classical approach is stoichiometric flux balancing (Vallino and Stephanopoulos, 1990). In this approach, the stoichiometry of the considered intracellular reactions is described in a stoichiometric matrix. Mass balancing around the intracellular metabolites allows to calculate the metabolic fluxes. Such calculations are based on a pseudo steady-state assumption for the intracellular metabolite concentrations, and measurement of extracellular reaction rates, as well as the macromolecular composition of the biomass to quantify metabolite requirements for biomass synthesis (Varma and Palsson, 1994). However, often there are more unknown fluxes than balancing equations in typical bioreaction networks. Consequently, biological assumptions are introduced to provide additional equations, thus to make the system solvable. However, these biological assumptions about energy stoichiometry or biological functions of metabolic systems are generally based on observations of wild-type organisms in their native environment. Under experimental conditions like carbon limitations or low growth rates, significant metabolic changes may occur and the assumptions may not be valid anymore (Sauer et al., 1997). Alternatively, isotopic-tracer experiments were used to determine flux ratios at certain branch points. For this purpose, nuclear magnetic resonance (NMR) spectroscopy is often used to detect differences in the isotope isomer, or isotopomer, composition of secreted metabolites or cellular components. This is achieved by growing microorganisms on minimal media containing a mixture of  $^{13}\text{C}$ -labeled and non-labeled carbon source. Depending on the labeling experiment, NMR is used to detect site-specific isotope enrichments in the metabolic intermediates (Cerdan and Seelig, 1990), or the isotopomer distributions (Malloy et al., 1990). A recent method is biosynthetically directed fractional  $^{13}\text{C}$ -labeling of the common proteinogenic amino acids, which is used to monitor metabolic flux ratios of metabolic key pathways (Szyperski, 1995). This method, also referred to as metabolic flux ratio (METAFoR) analysis (Sauer et al., 1999), can complement stoichiometric flux balancing by supplying additional constraints (or equations) in order to make the system solvable (Sauer et al., 1997).

Several attempts have been made to estimate the intracellular fluxes in the biotechnologically relevant yeast *Saccharomyces cerevisiae*, based on stoichiometric flux balancing. A relatively simple method was developed for estimating anabolic fluxes

(Cortassa et al., 1995), based on the calculation of anabolic fluxes from growth rate and the requirements for building blocks. This method allowed also to estimate fluxes through some central catabolic pathways. A similar study focused on the construction of metabolic networks using biochemical information from the literature. This information was used to describe the biochemistry of growth of *S. cerevisiae* and *Candida utilis* on several carbon substrates like glucose, ethanol, acetate and mixtures of glucose and ethanol (van Gulik and Heijnen, 1995). In this case, only two fitted parameters were used for all networks, the P-to-O ratio and the maintenance coefficient. In a follow-up study, it was shown that yield data for a number of mixtures of two substrates (glucose and ethanol) provide sufficient information for estimating the two energetic parameters P/O and  $k$ ; the operational P-to-O ratio and the growth-related maintenance factor, respectively. These two parameters were the only unknowns in the proposed stoichiometric description of *S. cerevisiae* metabolism (Vanrolleghem et al., 1996). In contrast to the studies mentioned above, stoichiometric flux analysis of anaerobic *S. cerevisiae* considered compartmentalization in the flux model (Nissen et al., 1997). However, several assumptions were necessary to make the system determined.

Apart from stoichiometric flux balancing, there are a few studies which employed  $^{13}\text{C}$ -NMR spectroscopy to determine certain flux ratios in *S. cerevisiae*. One example was investigation of the tricarboxylic acid (TCA) and glyoxylate cycles in *S. cerevisiae* using mathematical models based on the  $^{13}\text{C}$ -NMR spectra of glutamate obtained from cells fed with 100% 2- $^{13}\text{C}$  acetate (Tran-Dinh et al., 1996). The glutamate isotopomer population provided specific analytical equations for the deduction of the fluxes in the TCA and glyoxylate cycles. Similarly, the use of  $^{14}\text{C}$ -labelled glucose or glutamic acid and measurement of the radioactivity in the resulting compounds has also been employed to study the distribution of carbon from glucose and glutamate in anaerobically grown *S. cerevisiae* (Albers et al., 1998). It was concluded that the carbon flow follows two separate paths, and that the major reactions used in the TCA cycle are those involved in the conversion of 2-oxoglutarate to succinate. Additionally, it was found that the glutamate family of amino acids (glutamine, glutamic acid, proline, arginine and lysine) originate almost exclusively from the carbon skeleton of glutamic acid (Albers et al., 1998).

In the present study, we combined stoichiometric flux balancing and  $^{13}\text{C}$ -NMR analysis of proteinogenic amino acids to develop a more realistic and reliable metabolic flux model for *S. cerevisiae* that also considers compartmentalization. The primary goal of this work was to elucidate potential differences in pentose phosphate metabolism of the yeasts *S. cerevisiae* and *Pichia stipitis* during growth on glucose. The rationale for choosing these two yeasts was that the former is an efficient producer of ethanol, but

cannot utilize pentoses efficiently, even when engineered to do so. In contrast, the latter can utilize pentoses efficiently, but does not produce ethanol.

## MATERIALS AND METHODS

### Yeast Strains and Cultivation Conditions

*S. cerevisiae* wild-type strain CEN.PK 113.7D (*MATa*, *MAL2-8<sup>c</sup>*, *SUC2*) (obtained from Dr. P. Kötter, Johann Wolfgang Goethe-University, Frankfurt, Germany) and the *P. stipitis* wild-type strain CBS6054 (kindly provided by Prof. B. Hahn-Hägerdal, Lund University, Sweden) were used. Batch cultures were grown in baffled shake flasks and continuous cultivations in glucose-limited chemostats were performed at 30°C in a 1.5-L bioreactor (Bioengineering, Wald, Switzerland) with a working volume of 1 L, equipped with pH, dissolved oxygen, and temperature probes. The filter-sterilized mineral medium used for all cultivations contained the following components (per liter of distilled water): (NH<sub>4</sub>)<sub>2</sub>SO<sub>4</sub>, 5 g; MgSO<sub>4</sub>·7H<sub>2</sub>O, 0.5 g; KH<sub>2</sub>PO<sub>4</sub>, 3 g; 1 mL of vitamin solution (biotin, 0.05 mg/L; calcium pantothenate, 1 mg/L; nicotinic acid, 1 mg/L; inositol, 25 mg/L; thiamine-HCl, 1 mg/L; pyridoxine-HCl, 1 mg/L; and para-aminobenzoic acid 0.2 mg/L) and 1 mL of trace element solution (EDTA, 15 mg/L; ZnSO<sub>4</sub>·7H<sub>2</sub>O, 4.5 mg/L; CoCl<sub>2</sub>·6H<sub>2</sub>O, 0.3 mg/L; MnCl<sub>2</sub>·4H<sub>2</sub>O, 1 mg/L; CuSO<sub>4</sub>·5H<sub>2</sub>O, 0.3 mg/L; CaCl<sub>2</sub>·2H<sub>2</sub>O, 4.5 mg/L; FeSO<sub>4</sub>·7H<sub>2</sub>O, 3 mg/L; NaMoO<sub>4</sub>·2H<sub>2</sub>O; 0.4 mg/L; H<sub>3</sub>BO<sub>3</sub>, 1 mg/L; and KI, 0.1 mg/L) (Verduyn et al., 1992). The minimal medium was supplemented either with 3.6 g/L of glucose containing <sup>13</sup>C at natural abundance, or with 3.24 g/L of glucose at natural abundance and 0.36 g/L of uniformly labeled (<sup>13</sup>C<sub>6</sub>)-glucose (<sup>13</sup>C>98%, Isotech, Miamisburg, OH). The pH of the medium prior to adjustment was 4.5. Polypropylene glycol 2000 (PPG 2000) was added as an antifoam to the medium at a concentration of 2 mL PPG 2000 (1:10 diluted in dH<sub>2</sub>O) per liter of medium. For anaerobic *S. cerevisiae* chemostat cultures, 1.25 mL (per liter of medium) of filter-sterilized Tween 80/ergosterol solution containing 8 g ergosterol and 336 g Tween 80 per liter of ethanol was added to the medium.

For chemostat cultivations, the pH was controlled at 5.50±0.05 by the addition of 3 M KOH. The fermentation volume was kept constant using a weight-controlled pump. For aerobic chemostats, a constant air flow of 0.5 L/min was achieved by a mass flow controller and the agitation speed was adjusted to 1200 rpm. Anaerobic conditions were achieved by a constant flow of 0.5 L N<sub>2</sub> per min. Aliquots for further analysis were taken from chemostat cultures in steady state, which was defined as at least three volume changes of stable optical density readings, and oxygen and carbon dioxide concentrations in the fermenter off-gas, after any perturbation such as adjusting the dilution rate or withdrawal of aliquots. Labeling was achieved by changing the feed medium of a culture in steady state from the normal, unlabeled glucose medium to an identical medium that contained the same absolute concentration of glucose, but a 10% fraction of it was <sup>13</sup>C<sub>6</sub>-glucose. Samples of labeled biomass were taken after 1.00 (aerobic *S. cerevisiae*), 0.88 (anaerobic *S. cerevisiae*), and 1.00 (aerobic *P. stipitis*) volume changes, yielding an



overall degree of fractionally labeled biomass ( $x_b$ ), as calculated by using first order wash-out kinetics:  $x_b = 1 - e^{-Dt}$ , of 60, 59, and 57%, respectively. From each chemostat, about 0.1 g (cdw) of cells were harvested for NMR analysis.

### **Analytical Methods and Sample Preparation**

Cellular dry weight (cdw) measurements were performed using six parallel 10-mL suspensions, which were harvested by centrifugation at 5000 rpm for 20 min in a benchtop centrifuge (Sigma, USA). The pellets were washed once with distilled water, centrifuged again as above, and dried to constant weight at 85°C for 24 h. The concentrations of glucose, ethanol, and glycerol were determined with a Synchron CX5CE automated enzyme analysis system (Beckman, USA) with either kits supplied by the manufacturer or following standard protocols (Bergmeyer, 1985). Concentrations of additional fermentation (by-)products such as pyruvate, acetate, and succinate were determined using high-pressure liquid chromatography (Supelco-Hewlett Packard) at 30°C and 0.2 N ortho-phosphoric acid as the elution solvent. Protein determination was done using a modified Biuret method (Verduyn et al., 1990). RNA measurements were done as described elsewhere (Benthin et al., 1991). Total carbohydrate content was measured using the phenol method (Herbert et al., 1971). The remaining biomass components, mainly lipids and ash, were calculated on the basis of reported results (Nissen et al., 1997). The biomass precursor requirements for *Bacillus subtilis* (Sauer et al., 1996) were adapted for yeast by considering the biomass composition differences between yeast and bacteria, regarding especially the high glucose-6-phosphate requirements of yeast as a cell wall component. These data were then used in flux calculations. Off-gas concentrations of oxygen and carbon dioxide were determined with a quadrupole mass spectrometer (Fisons, Uxbridge, United Kingdom).

For NMR measurements, 0.1 g (cdw) of cellular biomass were harvested by centrifugation at 3800 rpm, 4°C, for 15 min in a benchtop centrifuge (Eppendorf, Germany). The pellets were washed once with 20 mM Tris-HCl, pH 7.6 and centrifuged at 14,000 rpm for 5 min in a benchtop centrifuge. The cells were then resuspended and hydrolyzed in 6 M HCl at 110°C for 24 h. Due to oxidation, cysteine and tryptophan were lost in the resulting samples, and asparagine and glutamine were deaminated. The hydrolysates were then lyophilized and redissolved in 700  $\mu$ L 0.1 M  $^2\text{HCl}$  in  $^2\text{H}_2\text{O}$ .

### **NMR Spectroscopy and Data Analysis**

NMR experiments were conducted at 40°C and a  $^{13}\text{C}$  resonance frequency of 125.8 MHz using a Bruker DRX500 spectrometer. The uniformly  $^{13}\text{C}$ -labeled glucose fraction in the medium was determined from the average degree of  $^{13}\text{C}$ -labeling that was determined from 1D  $^1\text{H}$  NMR spectra (Szyperski, 1995) and from the exchanged biomass fraction,  $x_b$ . For each of the three experiments, two ( $^{13}\text{C}$   $^1\text{H}$ )-COSY spectra were recorded, one for the aliphatic (data size 1500x256 complex points;  $t_{1\text{max}} = 353$  ms;  $t_{2\text{max}} = 102$  ms) and one

for the aromatic resonances (data size 800x128 complex points;  $t_{1\max} = 341$  ms;  $t_{2\max} = 102$  ms) (Szyperski, 1995). The information on the relative abundances of intact multi carbon fragments originating from glucose that are present in the precursor fragments for amino acid biosynthesis is provided by 18  $^{13}\text{C}$  scalar coupling fine structures in nine different amino acids (Szyperski, 1995; Szyperski et al., 1996). By means of probabilistic equations, the scalar coupling fine structures were related to the relative abundance of intact carbon fragments that can be extracted from such biosynthetically directed fractionally  $^{13}\text{C}$ -labeled amino acids (Szyperski, 1995). In order to estimate the experimental error for the relative abundances of intact multi-carbon fragments, 13 redundant fine structures were used. The other 14 observed  $^{13}\text{C}$  fine structures for the proteinogenic amino acids in the hydrolysate were checked for consistency with the known amino acid biosynthesis.

### **Computation of Fluxes**

The yeast biochemical reaction network that was used in our analyses is shown in Figure 1. Glycolysis and PPP intermediates were considered exclusively as cytosolic pools and the TCA intermediates as mitochondrial pools (Zimmermann and Entian, 1997). The only exceptions are pyruvate, acetyl-CoA, and oxaloacetate that occur as both mitochondrial and cytosolic pools. Amino acids from the pyruvate family were assumed to be synthesized from the mitochondrial pyruvate pool, based on biochemical evidence (Pronk et al., 1996; Jones and Fink, 1982). The METAFoR analysis principles were used first to elucidate the localization of certain biosynthetic intermediates in the cytosolic or mitochondrial compartments (Fiaux et al., unpublished). Information on pyruvate is embedded in the amino acids alanine, valine, isoleucine and leucine. The first step in the biosynthesis of isoleucine, leucine and valine is the condensation of pyruvate to  $\alpha$ -ketobutyrate for the former, and hydroxyethyl-TPP for the latter two, catalyzed by the mitochondrial enzyme acetolactate-pyruvate lyase (Jones and Fink, 1982). Hence, the  $^{13}\text{C}$ -multiplet fine structure of these amino acids reflects directly the mitochondrial pyruvate pool (Fiaux et al., unpublished). It is also known via subcellular fractionation studies that the malic enzyme in *S. cerevisiae* is located in the mitochondria (Boles et al., 1998). In contrast, based on METAFoR evidence, amino acids from the oxaloacetate pool were assumed to be synthesized from the cytosolic pool. Our previous findings with batch cultures of *S. cerevisiae* and *P. stipitis* revealed that, for biosynthesis of proteinogenic aspartate, threonine and methionine, the cytosolic oxaloacetate was used, and it did not equilibrate with the mitochondrial pool (Fiaux et al., unpublished). According to these results, the entire oxaloacetate pool originated from pyruvate via the pyruvate carboxylase and not from the TCA cycle. This view is consistent with the reported localization of pyruvate carboxylase in the cytoplasm (Pronk et al., 1996).

Several transport processes were considered in our model. Glucose uptake occurs via facilitated diffusion (Vanrolleghem et al., 1996). Ammonium is taken up by means of a proton symport (Roon et al., 1977). Oxaloacetate is transported into the mitochondria via a dicarboxylate carrier (Zimmermann and Entian, 1997). NADPH and NADH were previously assumed as both cytosolic and mitochondrial compounds (Nissen et al., 1997), because of the apparent absence of a transport system. However, it has recently been proposed that the glycerol-3-P shuttle, which is important for yeast under aerobic conditions to keep the redox balance, enables the transfer of these compounds (Larsson et al., 1998). Consequently, this was considered in our aerobic flux models. Although there is no reported mechanism for acetyl-CoA transport in and out of the mitochondrial membrane, our METAFoR analysis showed that some of the acetyl-CoA molecules embedded in 2-oxoglutarate were imported from the cytosol (Fiaux et al., unpublished). Thus, even if it is still unknown, there must be a transport mechanism for acetyl-CoA.

Our reaction network consists of 27 reactions with unknown fluxes and 26 metabolite balances, including CO<sub>2</sub> and O<sub>2</sub>. In the case of *P. stipitis* model, there is one more reaction, because the transhydrogenase reaction is considered to be present in this yeast (Bruinenberg, 1986), whereas for *S. cerevisiae* it is known that this yeast has no transhydrogenase activity (Lagunas and Gancedo, 1973). Compartmentalization was included in the model by defining mitochondrial and cytosolic pools of pyruvate, oxaloacetate, and acetyl-CoA, as denoted by subscripts.

The NMR data were then used to estimate fractional relationships between particular fluxes:

(1) the fraction of PYR<sub>mit</sub> originating from MAL (malic enzyme reaction, upper bound):

$$\alpha = v_{26}/(v_{26}+v_{19}) \quad (1)$$

(2) the fraction of OAA<sub>mit</sub> from PYR<sub>cyt</sub> (anaplerotic reaction):

$$\beta = v_{20'}/(v_{20'}+v_{15}) \quad (2)$$

(3) the fraction of PEP originating from OAA<sub>cyt</sub> (PEP carboxykinase reaction):

$$\gamma = v_9/(v_9+v_{18}) \quad (3)$$

(4) the upper limit for the fraction of PEP generated through PPP:

$$\delta = (5/3)v_3/v_9 \quad (4)$$

Mass balances for the 26 metabolites were constructed according to:

$$Nv + b + R_{mb} = 0, \quad (5)$$

where  $Nv$  is the  $26 \times 27$  (or  $26 \times 28$  for *P. stipitis*) stoichiometric matrix,  $b$  is the  $26 \times 1$  vector of measured fluxes for each metabolite mass balance, and  $R_{mb}$  is the  $26 \times 1$  vector of the residuals of the mass balances (Sauer et al., 1997). The nonlinear programming calculations with the objective to minimize the sum of the squares of the residuals were performed using the four NMR constraints given above. A MATLAB 4.2 program was used for this purpose (Dauner, unpublished). Thus, the 26 individual values of the  $R_{mb}$  vector, which are the 'residual errors' of each metabolic balance with the estimated flux values, were used as the criteria to evaluate the quality of the calculated flux estimations.

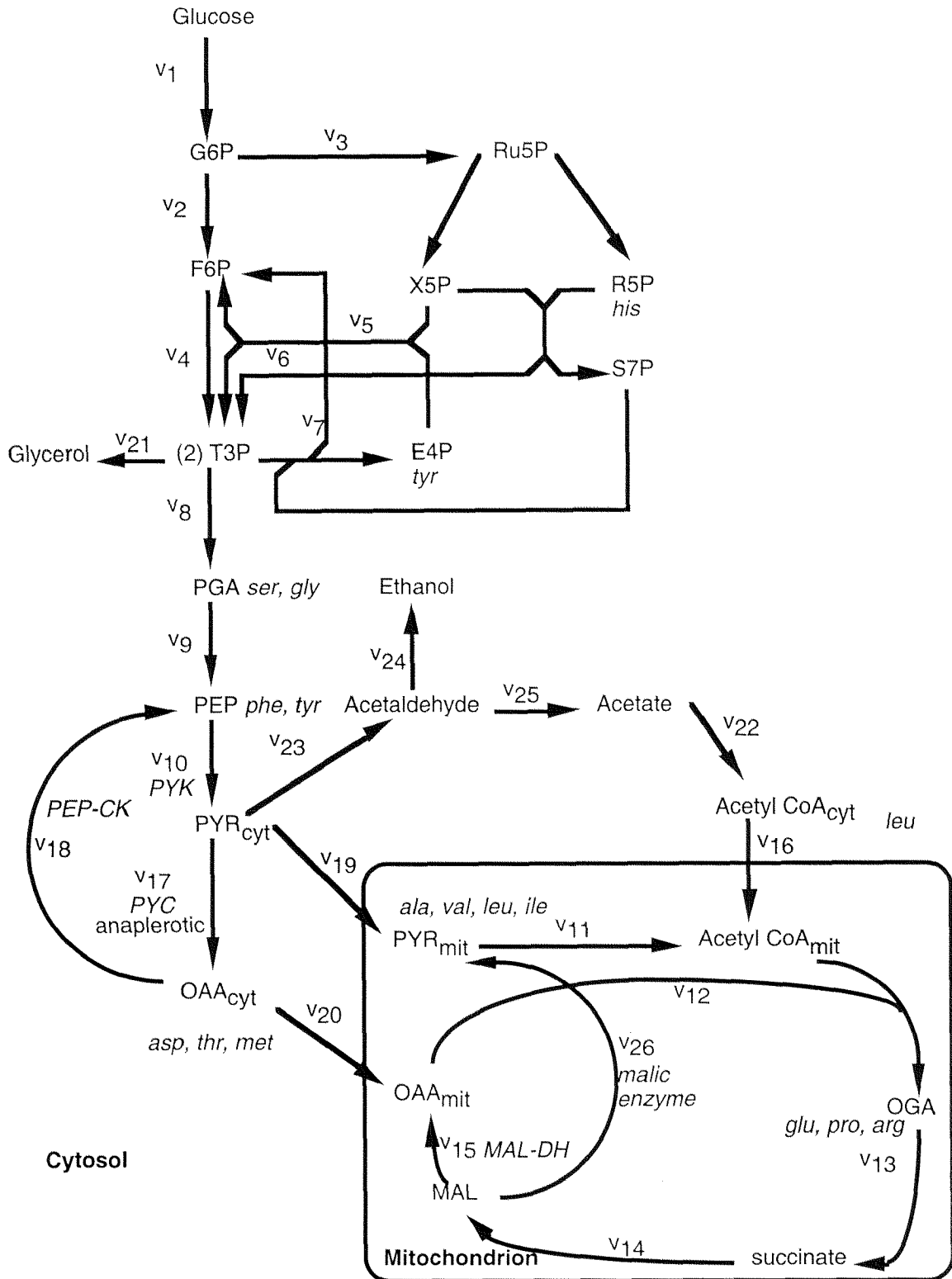


**Figure 1.** Biochemical pathway model for yeast. Abbreviations: G6P, glucose-6-phosphate; F6P, fructose-6-phosphate; Ru5P, ribulose-5-phosphate; X5P, xylulose-5-phosphate; E4P, erythrose-4-phosphate; S7P, seduheptulose-7-phosphate; R5P, ribose-5-phosphate; T3P, triose-3-phosphate; PGA, 3-phosphoglycerate; PEP, phosphoenolpyruvate; MAL, malate; PYR, pyruvate; OAA, oxaloacetate; OGA, oxoglutarate; PYK, pyruvate kinase; PYC, pyruvate carboxylase; PEP-CK, PEP carboxykinase; MAL-DH, malate dehydrogenase; *his*, histidine; *tyr*, tyrosine; *ser*, serine; *gly*, glycine; *phe*, phenylalanine; *leu*, leucine; *ala*, alanine; *val*, valine; *ile*, isoleucine; *asp*, aspartate; *thr*, threonine; *met*, methionine; *glu*, glutamate; *pro*, proline; *arg*, arginine. The subscripts 'cyt' and 'mit' indicate the cytosolic or mitochondrial localization of a given metabolite pool.

## RESULTS

Cells from glucose-limited chemostats were harvested after fractional  $^{13}\text{C}$ -labeling and the common amino acids in their hydrolysates were analysed using two-dimensional ( $^{13}\text{C}$ ,  $^1\text{H}$ )-COSY NMR (Szyperski, 1995). By determining the origin of the eight principal intermediates that are used as building blocks for amino acid biosynthesis, information was obtained on flux ratios through some key pathways of the central carbon metabolism (Table 1).

**Table 1.** METAFoR analysis of three chemostat experiments: *S. cerevisiae* aerobic, *S. cerevisiae* anaerobic, *P. stipitis* aerobic. The mitochondrial and cytosolic oxaloacetate pools equilibrate in the case of the *S. cerevisiae* anaerobic and *P. stipitis* aerobic cultivations.

Metabolites	Fraction of total pool (%)		
	<i>S. cerevisiae</i> , aerobic (D = 0.10 h <sup>-1</sup> )	<i>S. cerevisiae</i> , anaerobic (D = 0.08 h <sup>-1</sup> )	<i>P. stipitis</i> , aerobic (D = 0.10 h <sup>-1</sup> )
<b>Pentose phosphate pathway:</b>			
PEP from pentoses (upper bound)	39±8	6±5	58±11
Intact C5 in Ribose-5-P (lower bound)	41	5	28
<b>Glycolysis and TCA cycle:</b>			
PEP from OAA (PEP carboxykinase reaction)	1±7	not possible to determine	0±3
OAA transported from mitochondria	38±5	see legend	see legend
Glyoxylate shunt	inactive	inactive	inactive
<b>Mitochondria:</b>			
PYR from MAL (upper bound) (malic enzyme reaction)	6±5	not possible to determine	1±6
OAA from PYR (imported from cytosol) (Anaplerotic)	41±4	97±3	37±2
<b>C1-metabolism:</b>			
Serine from glycine + C1 (unknown subcellular localization)	34±2	35±2	26±2
Glycine from CO <sub>2</sub> + C1 (unknown subcellular localization)	5±3	5±2	3±3

The fraction of intact C<sup>(1)</sup>-C<sup>(2)</sup> fragments in the PEP pool that must originate from OAA, yielded an upper limit of 0% to 1% for the aerobic *S. cerevisiae* and *P. stipitis* cultures, for the generation of PEP molecules via PEP carboxykinase (Table 1). In the case of the anaerobic *S. cerevisiae* chemostat, however, it was not possible to determine this fraction. Thus, the aerobic chemostat results confirmed the previous assumption on the absence of

PEP carboxykinase activity during growth on glucose as the sole carbon source. Additionally, an upper limit on the amount of PYR resulting from MAL could be derived from the differences in relative abundance of intact C<sup>(1)</sup>C<sup>(2)</sup> fragments in PEP and PYR. The flux ratio for PYR from MAL was found to be 6% and 1% for aerobic *S. cerevisiae* and *P. stipitis*, respectively. The isotopomeric MAL pool composition was assumed to be identical to the isotopomeric OAA pool composition, which was based on the high exchangeability within the dicarboxylic acid portion of the TCA cycle (Table 1).

Analysis of the acetyl-CoA labeling pattern did not allow for precise localization of the observed pool. Similar multiplet fine structures were observed for acetyl-CoA incorporated in leucine and for the carbon atoms originating from acetyl-CoA in OGA. Acetyl-CoA was assumed to originate exclusively from PYR under the conditions investigated.

Information on the PPP was available from the isotopomer analysis of histidine and the aromatic ring of tyrosine, which correspond to the metabolites R5P and E4P, respectively. Regarding the non-oxidative branch of the PPP, PEP resulting from pentoses had an upper limit of only 39% and 6% in *S. cerevisiae* aerobic and anaerobic cultivations, respectively. In the case of *P. stipitis*, however, this value was 58%.

Among the TCA cycle intermediates, OAA and OGA could be directly observed from the data on the aspartate-threonine-methionine group and the glutamate-proline-arginine group, respectively. Their labeling patterns provided important information on the compartmentalization of the dicarboxylic acid pools as well as on the pathways active under specified conditions. Our previous findings with batch cultures of *S. cerevisiae* and *P. stipitis* revealed that the cytosolic OAA was used for biosynthesis of proteinogenic aspartate, threonine and methionine, and that this pool did not equilibrate with the mitochondrial pool, in which case the action of the TCA cycle would have been observed in the aerobic samples (Fiaux et al., unpublished). This result is consistent with the exclusively cytosolic location of pyruvate carboxylase (Pronk et al., 1996). Although it is known that the amino acids aspartate, threonine, and methionine can be synthesized from oxaloacetate in both mitochondria and cytosol (Jones and Fink, 1982), our data indicated that the amino acids incorporated into cellular proteins originate mainly from the cytosolic pool of OAA. It was also observed that molecules from the cytosolic pool were not converted to the symmetric metabolites succinate and fumarate, by activity of the TCA cycle in mitochondria.

As a TCA cycle intermediate, OGA is expected to be present mainly in the mitochondria. Consistent with this view, it exhibits the characteristic cleavage of the C2-C3 connectivity caused by condensation of OAA and acetyl-CoA. In anaerobiosis, its labeling pattern differs from that of the cytosolic OAA pool, which is affected by the exclusively mitochondrial TCA cycle reactions. Thus, mitochondrial OAA, which is the

precursor for OGA synthesis, must be a separate pool that is different from the cytosolic OAA pool, which does not undergo the exclusively mitochondrial TCA reactions. Consequently, the TCA cycle flux ratios could be derived from the OGA labeling patterns (Table 1). Hence, under aerobic conditions, the anaplerotic reaction of pyruvate carboxylase in the cytosol and OAA transport to the mitochondria accounts for about 41% of the mitochondrial OAA in *S. cerevisiae* and 37% in *P. stipitis*, and the rest is generated via the TCA cycle. During anaerobiosis, however, this value is much higher at about 97%. This is due to the interruption of the TCA cycle under anaerobic conditions, when it operates as a two-branch pathway to meet the biosynthetic demands for OGA and succinate (Zimmermann and Entian, 1997). Therefore, the flux of OGA to succinate and further to OAA should be zero, and mitochondrial and cytosolic OAA pools must be related by a simple transport step only.

### **Estimation of Metabolic Fluxes**

Detailed physiological analysis of the chemostat cultures revealed significant differences between the cultures (Table 2). Most prominently, *S. cerevisiae* produced significantly more ethanol than *P. stipitis* under aerobic conditions, whereas *P. stipitis* consumed less glucose and produced biomass more efficiently. Aerobic *S. cerevisiae* produced also small amounts of PYR and glycerol as by-products. As expected, under anaerobic cultivation conditions, *S. cerevisiae* exhibited the highest specific ethanol and glycerol production rates (Zimmermann and Entian, 1997). Additionally, the formation of other by-products like PYR, acetate and succinate also increased significantly. For flux estimations, precursor metabolite requirements for biomass formation of *S. cerevisiae* and *P. stipitis* were included using the biomass compositions of these yeasts (Tables 3 and 4). Under aerobic growth conditions in a glucose-limited chemostat with a dilution rate of 0.1 h<sup>-1</sup>, the precursor metabolite requirements for *P. stipitis* biomass formation were considered to be the same as those of *S. cerevisiae*.



**Table 2.** Physiology of aerobic and anaerobic *S. cerevisiae*, and aerobic *P. stipitis* in glucose-limited chemostats.

chemostat physiology	Growth parameters		
	<i>S. cerevisiae</i> ,	<i>S. cerevisiae</i> ,	<i>P. stipitis</i> ,
	aerobic	anaerobic	aerobic
	D = 0.10 h <sup>-1</sup>	D = 0.08 h <sup>-1</sup>	D = 0.10 h <sup>-1</sup>
Y <sub>x/s</sub> (g-cdw/g-glucose)	0.38±0.02	0.09±0.00	0.45±0.03
q <sub>gluc</sub> (mmol g <sup>-1</sup> h <sup>-1</sup> )	1.61±0.02	4.78±0.04	1.24±0.01
q <sub>O<sub>2</sub></sub> (mmol g <sup>-1</sup> h <sup>-1</sup> )	3.72±0.02	0±0	2.72±0.01
q <sub>CO<sub>2</sub></sub> (mmol g <sup>-1</sup> h <sup>-1</sup> )	3.27±0.05	6.16±0.18	2.68±0.05
q <sub>E<sub>1</sub>OH</sub> (mmol g <sup>-1</sup> h <sup>-1</sup> )	1.01±0.04	10.49±0.52	0.43±0.01
q <sub>pyr</sub> (mmol g <sup>-1</sup> h <sup>-1</sup> )	2.45x10 <sup>-4</sup> ±2x10 <sup>-6</sup>	1.09x10 <sup>-2</sup> ±2x10 <sup>-4</sup>	0±0
q <sub>gly</sub> (mmol g <sup>-1</sup> h <sup>-1</sup> )	2.66x10 <sup>-3</sup> ±3x10 <sup>-5</sup>	0.74±0.01	6.77x10 <sup>-4</sup> ±1x10 <sup>-5</sup>
q <sub>acet</sub> (mmol g <sup>-1</sup> h <sup>-1</sup> )	0±0	0.16±1x10 <sup>-3</sup>	0±0
q <sub>succ</sub> (mmol g <sup>-1</sup> h <sup>-1</sup> )	0±0	6.96x10 <sup>-2</sup> ±2x10 <sup>-3</sup>	0±0
Biomass concentration (g/L)	1.35±0.0	0.33±0.05	1.61±0.03

Y<sub>x/s</sub> is the biomass yield on glucose. q<sub>gluc</sub> and q<sub>O<sub>2</sub></sub> are specific utilization rates for glucose and O<sub>2</sub>, respectively. q<sub>CO<sub>2</sub></sub>, q<sub>E<sub>1</sub>OH</sub>, q<sub>pyr</sub>, q<sub>gly</sub>, q<sub>acet</sub>, and q<sub>succ</sub> are specific production rates for CO<sub>2</sub>, ethanol, pyruvate, glycerol, acetate and succinate, respectively. The experimental errors represent the standard deviations of three independent measurements for a given chemostat. Carbon balances are closed up to 102%, 97%, and 103% for *S. cerevisiae* aerobic and anaerobic, and *P. stipitis* aerobic cultivations, respectively. The percent error is within 5%.

**Table 3.** Experimentally determined macromolecular composition of *S. cerevisiae* and *P. stipitis* in glucose-limited chemostat cultures.

	Cellular composition (% w/w)		
	<i>S. cerevisiae</i> ,	<i>S. cerevisiae</i> ,	<i>P. stipitis</i> ,
	aerobic	anaerobic	aerobic
Protein	44±3	43±2	44±3
Carbohydrates	40±2	42±3	41±2
RNA	6±1	5±1	5±1
DNA	1±0.5	1±0.5	1±0.5
Lipids	4±0.2	4±0.1	4±0.2
Ash	5±0.2	5±0.2	5±0.2

**Table 4.** Precursor requirements for the formation of 1 g of yeast in aerobic and anaerobic chemostat cultures. Negative sign indicates generation.

Precursor metabolite	Amount required (mmol / g dry weight of cells)	
	<i>S. cerevisiae</i> , aerobic	<i>S. cerevisiae</i> , anaerobic
G6P	0.684	0.636
PGA	0.786	0.730
OAA	1.268	0.972
Ribose-5-P	0.282	0.262
NADPH	10.130	9.410
Pyruvate	2.101	1.953
Erythrose-4-P	0.246	0.228
PEP	0.492	0.457
OGA	0.734	0.551
NADH	-1.897	-1.766
Acetyl-CoA	0.993	0.923
T3P	0.086	0.079

Our NMR data yielded information on relative flux ratios. We used this essential information as constraints for our metabolic flux estimations in combination with classical stoichiometric flux balancing. Data on the PEP carboxykinase reaction and the anaplerotic PYR carboxylase reaction were used as equality constraints (Table 1). These equality constraints constitute additional, independent equations. Additionally, the information on PEP from pentoses and the malic enzyme reaction (Table 1) were used as inequality constraints (reaction bounds) in the least-squares calculations. The NMR-derived constraints provided the missing equations to arrive at fully determined bioreaction networks so that unique solutions of metabolic fluxes could be obtained.

According to these flux calculations, there are significant differences in the fraction of G6P that enters the PPP pathway ( $v_3$ ) (Figures 2, 3, and 4) in the three cultures. Among all cultures, *P. stipitis* had the highest percentage of oxidative PPP flux at about 55%, whereas in aerobic and anaerobic *S. cerevisiae* this flux was only 32% and 7%, respectively. Consistent with the METAFoR data, in anaerobic *S. cerevisiae*, the TCA cycle was found to be a two-branched pathway (Figure 3). Another interesting finding concerns the activity of the malic enzyme. Although no NMR equality constraint was available for the malic enzyme reaction in anaerobic *S. cerevisiae*, this reaction was assumed to be present under anaerobic conditions. However, this reaction was estimated to be zero by the flux analysis program, showing that the malic enzyme was not active under these conditions. Similar results were also obtained with the other two cultivations (Figures 2 and 4). In anaerobic *S. cerevisiae*, we did not consider the gluconeogenic PEP carboxykinase reaction ( $v_{18}$ ) to have a determined system. In our aerobic cultures, for which NMR equality constraints were available on this PEP carboxykinase reaction

(Table 1), the flux was estimated to be 0% and 2% for *P. stipitis* and *S. cerevisiae*, respectively.

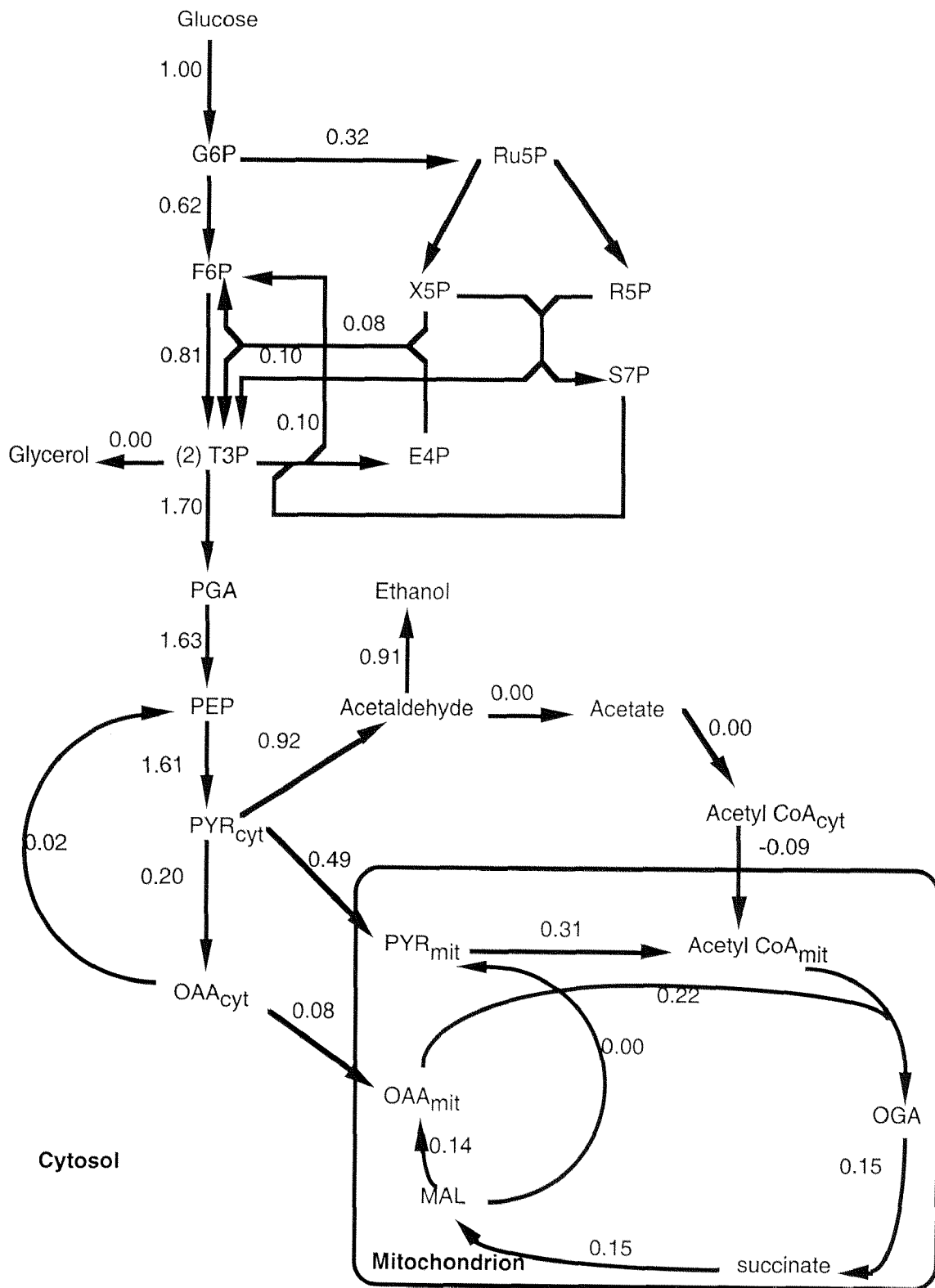


**Figure 2.** Estimated intracellular carbon fluxes of *S. cerevisiae* in aerobic chemostat at a dilution rate of  $0.1 \text{ h}^{-1}$ . The fluxes are normalized to the glucose uptake rate.

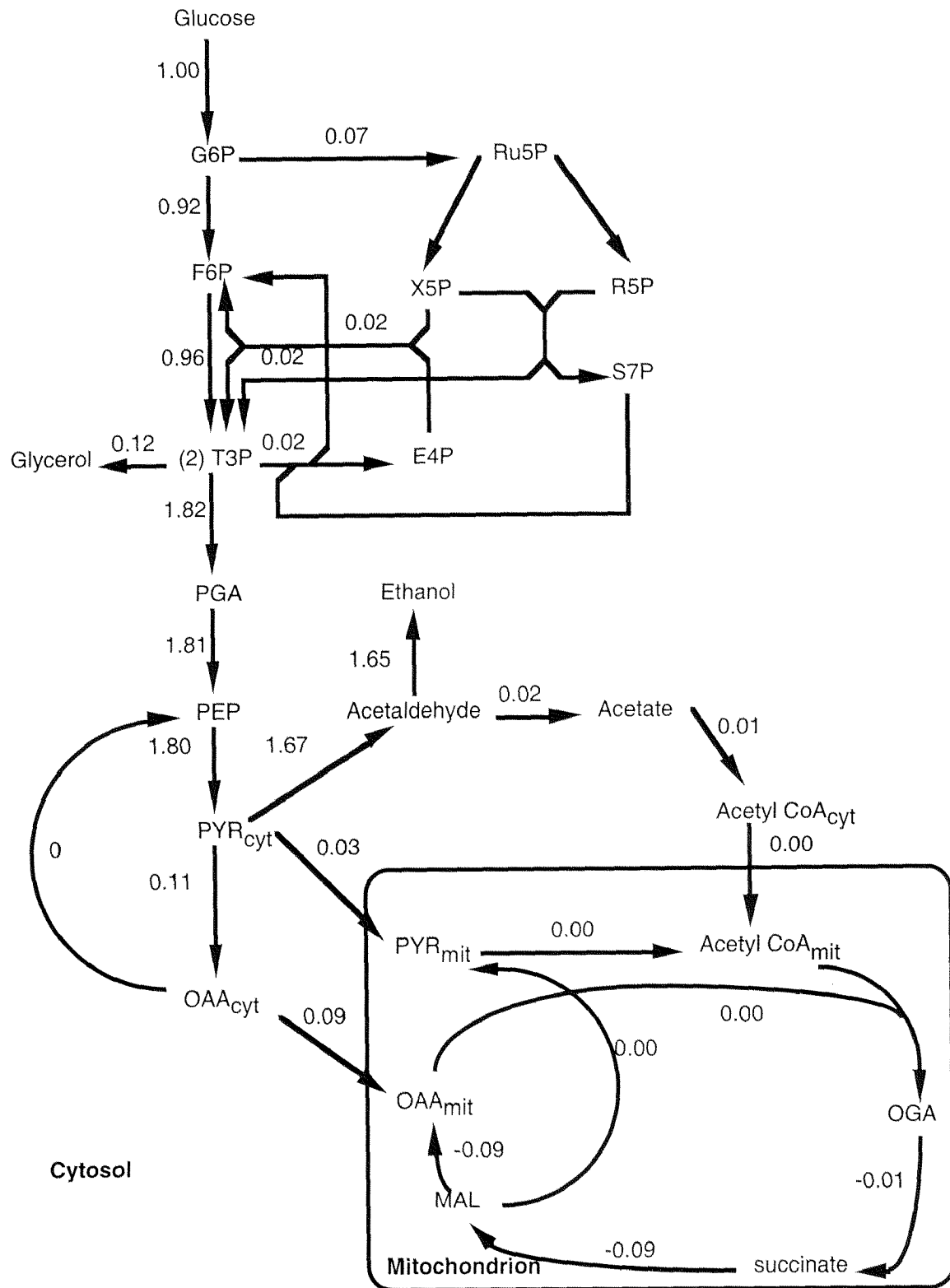


**Figure 3.** Estimated intracellular carbon fluxes of *S. cerevisiae* in anaerobic chemostat at a dilution rate of  $0.08 \text{ h}^{-1}$ . The fluxes are normalized to the glucose uptake rate. Negative signs indicate opposite flux direction.

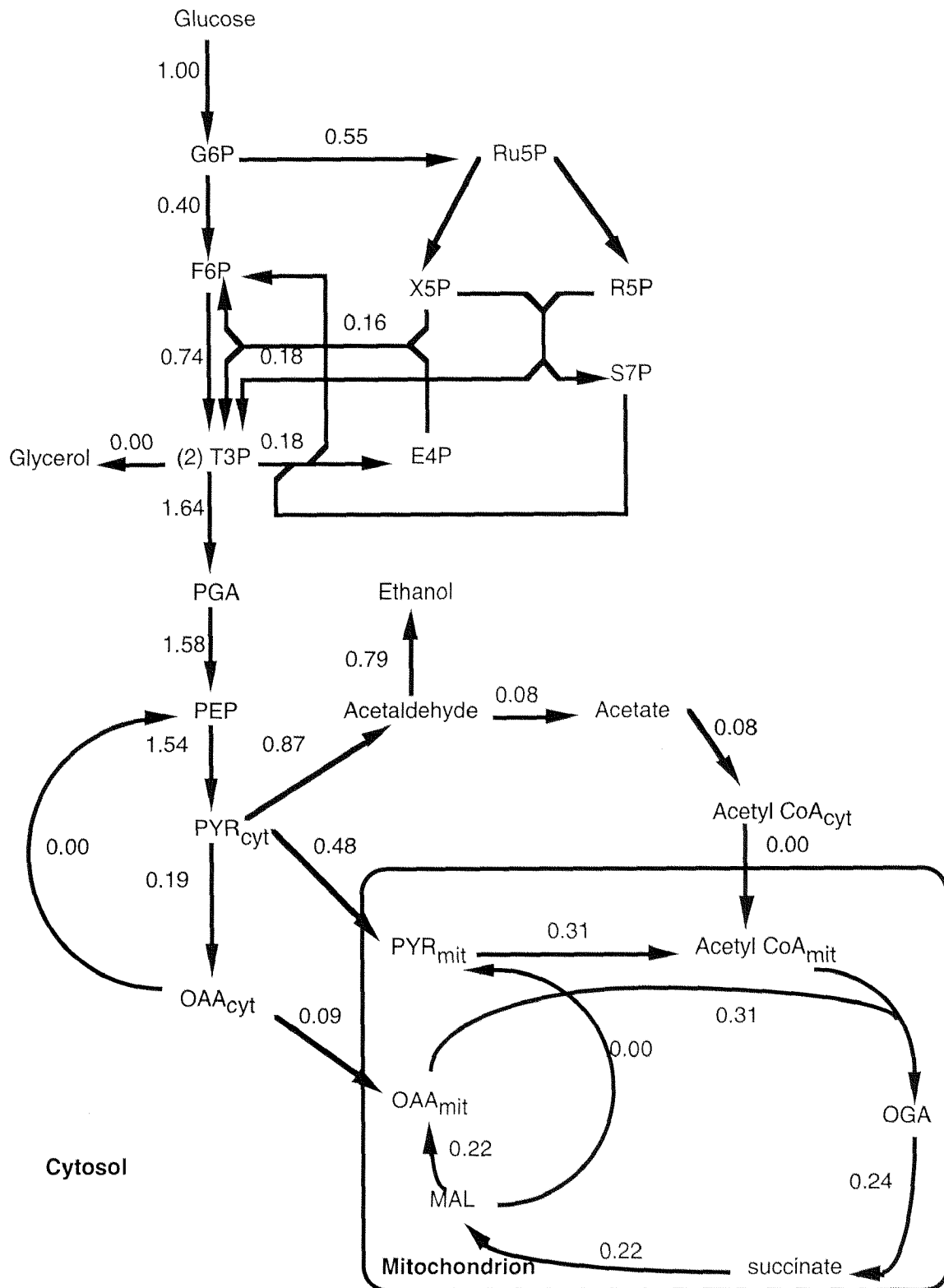


**Figure 4.** Estimated intracellular carbon fluxes of *P. stipitis* in aerobic chemostat at a dilution rate of  $0.1 \text{ h}^{-1}$ . The fluxes are normalized to the glucose uptake rate.

## DISCUSSION

In this study, we have obtained estimates for intracellular carbon flux ratios and net fluxes in *S. cerevisiae* and *P. stipitis* by using METAFoR analysis by NMR alone and in combination with stoichiometric flux balancing. This is the first time such an analysis is applied to eukaryotic cells. Unlike many former yeast flux analysis studies, we had sufficient information that allowed us to include compartmentalization in our flux model to arrive at a more realistic view of yeast metabolism. Moreover, METAFoR analysis allowed us in some cases to distinguish between cytosolic and mitochondrial localization of reactions. Thus, METAFoR analyses provided detailed insights into the carbon flux distribution in *S. cerevisiae* and *P. stipitis* by independent assessment of *in vivo* operating reactions, thus reducing assumptions on absence or presence of reactions.

Our flux estimations for *S. cerevisiae* are generally similar to those reported in the literature. Regarding the main concepts like the interruption of the TCA cycle during anaerobiosis, our anaerobic flux estimations are in agreement with those of the anaerobic flux study considering compartmentalization (Nissen et al., 1997). Similar to their results, we have also obtained fluxes in the reverse direction between the succinate-MAL-OAA part of the TCA cycle, because of the presence of succinate as a by-product in the culture supernatant. Additionally, TCA cycle provided OGA as a biosynthetic requirement (Figure 3).

Most prominently, our flux ratio and net flux analyses revealed significant differences in the pentose phosphate pathway operation between aerobic cultures of *S. cerevisiae* and *P. stipitis*. The upper bound for the amount of PEP molecules originating from pentoses, as obtained by METAFoR analysis, as well as the net flux estimates showed a smaller contribution of the pentose phosphate pathway to glucose catabolism in *S. cerevisiae*, compared to *P. stipitis*.

These major differences are related to the absence of a transhydrogenase reaction in *S. cerevisiae*. Transhydrogenase catalyzes the reversible transfer of a hydride ion equivalent between NAD(H) and NADP(H). One of the functions of this enzyme is to provide NADPH for biosynthesis (Hoek and Rydström, 1988). There have been several studies that investigated the presence or absence of transhydrogenase activity in yeasts. Studies with *Candida utilis* revealed that the steady-state cell yield on glucose increased with increasing amounts of formate in the medium as an additional energy source, until growth became carbon-limited (Bruinenberg et al., 1985). The maximum growth yield on glucose in the presence of excess formate was dependent on the nitrogen source. This difference in maximum growth yield was found to correlate with the NADPH requirement for biomass formation with the two different nitrogen sources used, which suggested that NADH produced from formate oxidation cannot replace the NADPH needed for biomass formation. Thus, it was concluded that *C. utilis* had no transhydrogenase activity. A

similar conclusion, based on radiorespirometric studies, was also drawn for glucose-grown *S. cerevisiae* (Lagunas and Gancedo, 1973). A homology search in *S. cerevisiae* genome database for *E. coli* transhydrogenase genes also supported this view (data not shown). Moreover, it was suggested that one of the consequences of the lack of transhydrogenase activity in yeast may be its inability to ferment xylose (Bruinenberg et al., 1983). Consistently, our flux results provide further evidence for the absence or presence of transhydrogenase activity in *S. cerevisiae* and *P. stipitis*, respectively. This follows from our finding that, when we assumed transhydrogenase activity in *S. cerevisiae* and the absence of this activity in *P. stipitis*, the residual errors of the flux estimations increased significantly (data not shown). These residual errors are crucial criteria to judge the reliability of flux estimates. Thus, any assumption that increases the absolute values of residual errors is likely to be less realistic.

The extensive genomic information on *S. cerevisiae* has also been used for genome-wide analysis of transcripts in aerobic and anaerobic chemostat cultures of *S. cerevisiae* (Ter Linde et al., 1999). In that particular chemostat study, it was found that in glucose-limited chemostat cultures, 93% of the open reading frames (ORFs) were transcribed at a detectable level under aerobic or anaerobic growth conditions, a value much higher than that obtained with batch cultures. This difference was explained as a possible alleviation of glucose catabolite repression under glucose-limited chemostat conditions with very low residual glucose concentration (Ter Linde et al., 1999). This emphasizes the physiological and metabolic differences between batch and chemostat cultivation conditions that we have also seen with our batch and chemostat METAFoR analyses (Fiaux et al., unpublished).

Lignocellulosic biomass is the most-abundant low-cost carbon source. Thus it is suitable as a raw material for biotechnological production of fuel ethanol. The hexose glucose is the most abundant component of lignocellulose. It is followed by xylose, which constitutes 3-23% of the dry weight (Hayn et al., 1993). Although *S. cerevisiae* is a very important host for bioethanol production, it cannot metabolize xylose (Barnett, 1976). Therefore, it is biotechnologically relevant to metabolically engineer xylose utilization in *S. cerevisiae* to produce fuel ethanol from low-cost lignocellulosic biomass. For this reason, the *XYL1* and *XYL2* genes from *P. stipitis*, a naturally xylose utilizing yeast, were cloned into *S. cerevisiae* (Kötter and Ciriacy, 1993). These genes code for the NADPH-dependent xylose reductase (XR) for the reduction of xylose to xylitol; and for the NAD-linked xylitol dehydrogenase for the oxidation of xylitol to xylulose, respectively. However, physiological studies with these recombinant *S. cerevisiae* indicated that xylose conversion to ethanol in *S. cerevisiae* may be limited by cofactor imbalance and/or by an insufficient capacity of xylulose conversion by PPP (Kötter and Ciriacy, 1993). Thus, there seems to be a link between PPP capacity and xylose



utilization. In this respect, the differences we have found between wild-type *S. cerevisiae* and *P. stipitis* during growth on glucose support this view of a limited PPP capacity. The flux analysis methods applied here can, therefore, be further exploited to compare the metabolism of xylose-utilizing recombinant *S. cerevisiae* and wild-type *P. stipitis* during growth on xylose. This can possibly reveal metabolic bottlenecks in recombinant *S. cerevisiae* metabolism for xylose utilization.

#### **ACKNOWLEDGEMENTS**

We would like to thank Bärbel Hahn-Hägerdal for providing the *P. stipitis* strain CBS6054, Jocelyne Fiaux for NMR analysis, and Michael Dauner for the flux analysis program.

## REFERENCES

- Albers, E., Gustafsson, L., Niklasson, C., Liden, G. 1998. Distribution of  $^{14}\text{C}$ -labelled carbon from glucose and glutamate during anaerobic growth of *Saccharomyces cerevisiae*. *Microbiol.* **144**: 1683-1690.
- Barnett, J. A. 1976. The utilization of sugars by yeasts. *Adv. Carbohydr. Chem. Biochem.* **32**: 126-228.
- Benthin, S., Nielsen, J., Villadsen, J. 1991. A simple and reliable method for the determination of cellular RNA content. *Biotechnol. Tech.* **5**: 39-42.
- Bergmeyer, H. U. 1985. *Methods of enzymatic analysis*, vol. IV. VCH Publishers, Deerfield Beach, Fla.
- Boles, E., de Jong-Gubbels, P., Pronk, J. T. 1998. Identification and characterization of *MAE1*, the *Saccharomyces cerevisiae* structural gene encoding mitochondrial malic enzyme. *J. Bacteriol.* **180**: 2875-2882.
- Bruinenberg, P. M., Van Dijken, J. P., Scheffers, A. W. 1983. An enzymic analysis of NADPH production and consumption in *Candida utilis*. *J. Gen. Microbiol.* **129**: 965-971.
- Bruinenberg, P. M., Jonker, R., Van Dijken, J. P., Scheffers, A. W. 1985. Utilization of formate as an additional energy source by glucose-limited chemostat cultures of *Candida utilis* CBS621 and *Saccharomyces cerevisiae* CBS8066. *Arch. Microbiol.* **142**: 302-306.
- Bruinenberg, P. M. 1986. The NADP(H) redox couple in yeast metabolism. *Ant. Leeuwenhoek* **52**: 411-429.
- Cerdan, S., Seelig, J. 1990. NMR studies of metabolism. *Annu. Rev. Biophys. Biophys. Chem.* **19**: 43-67.
- Cortassa, S., Aon, J. C., Aon, M. A. 1995. Fluxes of carbon, phosphorylation, and redox intermediates during growth of *Saccharomyces cerevisiae* on different carbon sources. *Biotechnol. Bioeng.* **47**: 193-208.
- Hayn, M., Steiner, W., Klinger, R., Steinmuller, H., Sinner, M., Esterbauer, H. 1993. Basic research and pilot studies on the enzymatic conversion of lignocellulosics. In: *Bioconversion of forest and agricultural plant residues*, pp. 33-72, (ed.) J. N. Saddler, CAB International, Wallingford, UK.
- Herbert, D., Phipps, P. J., Strange, R. E. 1971. Chemical analysis of microbial cells. *Methods Microbiol.* **5B**: 209-344.
- Hoek, J. B., Rydström, J. 1988. Physiological roles of nicotinamide nucleotide transhydrogenase. *Biochem. J.* **254**: 1-10.
- Jones, E. W., Fink, G. R. 1982. Regulation of amino acid and nucleotide biosynthesis. In: *The molecular biology of the yeast Saccharomyces, metabolism and gene*

- expression', eds. Strathern, J. N., Jones, E. W., Broach, J. R., Cold Spring Harbor Press, New York (vol 2, pp. 181-299).
- Kötter, P., Ciriacy, M. 1993. Xylose fermentation by *Saccharomyces cerevisiae*. Appl. Microbiol. Biotechnol. **38**: 776-783.
- Lagunas, R., Gancedo, J. M. 1973. Reduced pyridine-nucleotides balance in glucose-growing *Saccharomyces cerevisiae*. Eur. J. Biochem. **37**: 90-94.
- Larsson, C., Pahlmann, I.-L., Ansell, R., Rigoulet, M., Adler, L., Gustafsson, L. 1998. The importance of the glycerol 3-phosphate shuttle during aerobic growth of *Saccharomyces cerevisiae*. Yeast **14**: 347-357.
- Malloy, C. R., Sherry, A. D., Jeffrey, F. M. H. 1990. Analysis of tricarboxylic acid cycle of the heart using  $^{13}\text{C}$  isotope isomers. Am. J. Physiol. **259**: H987-H995.
- Nissen, T. L., Schulze, U., Nielsen, J., Villadsen, J. 1997. Flux distributions in anaerobic, glucose-limited continuous cultures of *Saccharomyces cerevisiae*. Microbiol. **143**: 203-218.
- Pronk, J. T., Steensma, H. J., Van Dijken, J. 1996. Pyruvate metabolism in *Saccharomyces cerevisiae*. Yeast **12**: 1607-1633.
- Roon, R. J., Levy, J. S., Larimore, F. 1977. Negative interactions between amino acid and methylamine/ammonia transport systems of *Saccharomyces cerevisiae*. J. Biol. Chem. **252**: 3599-3604.
- Sauer, U., Hatzimanikatis, V., Hohmann, H.-P., Manneberg, M., van Loon, A. P. G. M., Bailey, J. E. 1996. Physiology and metabolic fluxes of wild-type and riboflavin-producing *Bacillus subtilis*. Appl. Env. Microbiol. **62**: 3687-3696.
- Sauer, U., Hatzimanikatis, V., Bailey, J. E., Hochuli, M., Szyperski, T., Wüthrich, K. 1997. Metabolic fluxes in riboflavin-producing *Bacillus subtilis*. Nat. Biotechnol. **15**: 448-452.
- Szyperski, T. 1995. Biosynthetically directed fractional  $^{13}\text{C}$ -labeling of proteinogenic amino acids. An efficient analytical tool to investigate intermediary metabolism. Eur. J. Biochem. **232**: 433-448.
- Szyperski, T., Bailey, J. E., Wüthrich, K. 1996. Detecting and dissecting metabolic fluxes using biosynthetic fractional  $^{13}\text{C}$ -labeling and two-dimensional NMR spectroscopy. Trends Biotechnol. **14**: 453-459.
- Ter Linde, J. J. M., Liang, H., Davis, R. W., Steensma, H. Y., Van Dijken, J. P., Pronk, J. T. 1999. Genome-wide transcriptional analysis of aerobic and anaerobic chemostat cultures of *Saccharomyces cerevisiae*. J. Bacteriol. **181**: 7409-7413.
- Tran-Dinh, S., Bouet, F., Huynh, Q.-I., Herve, M. 1996. Mathematical models for determining metabolic fluxes through the citric acid and the glyoxylate cycles in *Saccharomyces cerevisiae* by  $^{13}\text{C}$ -NMR spectroscopy. Eur. J. Biochem. **242**: 770-778.

- Vallino, J. J., Stephanopoulos, G. 1990. Flux determinations in cellular bioreaction networks: application to lysine fermentations. In: *Frontiers in Bioprocessing* (eds. S. K. Sikdar, M. Bier, P. Todd), pp. 205-219, CRC Press, Boca Raton.
- van Gulik, W. M., Heijnen, J. J. 1995. A metabolic network stoichiometry analysis of microbial growth and product formation. *Biotechnol. Bioeng.* **48**: 681-698.
- Vanrolleghem, P. A., de Jong-Gubbels, P., van Gulik, W. M., Pronk, J. T., van Dijken, J. P., Heijnen, S. 1996. Validation of a metabolic network for *Saccharomyces cerevisiae* using mixed substrate studies. *Biotechnol. Prog.* **12**: 434-448.
- Varma, A., Palsson, B. O. 1994. Metabolic flux balancing: basic concepts, scientific, and practical use. *Bio/Technol.* **12**: 994-998.
- Verduyn, C., Postma, E., Scheffers, W. A., van Dijken, J. P. 1992. Effect of benzoic acid on metabolic fluxes in yeasts: a continuous culture study on the regulation of respiration and alcoholic fermentation. *Yeast* **8**: 501-517.
- Zimmermann, F. K., Entian, K.-D. (eds.) 1997. *Yeast Sugar Metabolism*. Technomic Publishing Co., Inc. Basel.

**Chapter 4**

**Metabolic Engineering of Yeast:  
the Perils of Auxotrophic Hosts**

**Z. Petek Çakar, Uwe Sauer, and James E. Bailey**

published in *Biotechnol. Lett.* 1999, **21**: 611-616.

**SUMMARY**

Auxotrophic mutants may have physiological alterations and sensitivities which are not generally recognized. Such features are shown here by observations that final cell densities attained by several leucine-auxotrophic *Saccharomyces cerevisiae* strains depend differently on the initial leucine concentration in the medium. Furthermore, complementing such auxotrophic strains with the plasmid-based *LEU2* selection marker resulted in different final cell densities than chromosomal expression of *LEU2* in the otherwise isogenic, prototrophic strains. These results warn that auxotrophic host-related physiological influences overlay any metabolic effect of a cloned gene expressed in such a host, clearly complicating interpretation of the effect of that gene's product in scientific or metabolic engineering research.

## INTRODUCTION

In metabolic engineering (Bailey, 1991), auxotrophic host systems are often used to ensure maintenance of plasmids with selectable markers. A typical example is the yeast *Saccharomyces cerevisiae*, an important host for many traditional biotechnological applications and heterologous protein production (Buckholz and Gleeson, 1991). In this organism, the most common dominant selection markers are *URA3*, *LEU2*, *TRP1*, or *HIS3*. They are used in auxotrophic yeast strains that are unable to synthesize uracil, leucine, tryptophan, or histidine, respectively, and selection is achieved by cultivation in minimal media without the relevant nutrient. Such auxotrophic hosts are not only employed for genetic experiments, but also for heterologous protein production (Kuriyama et al., 1992; Shu and Yang, 1996).

There are several problems associated with the use of such auxotrophic strains. First, auxotrophic strains that are grown in a nutrient-supplemented medium are not necessarily physiologically equivalent to the complemented transformants (Pronk et al., 1996). Second, it is a priori not clear how much of the substrate for which the organism is auxotrophic must be added to the growth medium, and there is a high degree of variation in concentrations given in prior publications. Recently, for example, media optimization studies revealed that the optimal L-leucine concentration in defined yeast media for cultivation of L-leucine *S. cerevisiae* auxotrophs must be 100 mg/L (Adams et al., 1998), more than 3-fold of the concentration that was previously recommended (30 mg/L) in the standard yeast methods handbook (Rose et al., 1990). When one or more of such substrates are supplemented insufficiently, dramatic changes in physiology and growth behavior of a strain can be expected. Third, under auxotrophic substrate-limiting conditions there is a strong selection pressure for revertants. If not recognized, such effects may be misleading when the physiology of engineered and control strains is compared.

In this paper we present systematic experiments designed to expose generally unrecognized physiological sensitivities in auxotrophic yeast strains, with a focus on yeast expression systems used in the context of metabolic engineering studies. For this purpose, leucine demands and growth physiology of various *S. cerevisiae* hosts were studied, including the well-defined CEN.PK strains which were found to be the best academic model for industrial yeast strains (Brown, 1997).

## MATERIALS AND METHODS

### Strains and Plasmids

The following *S. cerevisiae* strains were used in this study: CBS7752 (*MATa, ura3-52, leu2-3/112, trp1*), Centraalbureau voor Schimmelcultures (Delft, the Netherlands); W303-1A (*MATa, ade2-1, ura3-1, his3-11/15, can1-100, leu2-3/112, trp1-1*), Prof. F. Thoma (Institute of Cell Biology, ETH Zürich, Switzerland); INVSC1 (*MAT $\alpha$ , ura3-52, his3- $\Delta$ 1, leu2-3/112, trp1-289*), Invitrogen BV (Leek, the Netherlands); and the CEN.PK strains 102-5B (*MATa, ura3-52, his3- $\Delta$ 1, leu2-3/112, TRP1, MAL2-8<sup>c</sup>, SUC2*), 113-6B (*MATa, ura3-52, HIS3, leu2-3/112, trp1-289, MAL2-8<sup>c</sup>, SUC2*), 113-11C (*MATa, ura3-52, his3- $\Delta$ 1, LEU2, TRP1, MAL2-8<sup>c</sup>, SUC2*), and 113-14A (*MATa, ura3-52, HIS3, LEU2, trp1-289, MAL2-8<sup>c</sup>, SUC2*), Dr. P. Kötter (Institute of Microbiology, Johann Wolfgang Goethe-University, Frankfurt, Germany). The constitutive yeast expression vectors pAAH5 (Ammerer, 1983) and YEP24 (Botstein et al., 1979) were kindly provided by Prof. T. Wallimann (Institute of Cell Biology, ETH Zürich, Switzerland).

### Transformations

The strains CBS7752 and W303-1A were transformed by electroporation as described previously (Becker and Guarante, 1990). INVSC1 and CEN.PK strains were transformed by using the *S. cerevisiae* EasyComp™ transformation kit (Invitrogen BV). Transformants were selected by means of the LEU or URA markers on the plasmids pAAH5 or YEP24, respectively.

### Growth Media and Culture Conditions

For cultivations prior to transformation, YPD-medium (10 g yeast extract/L, 20 g peptone/L, and 20 g dextrose/L) was used. Yeast minimal medium (YMM), containing 6.7 g yeast nitrogen base without amino acids (Difco)/L and glucose (2.0% w/v) as the carbon source was used in physiological analyses. Filter-sterilized adenine sulfate, histidine, tryptophan and uracil were added where appropriate to give 20 mg/L each. Leucine was varied between 80-300 mg/L. Cells were grown until stationary phase using a rotary shaker at 30°C and 200 rpm, in 500 mL baffled shake flasks containing 100 mL medium. Achievement of stationary phase was verified by at least three consecutive OD<sub>600</sub> readings.

### Analytical Methods

Growth was monitored spectrophotometrically by measuring the optical density of cultures at 600 nm (OD<sub>600</sub>) (1 OD<sub>600</sub>  $\approx$  0.5 g cellular dry weight (cdw)/L). For determination of cellular dry weight (cdw), Eppendorf tubes were dried at 80°C for 48 h, cooled in a desiccator for 30 min and weighed. Two mL aliquots of culture broth were centrifuged in these Eppendorf tubes at 15,800 g for 10 min in a benchtop centrifuge. The resulting cell pellets were washed twice with 2 mL deionized water and dried at 80°C for 24 h. They were then placed in a desiccator for 30 min and weighed afterwards. The total



cell number was determined by counting the yeast cells in 13  $\mu\text{L}$  of diluted (1:10) samples by using an improved Neubauer haemocytometer. The cells were counted at 400x magnification using a light microscope (Olympus BH-2, Japan).

## RESULTS

### Leucine Requirements of Auxotrophic *S. cerevisiae* CEN.PK Strains

Initially, we determined the leucine requirements for auxotrophic strains of the industrial *S. cerevisiae* model strain CEN.PK (Brown, 1997). In particular, dependence of final cell density was determined as a function of initial leucine concentration. For this purpose, auxotrophic CEN.PK 102-5B and 113-6B strains were grown in batch cultures initiated with various leucine concentrations.

The results reveal that the leucine concentration required for optimum growth of auxotrophic CEN.PK strains was much higher than the values suggested in the literature for yeast growth (Figure 1, Table 1). For both strains, increasing leucine concentrations up to around 240 mg/L had a positive effect on the final cell density. For all strains investigated, the final cell density was determined by means of cellular dry weight (cdw), microscopic cell counting (data not shown), and optical density (OD<sub>600</sub>) measurements (data not shown), all of which were consistent. Variations in the initial leucine concentration did not affect the specific glucose uptake rates of these cultures. Extracellular pH is probably not a relevant factor, because cultures with a higher final cell density had even lower final pH values (approximately 0.5 pH units) than those with a lower final cell density (data not shown). These cell density effects are most likely related to the leucine requirements and not to the potential use of leucine as a nitrogen source, since leucine is poorly utilized during nitrogen starvation and known to play a minor role in nitrogen metabolism (Watson, 1976). Additionally, it should be noted that in all the cases the cultures were not limited by nitrogen supply.

### Leucine Requirements of Other *S. cerevisiae* Strains

The *S. cerevisiae* strain INVSC1 reached final cell densities essentially identical to those attained by CEN.PK (Table 1). Similar responses with respect to leucine supplementation were also observed with two other commonly used strains, CBS7752 and W303-1A, the latter of which is the haploid form of the genomic functional analysis strain W303 (Rieger et al., 1997).

For optimal growth, W303-1A has a leucine requirement higher than 80 mg/L, which is also supported by a color change observation. The *ade1* and *ade2* mutants of *S. cerevisiae*, such as W303-1A, produce a red pigment upon induction of their defective adenine biosynthetic pathway, which happens normally when the cells exceed a certain cell density. The lack of color change from white to pink in the case of W303-1A grown with 80 mg leucine/L is caused by its growth at sub-optimal leucine levels, which results in a delay or absence of pigment production, as was described previously for amino acid auxotrophs carrying mutations in *ade1* or *ade2* (Pearson et al., 1986). Light absorption of this pink pigment did not have a significant effect on OD<sub>600</sub> determinations.

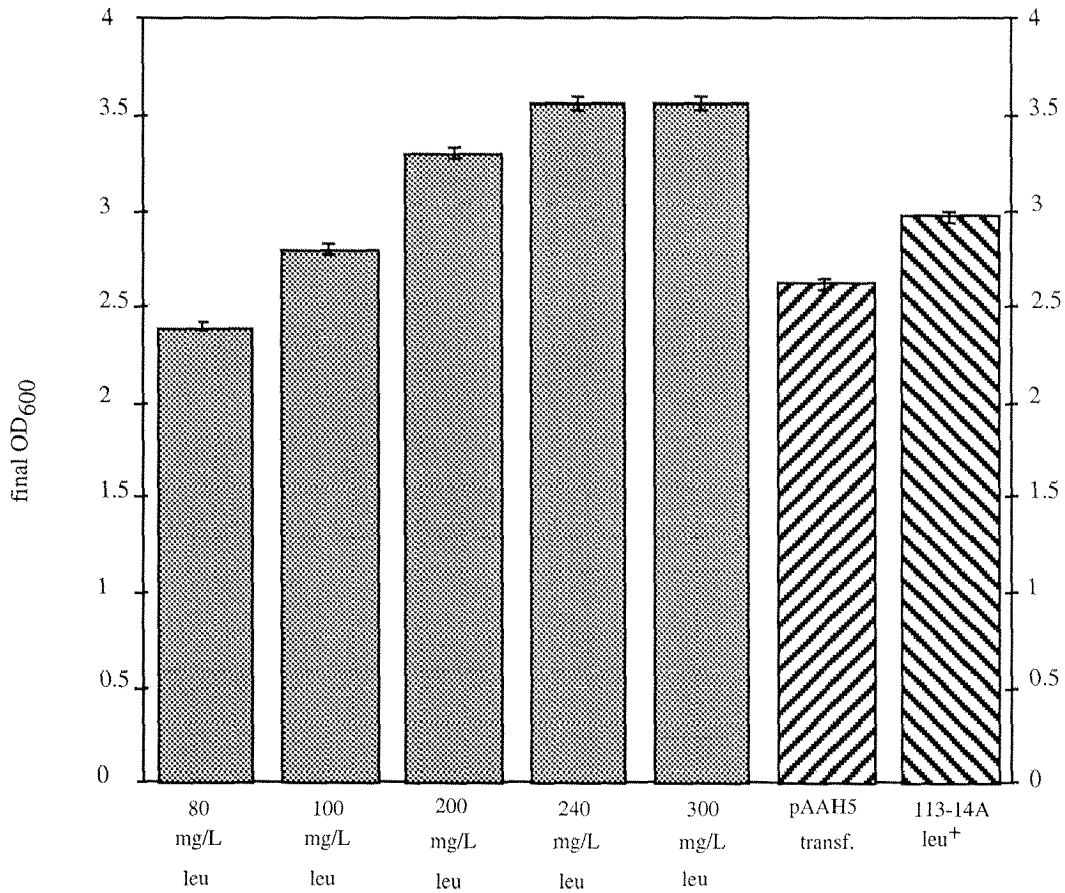


**Figure 1.** Comparison of final cell densities (OD<sub>600</sub>) of *S. cerevisiae* CEN.PK 113-6B, its pAAH5-transformant, and the isogenic leucine-prototrophic CEN.PK 113-14A grown in minimal medium with 2% glucose. For CEN.PK 113-6B, leucine concentration in the medium was varied between 80 and 300 mg/L. No leucine was supplied for the transformant and the leucine-prototroph.

**Table 1.** Final cellular dry weight (g/L) of *S. cerevisiae* strains grown in minimal medium with 2% glucose and various leucine concentrations. The values given are the mean values of three independent measurements.

Strains	No leucine	80 mg leucine/L	240 mg leucine/L	300 mg leucine/L
CEN.PK 102.5B	-	1.07±0.05	-	1.60±0.07
CEN.PK 102.5B+ pAAH5	1.25±0.05	-	-	-
CEN.PK 113.11C <sup>a</sup>	1.55±0.08	-	-	-
CEN.PK 113.6B	-	1.15±0.05	-	1.75±0.07
CEN.PK 113.6B+ pAAH5	1.37±0.05	-	-	-
CEN.PK 113.14A <sup>b</sup>	1.50±0.06	-	-	-
INVSCI	-	1.06±0.05	-	1.62±0.07
INVSCI+pAAH5	1.15±0.05	-	-	-
W303-1A	-	1.27±0.06	1.72±0.09	-
W303-1A+pAAH5	1.81±0.10	-	-	-
CBS7752	-	0.94±0.05	1.05±0.08	-
CBS7752+pAAH5	0.44±0.04	-	-	-
CBS7752* <sup>c</sup>	-	0.83±0.04	1.08±0.06	-
CBS7752*+pAAH5	1.12±0.06	-	-	-

<sup>a</sup>Isogenic to CEN.PK 102-5B except for the leucine prototrophy.

<sup>b</sup>Isogenic to CEN.PK 113-6B except for the leucine prototrophy.

<sup>c</sup>A tryptophan-revertant mutant strain obtained from CBS7752.

### Plasmid-based Leucine Complementation

To investigate the physiological effects of plasmid-based leucine complementation on the hosts mentioned above, their transformants with LEU marker-carrying plasmids were grown in leucine-free media. In the case of CEN.PK strains, the corresponding isogenic leucine-prototrophic strains were also investigated under the same growth conditions as those of the transformants. The final cell densities of the isogenic leucine-prototrophic CEN.PK strains cultivated in minimal medium without leucine supplementation were in the range of those of the auxotrophs grown in minimal medium with about 150 mg leucine/L (Figure 1, Table 1). These results clearly indicate that leucine concentrations for auxotrophic CEN.PK strains should be at least 150 mg/L to make them comparable, with respect to final cell density, to their isogenic leucine-prototrophs grown without leucine supplementation. When grown in minimal medium without leucine supplementation, pAAH5-transformants exhibited lower final cell densities than the prototrophic strains. Growing these pAAH5-transformants in the presence of 80-240 mg leucine/L had no

discernible influence on the final cell densities (data not shown). Therefore, it appears that metabolic perturbations of plasmid maintenance overlay leucine requirement, and, for that matter, probably also other metabolic effects of cloned gene expression.

Surprisingly, the final cell density of W303-1A's pAAH5-transformant was comparable to that of the host grown with the highest leucine supplementation (Figure 2, Table 1). Similar to the transformants of CEN.PK strains, growth of the transformant of W303-1A in the presence of leucine did not further increase its final cell density (data not shown). However, the pAAH5-transformant of CBS7752 grew only to extremely low densities, less than half the value reached by the host supplied with 80 mg leucine/L (Figure 2, Table 1). The presence of 300 mg leucine/L in the medium increased the final cell density of this transformant more than two-fold (data not shown), which indicates an intracellular limitation of leucine in the transformants.

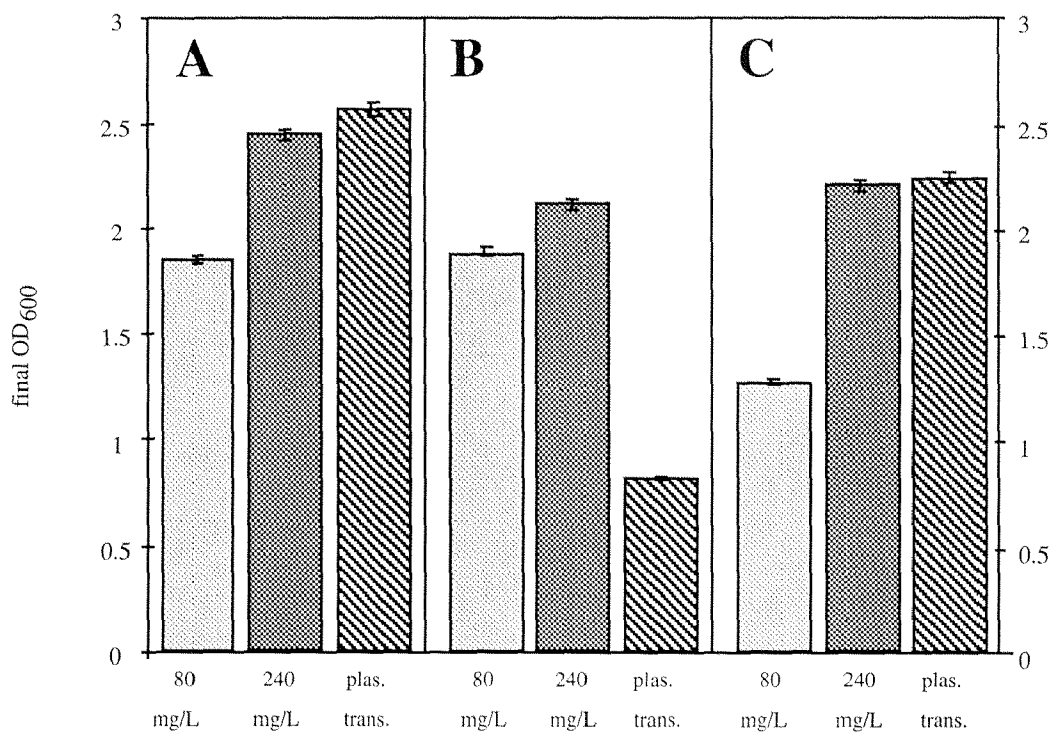


**Figure 2.** Comparison of final cell densities ( $OD_{600}$ ) of wild-type *S. cerevisiae* W303-1A (A), CBS7752 (B), and CBS7752\* (tryptophan revertant) (C) with those of their corresponding pAAH5-transformants grown in minimal medium with 2% glucose. The leucine concentration in the medium was either 80 or 240 mg/L, and no leucine was supplied for the transformants. CBS7752\* was grown without tryptophan supplementation.

**Auxotrophic Reversion Interferes with a Seemingly Unrelated Auxotrophy**

At least one auxotrophy of *S. cerevisiae* CBS7752 has an unexpectedly high frequency of reversion with strong pleiotropic effects. We encountered this problem recently when CBS7752 was co-transformed with the plasmids pAAH5 and YEP24. Transformants were grown in yeast minimal medium containing 20 mg tryptophan/L, and, after about 100 generations, a tryptophan revertant was predominant. Plasmid curing studies showed that the 'new' host was auxotrophic for uracil and leucine only and was denoted CBS7752\*. As a result of this reversion, cell physiology and response to plasmid transformation were affected. Both CBS7752 and CBS7752\* showed a similar behavior with respect to leucine supplementation, while the presence or absence of 20 mg tryptophan/L did not change the response of CBS7752\*, illustrating that the change is permanent and no longer tryptophan-dependent. Unexpectedly, CBS7752\* was always found to reach lower final cell densities than CBS7752 at 80 mg leucine/L supplementation. The pAAH5-transformants of CBS7752\* grew to much higher final cell densities than the pAAH5-transformants of CBS7752 (Figure 2, Table 1). In contrast to the transformants of CBS7752, the presence of leucine in the medium did not further increase the final cell density of the transformants of CBS7752\* (data not shown). Thus, it remains unclear whether growth of transformants of CBS7752 is limited by leucine, tryptophan or another yet unidentified component. These results indicate that seemingly unrelated mutations in auxotrophic markers can augment the effects of limiting supply of leucine and possibly other amino acids. Such mutations add a further difficulty to the interpretation of the results obtained with auxotrophic hosts, in particular those with multiple auxotrophies.

## DISCUSSION

Physiological perturbations of enzyme overexpression or high-copy-number plasmid burden are generally recognized (Bailey, 1993). Here we clearly show previously neglected physiological sensitivities arising in auxotrophic yeasts and in these strains with complementing vectors. Therefore, metabolic changes which occur when cloned genes are expressed in such host-vector systems may well arise from peculiarities of the auxotrophic host rather than from activity of the cloned proteins. Exogeneous supplementation of leucine has a strong influence on the final cell density of all strains investigated. Expression of a plasmid-based leucine marker gene has more heterogeneous effects in a highly strain-specific fashion and may lead to final cell densities similar to those obtained with the highest leucine supplementation of auxotrophs or much lower values. The decrease can in some cases, but not in all, be partly cured by exogeneous addition of leucine.

The problems of using auxotrophic host strains in physiological research are not confined to yeast. Amino acid limitations were also observed at higher growth rates in glucose-limited chemostat cultures of a methionine-auxotrophic *Bacillus subtilis* 1012 strain (Saito et al., 1979), supplemented with 50 mg methionine/L. At dilution rates higher than  $0.15 \text{ h}^{-1}$ , the methionine-auxotrophic strain started to secrete substantial amounts of acetate and the cell density dropped significantly (Sauer, unpublished). The prototrophic wild-type strain and a riboflavin-producer, on the other hand, never excreted acetate below a dilution rate of  $0.7 \text{ h}^{-1}$ , and their cell density increased steadily up to a dilution rate of  $0.5 \text{ h}^{-1}$  (Sauer et al., 1996). Thus, the auxotrophic strain was apparently limited by methionine, although the methionine supplementation provided was more than two to three times the theoretical requirement for *B. subtilis* biomass.

Similar observations were made with auxotrophic *Escherichia coli* strains that are frequently used in metabolic engineering and physiological research, such as HB101 ( $\Delta(gpt-proA)62, leu$ ) and C600 (*thi-1, thr-1, leuB6*) (Boyer and Roulland-Dussoix, 1969; Appleyard, 1954). Although compensating compounds were added to the feed stocks, such strains are known to reach only medium cell densities in fed-batch cultivations with minimal media (Riesenber, 1991), supporting the view expressed here that the phenotype of supplemented auxotrophs often does not compare well with those of their prototrophic counterparts. Without rationalization, these factors are avoided in industrial bioprocesses, where it is common practice to use prototrophic *E. coli* strains.

Amino acid auxotrophies are of particular importance in amino acid-producing *Corynebacterium glutamicum*, because they are often used as growth-limiting nutrients in fed-batch processes, or they interfere with the biosynthetic regulation of the produced amino acid. Media optimization studies with the well-characterized leucine-auxotrophic *C. glutamicum* MH20-22B revealed that for optimal lysine production, the initial leucine

concentration should be 315 mg/L in the first inoculum, but 1300 mg/L in the fed-batch process, which reflects the dependence on cultivation conditions (Weuster-Botz et al., 1997). However, another leucine-auxotrophic *C. glutamicum* strain has its highest specific lysine production rate at low leucine concentrations that were achieved by pulsewise supplementation (Takiguchi et al., 1997).

To avoid artifacts in metabolic engineering studies, we strongly recommend avoiding auxotrophic host systems. The use of regulated promoters, which allow the protein introduced to effect metabolic engineering to be turned on or off, minimizes artifacts which may arise when using different genotypes to study the physiological effects of this protein. However, even in this situation, changes in cultivation conditions required for regulation of cloned gene expression may themselves have nontrivial consequences (see, for example, Kosinski et al., 1992; Prati et al., 1999), reiterating the importance of careful control experiments.

#### **ACKNOWLEDGEMENTS**

We thank Daniel E. Gottschling for advice on leucine requirements in supplemented yeast minimal media, and Bärbel Hahn-Hägerdal, Johan Thevelein, Theo Wallimann, Uwe Schlattner, and Martin Stolz for discussions of various aspects of this work.

This work was supported by the Swiss Bundesamt für Bildung und Wissenschaft (BBW) within the Framework IV Biotechnology Programme of the European Commission.



## REFERENCES

- Adams, A., Gottschling, D. E., Kaiser, C. A., Stearns, T. 1998. Methods in yeast genetics: a Cold Spring Harbor Laboratory course manual, 1997 edition, Cold Spring Harbor Laboratory Press, New York.
- Ammerer, G. 1983. Expression of genes in yeast using the *ADCI* promoter. Meth. Enzymol. **101**: 192-211.
- Appleyard, R. K. 1954. Segregation of new lysogenic types during growth of a doubly lysogenic strain derived from *Escherichia coli* K12. Genetics **39**: 440-452.
- Bailey, J. E. 1991. Toward a science of metabolic engineering. Science **252**: 1668-1675.
- Bailey, J. E. 1993. Host-vector interactions in *Escherichia coli*. Adv. Biochem. Eng. Biotechnol. **48**: 29-52.
- Becker, D. M., Guarante, L. 1990. High efficiency transformation of yeast by electroporation. Meth. Enzymol. **194**: 182.
- Botstein, D., Falco, S. C., Stewart, S. E., Breenan, M., Scherer, S., Stinchcomb, D. T., Struhl, K., Davis, R. W. 1979. Sterile host yeasts (shy): a eukaryotic system of biological containment for recombinant DNA experiments. Gene **8**: 17-24.
- Boyer, H. W., Roulland-Dussoix, D. 1969. A complementation analysis of the restriction and modification of DNA in *Escherichia coli*. J. Mol. Biol. **41**: 459-472.
- Brown, A. J. P. 1997. Control of metabolic flux in yeasts and fungi. Trends Biotechnol. **15**: 445-447.
- Buckholz, R. G., Gleeson, M. A. G. 1991. Yeast systems for the commercial production of heterologous proteins. Bio/Technol. **9**: 1067-1071.
- Kosinski, M. J., Rinas, U., Bailey, J. E. 1992. Isopropyl- $\beta$ -D-thiogalactopyranoside influences the metabolism of *Escherichia coli*. Appl. Microbiol. Biotechnol. **36**: 782-784.
- Kuriyama, M., Morita, S., Asakawa, N., Nakatsu, M., Kitano, K. 1992. Stabilization of a recombinant plasmid in yeast. J. Ferment. Bioeng. **74**: 139-144.
- Pearson, B. M., Fuller, L. J., Mackenzie, D. A., Keenan, M. H. J. 1986. A red/white selection for *Saccharomyces cerevisiae* auxotrophs. Lett. Appl. Microbiol. **3**: 89-91.
- Prati, E. G. P., Sutter, T. B., Matasci, M., Dinter, A., Sburlati, A. R., Bailey, J. E. 1999. Partial cloning and inducible inhibition of Gal $\beta$ 1,3GalNAc $\alpha$ 2,3-sialyltransferase in chinese hamster ovary (CHO) cells. Biotechnol. Bioeng. (in press).
- Pronk, J. T., Steensma, H. Y., Van Dijken, J. P. 1996. Pyruvate metabolism in *Saccharomyces cerevisiae*. Yeast **12**: 1607-1633.
- Rieger, K.-J., Kaniak, A., Coppée, J.-Y., Aljinovic, G., Baudin-Baillieu, A., Orłowska, G., Gromadka, R., Groudinsky, O., Di Rago, J.-P., Slonimski, P. P. 1997. Large-scale phenotypic analysis- the pilot project on yeast chromosome III. Yeast **13**: 1547-1562.

- Riesenberg, D. 1991. High-cell-density cultivation of *Escherichia coli*. Curr. Op. in Biotech. **2**: 380-384.
- Rose, M. D., Winston, F., Hieter, P. 1990. Methods in yeast genetics: a laboratory manual, Cold Spring Harbor Laboratory Press, New York.
- Saito, H., Shibata, T., Ando, T. 1979. Mapping of genes determining nonpermissiveness and host specific restriction to bacteriophages in *Bacillus subtilis* Marburg. Mol. Gen. Genet. **170**: 117-122.
- Sauer, U., Hatzimanikatis, V., Hohmann, H., Manneberg, M., van Loon, A. P. G. M., Bailey, J. E. 1996. Physiology and metabolic fluxes of wild-type and riboflavin-producing *Bacillus subtilis*. Appl. Environ. Microbiol. **62**: 3687-3696.
- Shu, C., Yang, S. 1996. Kinetics of continuous GM-CSF production by recombinant *Saccharomyces cerevisiae* in an airlift bioreactor. J. Biotechnol. **48**: 107-116.
- Takiguchi, N., Shimizu, H., Shioya, S. 1997. An on-line physiological state recognition system for the lysine fermentation process based on a metabolic reaction model. Biotechnol. Bioeng. **55**: 170-181.
- Watson, T. G. 1976. Amino-acid pool composition of *Saccharomyces cerevisiae* as a function of growth rate and amino-acid nitrogen source. J. Gen. Microbiol. **96**: 263-268.
- Weuster-Botz, D., Kelle, R., Frantzen, M., Wandrey, C. 1997. Substrate controlled fed-batch production of L-lysine with *Corynebacterium glutamicum*. Biotechnol. Prog. **13**: 387-393.

**Chapter 5****Vacuolar Morphology and Cell Cycle Distribution  
are Modified by Leucine Limitation in Auxotrophic  
*Saccharomyces cerevisiae***

**Z. Petek Çakar, Uwe Sauer, James E. Bailey, Martin Müller<sup>a</sup>,  
Martin Stolz<sup>b</sup>, Theo Wallimann<sup>b</sup>, and Uwe Schlattner<sup>b</sup>**

<sup>a</sup> Laboratory of Electron Microscopy I, ETH Zurich

<sup>b</sup> Institute of Cell Biology, ETH Zurich

## SUMMARY

Yeast vacuoles are highly dynamic and flexible organelles. In this paper, we demonstrate for the first time an interrelation of vacuolar morphology, cell cycle and amino acid availability in auxotrophic *Saccharomyces cerevisiae* strains. To study cell morphology by transmission electron microscopy, advanced high pressure freezing-freeze substitution techniques were used for sample preparation, which so far have been barely successful in yeast. Slight leucine limitation of leucine-auxotrophic *S. cerevisiae* led to growth restriction and cells that were characterized by single, large vacuoles, a hexagonal tonoplast pattern and a partial arrest in G1-phase of cell cycle during later growth phases. Relieving such limitations, either by providing unusually high extracellular leucine concentrations in the medium, or via enhanced intracellular leucine biosynthesis due to plasmid-based expression of a leucine marker gene, led to more than two-fold higher final optical densities in stationary phase. Vacuoles fragmented to a different degree into several smaller vesicles with rather homogenous membranes and only an inferior proportion of cells remaining in G1 phase. These results reveal that not only nitrogen, phosphate, or sulfate starvation, but also subtle, often unrecognized amino acid limitations of commonly used auxotrophic *S. cerevisiae* strains can drastically affect cell physiology, vacuolar morphology and cell cycle distribution. This presents a note of caution for morphological and cell cycle studies in yeast. Our results further indicate that vacuolar morphology and cell cycle can be related under batch growth conditions, in a similar way as has been shown in synchronized cultures.

## INTRODUCTION

The vacuole of *S. cerevisiae* is central to the physiology of this organism and is involved in pH- and osmoregulation, protein degradation and storage of various compounds (reviewed in Jones et al., 1997). Vacuoles are also highly dynamic and flexible organelles that are sensitive to many factors, including the genetic background of a particular strain as well as growth conditions (Weisman et al., 1987; Raymond et al., 1990). For example, yeast vacuoles may change size and shape, alter the morphology of their tonoplast (Moeller and Thomson, 1979a,b), move around or remain in close contact with the nucleus (Jones et al., 1993). In addition, they may fragment into multiple small vacuoles or, vice versa, fuse into one single large vacuole (Wiemken et al., 1970; Bryant and Stevens, 1998). Although these phenomena were described in some detail, it has remained unclear whether they are triggered by general, well-defined molecular or physiological events or whether they simply depend on the yeast strain or the experimental procedure (Weisman et al., 1987; Willison and Johnson, 1985).

Yeast cells have mostly a single, large spherical vacuole (Wiemken et al., 1970), at least during the G1-phase of the cell cycle. Moeller and Thomson (1979a,b) have analyzed in detail the morphology of tonoplast membranes during growth of *S. cerevisiae* A364A batch cultures. They described aggregated states of intramembrane particles at the transition from exponential to stationary phase, which form geometric, mostly hexagonal patterns of particle-free regions. Similar patterns were observed in strain HMSF1, using the temperature-sensitive secretory mutant *sec1* at restrictive temperature (Necas and Svoboda, 1986), but were not detected in other strains (Willison and Johnson, 1985). A fragmentation of the large G1-phase vacuole into several smaller vacuoles was first observed in synchronized cultures prior to bud formation in S-phase (Wiemken et al., 1970; Severs et al., 1976). In fact, as the cell cycle proceeds, some small vacuoles migrate into the bud. When mitosis and cytokinesis are completed, bud and mother cell vacuoles fuse, resulting in a single, large vacuole in each cell. Thus, fragmentation and fusion of yeast vacuoles are integral part of vacuolar inheritance and their molecular basis has been studied to some extent (Gaits and Russell, 1999; reviewed in Bryant and Stevens, 1998). Vacuole fragmentation was also observed in certain vacuole protein sorting (*vps*) mutants (Banta et al., 1988; reviewed in Bryant and Stevens, 1998), and after treatment with microtubuli-inhibitors (Guthrie and Wickner, 1988), suggesting a structural basis of this phenomenon. However, no correlation between vacuole fragmentation and cell cycle was found in asynchronous batch cultures, except for an adenine-supplemented *ade* mutant strain (Weisman et al., 1987). These authors concluded vacuolar morphology to be cell cycle independent.

It is well known that the cell cycle of yeast is controlled by the availability of nutrients. Deprivation of nutrients like glucose, ammonia, sulfate, phosphate, biotin, or

potassium leads to an arrest of cell division at the unbudded G1-phase of *S. cerevisiae* (Williamson and Scopes, 1962; Johnston et al., 1977). Other deprivations like auxotrophic starvation may cause yeast cells to arrest at various points in the cell cycle (Cooper et al., 1979). Our previous studies revealed that variations in leucine supplementation of leucine-auxotrophic *S. cerevisiae* cause dramatic changes in growth physiology (Çakar et al., 1999). Cells that were grown with insufficient leucine attained much lower final cell densities in batch culture than with optimal leucine concentrations. This raised the question if insufficient supply of auxotrophic amino acid(s) induces G1-arrest in these cultures. We also observed the frequent appearance of *trp*<sup>+</sup> revertants of strain CBS77752, denoted as CBS7752\*. When transformed with pAAH5 (carrying the *LEU2* gene), CBS7752\* grew to much higher cell densities than the wild type transformant (Çakar et al., 1999). In addition, the presence of leucine in the medium further increased the final cell density of CBS7752 transformants, but not that of CBS7752\* transformants, indicating that CBS7752 transformants are limited while CBS7752\* transformants essentially behaved like other auxotrophic yeast strains (Çakar et al., 1999).

On the basis of these results, our present study aims to evaluate possible interrelations between leucine starvation, cell cycle G1-phase arrest and vacuolar morphology in leucine-auxotrophic *S. cerevisiae* under leucine limitation. Slight leucine starvation in the later growth phase was induced in two ways: (i) decreasing leucine supplementation via the medium, and (ii) the use of wild type CBS7752 that grows only to suboptimal final cell densities if a leucine marker gene is supplied on a plasmid, together with the close descendant CBS7752\* that grows normally if transformed with the same plasmid.

## MATERIALS AND METHODS

### Strains and Plasmids, Transformation Protocol

*S. cerevisiae* strain CBS7752 (*MATa*, *ura3-52*, *leu2-3/112*, *trp1*) was from the Centraalbureau voor Schimmelcultures (Delft, the Netherlands), and CEN.PK strain 113-6B (*MATa*, *ura3-52*, *HIS3*, *leu2-3/112*, *trp1-289*, *MAL2-8c*, *SUC2*) was provided by Dr. P. Kötter (Institute of Microbiology, Johann Wolfgang Goethe-University, Frankfurt, Germany). For auxotrophic complementation we used the constitutive yeast expression vectors pAAH5 (Ammerer, 1983) and YEP24 (Botstein et al., 1979). Strain CBS7752 was transformed by electroporation (Becker and Guarante, 1990), CEN.PK by using the *S. cerevisiae* EasyComp™ transformation kit (Invitrogen BV). Transformants were selected by means of the *leu* or *ura* markers on the plasmids pAAH5 or YEP24, respectively.

### Growth Media and Culture Conditions

Yeast minimal medium (YMM), containing 6.7 g/L yeast nitrogen base without amino acids (Difco) and glucose (0.5% w/v) as the carbon source, was used in all physiological analyses. Filter-sterilized tryptophan and uracil were added where appropriate to a final concentration of 20 mg/L each. The leucine concentration of the CEN.PK growth medium was either 80 or 240 mg/L. Cells were grown until stationary phase using a rotary shaker at 30°C and 200 rpm, in 1-L baffled shake flasks containing 250 mL medium. Achievement of stationary phase was verified by at least three consecutive optical density readings at 600 nm ( $OD_{600}$ ).

### FACS Analysis

Sample preparation for FACS analysis was done as described before (Lew et al., 1992; Deere et al., 1998) with some modifications. Liquid culture samples of 1 mL and  $1 \times 10^6$  cells/mL density were harvested and washed with ice-cold, sterile dH<sub>2</sub>O. Absolute ethanol was then added to the cells to a final concentration of 70%. The cells were kept at 4°C overnight, for membrane permeabilization and fixation. They were then centrifuged and washed once with Na-citrate (50 mM, pH 7.0), and resuspended in 500  $\mu$ L Na-citrate. RNase A was added to a final concentration of 1 mg/mL, and the cells were incubated for 2 h at 37°C and subsequently transferred on ice. Cell densities were again adjusted to  $1 \times 10^6$  cells/mL by addition of cold, sterile PBS buffer (140 mM NaCl, 3 mM KCl, 10 mM Na<sub>2</sub>HPO<sub>4</sub>, 2 mM KH<sub>2</sub>PO<sub>4</sub>) and 3  $\mu$ L of propidium iodide (1 mg/ml in PBS buffer) was added. Samples were incubated on ice in the dark for up to 2 hours before analysis. FACS analysis was performed using an EPICS ELITE Analyzer (Coulter, USA), and data were evaluated using the MultiCycle software.

### Labeling of Yeast Vacuoles and Light Microscopy

Three mL of yeast culture in a light-protected tube were supplemented with 20  $\mu$ L Cell Tracker™ Blue CMAC (10 mM stock solution, Molecular Probes, Eugene, OR, USA),

a cell-permeable fluorescent marker that accumulates specifically in vacuoles. After incubation of the culture for 0.5-1 h at 30°C, yeast cells were harvested by centrifugation at 4°C, washed once with ice-cold SPM buffer (1.2 M sorbitol, 1 mM MgCl<sub>2</sub>, 50 mM KH<sub>2</sub>PO<sub>4</sub>, 0.1 mM EDTA, pH 7.3), resuspended in 100 µL SPM buffer and finally kept at 4°C in the dark. On a glass slide coated with Concanavalin-A and poly-L lysine, a drop of this suspension was immobilized under a coverslip and sealed with nail polish. Cells were observed using a Carl Zeiss Inc. Axiophot microscope with a 100x oil-immersion objective, equipped for differential interference optics (DIC), i.e. Nomarski optics, and epifluorescence. Fluorescence filters used were Carl Zeiss Inc. G365 (excitation), FT 395 (beam splitter), and LP420 (emission barrier). All DIC and fluorescent images were photographed using a Kappa CF8/1 FMCC video-camera.

### **Transmission Electron Microscopy**

Cells were conventionally fixed (Luft, 1961) with 2.5% glutaraldehyde, followed by 1% OsO<sub>4</sub> and 1% K-ferrocyanide as described previously (van Tuinen and Riezman, 1987; Banta et al., 1988), rendering the cell walls permeable by treatment with 1% sodium metaperiodate. Thin sections were cut from Epon/Araldite blocks and poststained with 2% aqueous uranylacetate, followed by lead citrate (Reynolds, 1963). Micrographs were taken on a Jeol 200 transmission electron microscope at 80 kV. Cryopreparation of cells for thin section TEM was performed as described previously (Hohenberg et al., 1994). The suspensions were sucked into porous cellulose capillary tubes and cryoimmobilized in their growth medium by high pressure freezing (Studer et al., 1979), using a Baltec HPM 010 instrument. Freeze substitution was performed in 2% OsO<sub>4</sub> in acetone (van Harreveld and Crowell, 1964). Embedding, sectioning, poststaining and microscopy were done as outlined above.

### **Cryo-scanning Electron Microscopy**

Samples for cryo-scanning electron microscopy (cryo-SEM) were prepared and imaged as described elsewhere (Walther et al., 1995; Walther and Müller, 1997). A 100-mesh copper grid (diameter 3 mm) was dipped into the yeast suspension and mounted between two aluminum platelets. This sandwich was frozen in a high pressure freezing machine (HPM 010, Baltec, Balzers, Liechtenstein), and subsequently cryofractured in a freeze etching device (BAF 300, Baltec) by removing one aluminum platelet with the microtome knife (temperature 163 K, vacuum about  $2 \times 10^{-7}$  mbar). After 2 min of etching (sublimation of some water at the fracture face), the sample was coated by electron beam evaporation with 3 nm of platinum-carbon, from an angle of 45°, and 8 nm of carbon, perpendicularly. After coating, the samples were cryo-transferred under liquid nitrogen into a cryo-SEM (Hitachi S-900 in-lens field emission) and analyzed in the frozen-hydrated state on a cold stage (Gatan) at a temperature of 140 K. Images were recorded using the backscattered electron signal.



## RESULTS

### **Leucine Limitation Dramatically Affects Growth Behavior, Vacuolar Morphology, and Cell Cycle Distribution of a *S. cerevisiae* CEN.PK Strain**

Based on our previous study of leucine effects on growth physiology (Çakar et al., 1999), we hypothesized that unexpected growth limitation in batch cultures may be caused by the intracellular availability of amino acids. Since amino acid starvation leads to cell cycle arrest in G1-phase and cell cycle may be related to vacuolar morphology (Wiemken et al., 1970; Severs et al., 1976), we examined if slight leucine limitation of a leucine-auxotrophic *S. cerevisiae* strain alone could alter both, vacuolar morphology and cell cycle distribution.

For this study, we chose CEN.PK 113-6B, a leucine-auxotrophic strain of the well-defined *S. cerevisiae* CEN.PK family (Brown, 1997). The amino acid availability was modulated by growing the strain in minimal medium with different initial leucine concentrations. 80 mg/L leucine were insufficient for optimal growth, since cultures grown with 240 mg/L leucine attained 50% higher cell densities (Figure 1). Vacuole-specific fluorescence staining revealed a single, large vacuole without any fragmentation in the late exponential growth phase with 80 mg/L leucine (Figure 2a,b). However, cultivation with 240 mg/L leucine led to a pronounced, although not complete vacuolar fragmentation during later phases of growth (Figure 2c,d), where growth rates differed largely between both culture conditions (see Figure 1). We then used FACS analysis to investigate whether indeed slight leucine limitation was correlated not only with vacuole morphology, but also with the cell cycle distribution, as was previously hypothesized (Wiemken et al., 1970; Severs et al., 1976). With 80 mg/L initial leucine concentration, a higher percentage of the CEN.PK 113-6B cells was in G1-phase, and also in S-phase, as compared to cells grown with 240 mg/L initial leucine concentration (Figure 3). This difference was most pronounced at later stages of growth (i.e. 16 h). These results support our hypothesis that insufficient supplementation of leucine prevents growth and cell division of yeast cells and leads to altered vacuolar morphology.

### **Insufficient Leucine Biosynthesis Through Marker Gene Expression Affects Vacuolar Morphology**

In many experimental systems, auxotrophic mutations are not countered by extracellular supplementation of the nutrient, but by transformation with plasmid-encoded auxotrophic marker genes. While we have shown above that suboptimal extracellular supply of leucine induced partial G1 arrest and altered vacuolar morphology, we here investigate the effects of suboptimal leucine biosynthesis by strain-specific marker gene expression. For this purpose, we chose the two *S. cerevisiae* strains CBS7752, a wild-type strain, and CBS7752\*, a previously described pleiotropic mutant of this strain, which responds very

differently to plasmid-based marker gene expression (Çakar et al., 1999). For the wild-type, these data indicated that plasmid-based expression of the *leu2* marker gene was insufficient for optimal leucine supply, as was evidenced by higher final cell densities when extracellular leucine was added to the transformants. In contrast, final cell densities attained by transformants of the mutant strain CBS7752\* were similar to those of other transformed leucine auxotrophic yeast strains, including CEN.PK (Çakar et al., 1999).

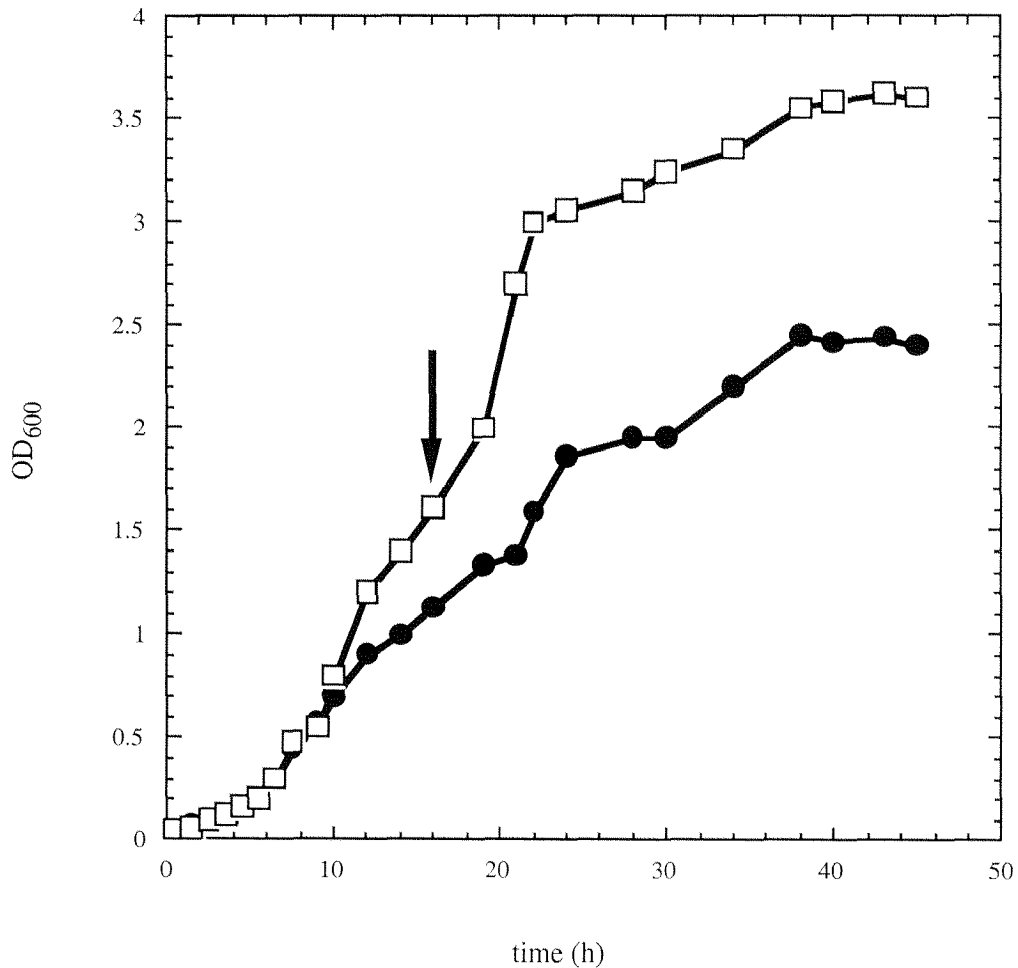


**Figure 1.** Growth behavior of CEN.PK 113.6B on 0.5% glucose-YMM and at two different initial leucine concentrations, 80 mg/L (circles) and 240 mg/L (squares). The arrow indicates the sampling time for microscopy and FACS analysis.

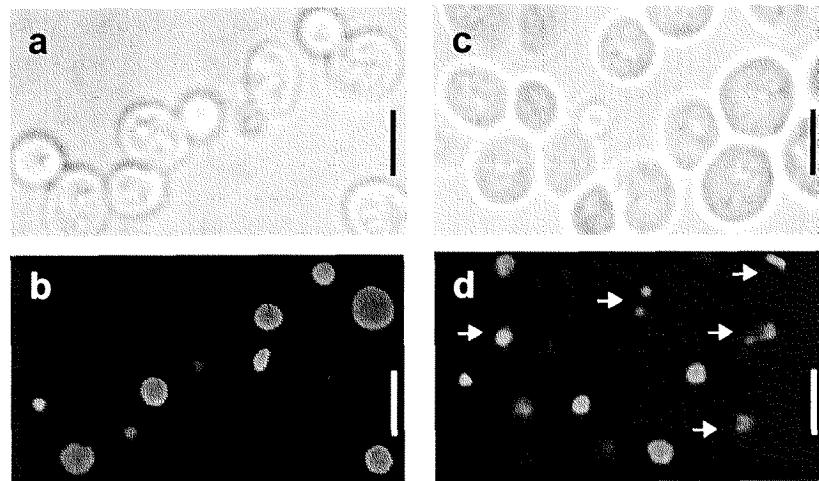


**Figure 2.** Vacuole fragmentation of CEN.PK 113.6B grown at 80 mg/L (a,b) and 240mg/L (c,d) initial leucine concentration in the late exponential growth phase (16 h). Cells were grown on 0.5% glucose-YMM and native stained with the vacuole-specific fluorescent marker dye Cell Tracker™ Blue CMAC. Images were taken with DIC (a,c) or fluorescence microscopy (b,d). Note that each cell has a single, large vacuole in (b), but smaller, ‘diffuse’, or partially fragmented vacuoles in (d). See arrows for fragmented vacuoles. Bars: 3  $\mu$ m.

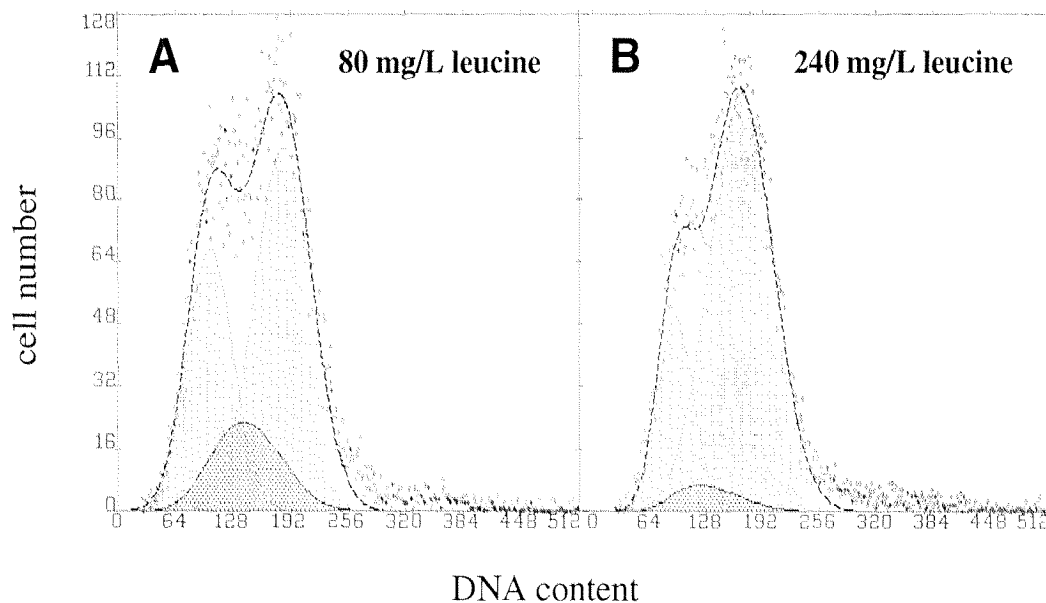


**Figure 3.** Cell cycle distribution of CEN.PK 113-6B in late exponential growth phase (16 h). Cells were grown on 0.5% glucose-YMM at two different initial leucine concentrations, 80 mg/L (A) and 240 mg/L (B). FACS was performed as described in Materials and Methods. The distribution of cell number versus propidium iodide fluorescence is recalculated as a distribution of cells in phase G1 (DNA content  $1n$ ), S and G2 ( $2n$ ) (see gray peaks, from left to right). Note the higher proportion of cells in G1- and S-phase at 80 mg/L initial leucine concentration.

To investigate whether insufficient synthesis of leucine via plasmid-based leucine marker gene expression in wild-type CBS7752 causes similar morphological and cell cycle effects as shown before with CEN.PK, we grew CBS7752 and CBS7752\* in 0.5% glucose-containing minimal medium (Figure 4). In stationary phase, transformants of CBS7752\* reached at least two-fold higher final optical densities compared to transformants of CBS7752. These  $OD_{600}$  measurements were consistent with cellular dry weight measurements and microscopic cell counts (data not shown). When CBS7752 and CBS7752\* transformants attained  $OD_{600}$  values of about 0.5 and 0.9, respectively, glucose was completely consumed in the CBS7752\* culture, while the CBS7752 culture retained about 55% of the initial glucose (data not shown).

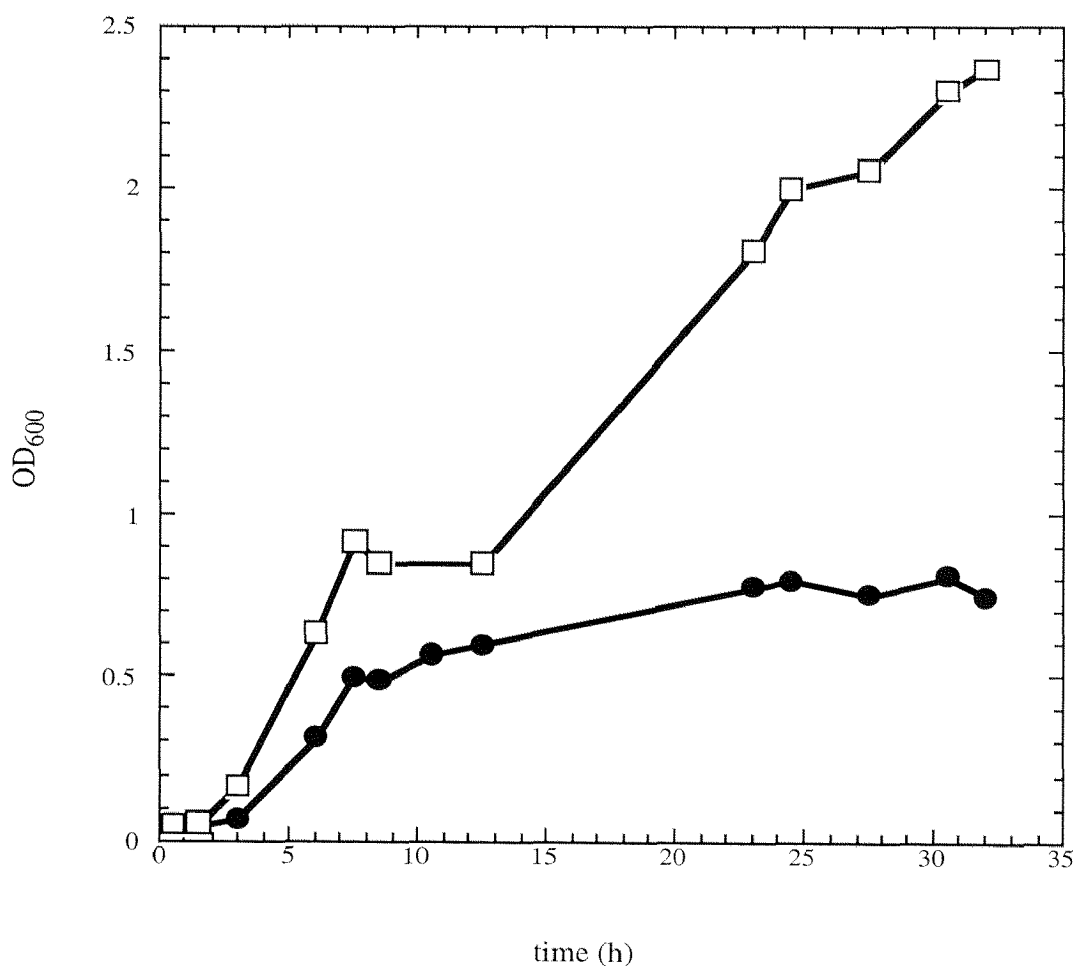


**Figure 4.** Growth behavior of transformants of CBS7752 (circles) and revertant CBS7752\* (squares) on 0.5% glucose-YMM.

Staining with a vacuole-specific fluorescent dye revealed a significant difference in vacuolar morphology of these two strains (Figure 5). CBS7752 transformants generally had a single, large vacuole that persisted throughout their entire growth (Figure 5b), as seen already in CEN.PK with suboptimal leucine supply (Figure 2b). By contrast, transformants of the revertant strain CBS7752\* showed pronounced fragmentation of the vacuole, especially when approaching late growth phase (Figure 5d), where the difference in growth rate between CBS7752 and CBS7752\* transformants became most prominent (see Figure 4). Vacuolar fragmentation was accompanied by a significant reduction of cellular volume occupied by the vacuoles and by an increased background staining in the cytosol with a vacuole-specific marker dye (Figure 5d).

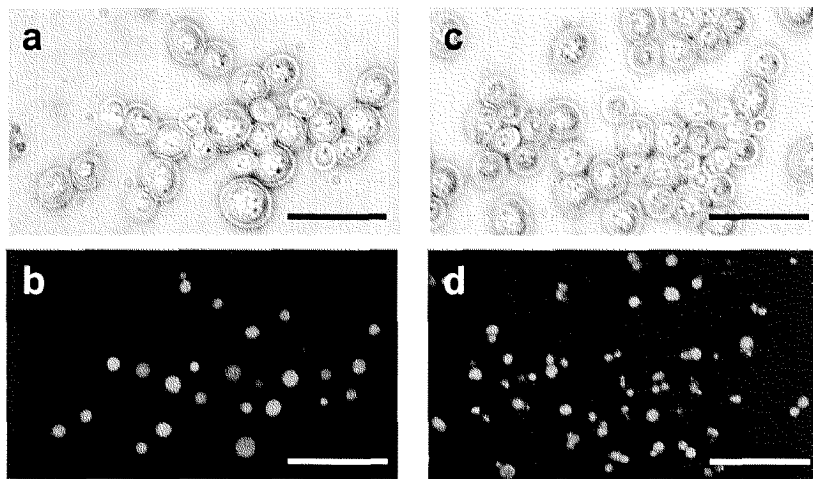


**Figure 5.** Vacuole fragmentation of transformants of CBS7752 (a,b) and revertant CBS7752\* (c,d) at late stages of growth. Cells were grown on 0.5% glucose-YMM and native staining of cells was performed with the vacuole-specific fluorescent marker dye Cell Tracker™ Blue CMAC. Images were taken with DIC (a,c) or fluorescence microscopy (b,d). Note that each cell has a single, large vacuole in (b), but multiple, smaller vacuoles in (d). Bars: 10  $\mu$ m.

Cellular morphology of both yeast strains was further analyzed by different EM methods (Müller and Moor, 1984; Studer et al., 1989; for a review see Kiss and Staehelin, 1995), including conventional TEM (Figure 6a,d) and cryofixation-based (high pressure-freezing-freeze-substitution) procedures for TEM (Figure 6b,e), as well as by Cryo-SEM of high pressure frozen and freeze-fractured samples (Figure 6c,f). The single, spherical vacuole of the CBS7752 transformant was found adjacent to the nucleus. The tonoplast showed a very regular, geometric pattern of smooth hexagonal areas ( $\varnothing$  ~200 nm, Figure 6c), which were depressed towards the organelle interior and separated by particle-rich rows. These rows corresponded to the edges of the scalloped pattern of tonoplasts seen in thin-sectioned cells, especially after high-pressure cryofixation (Figure

6b). The typical CBS7752\* transformant had multiple vacuoles with highly variable size, distributed all over the cell and a rather smooth tonoplast surface without geometric patterns (Figure 6f). In addition, the number of electron-microscopically isomorphous vesicles, already seen in the CBS7752 transformant, increased significantly in the CBS7752\* transformant (Figure 6d,f). These vesicles, representing most likely lipid droplets, were surrounded by a single lipid membrane and did not stain with our vacuole-specific dye (Figures 2 and 5).

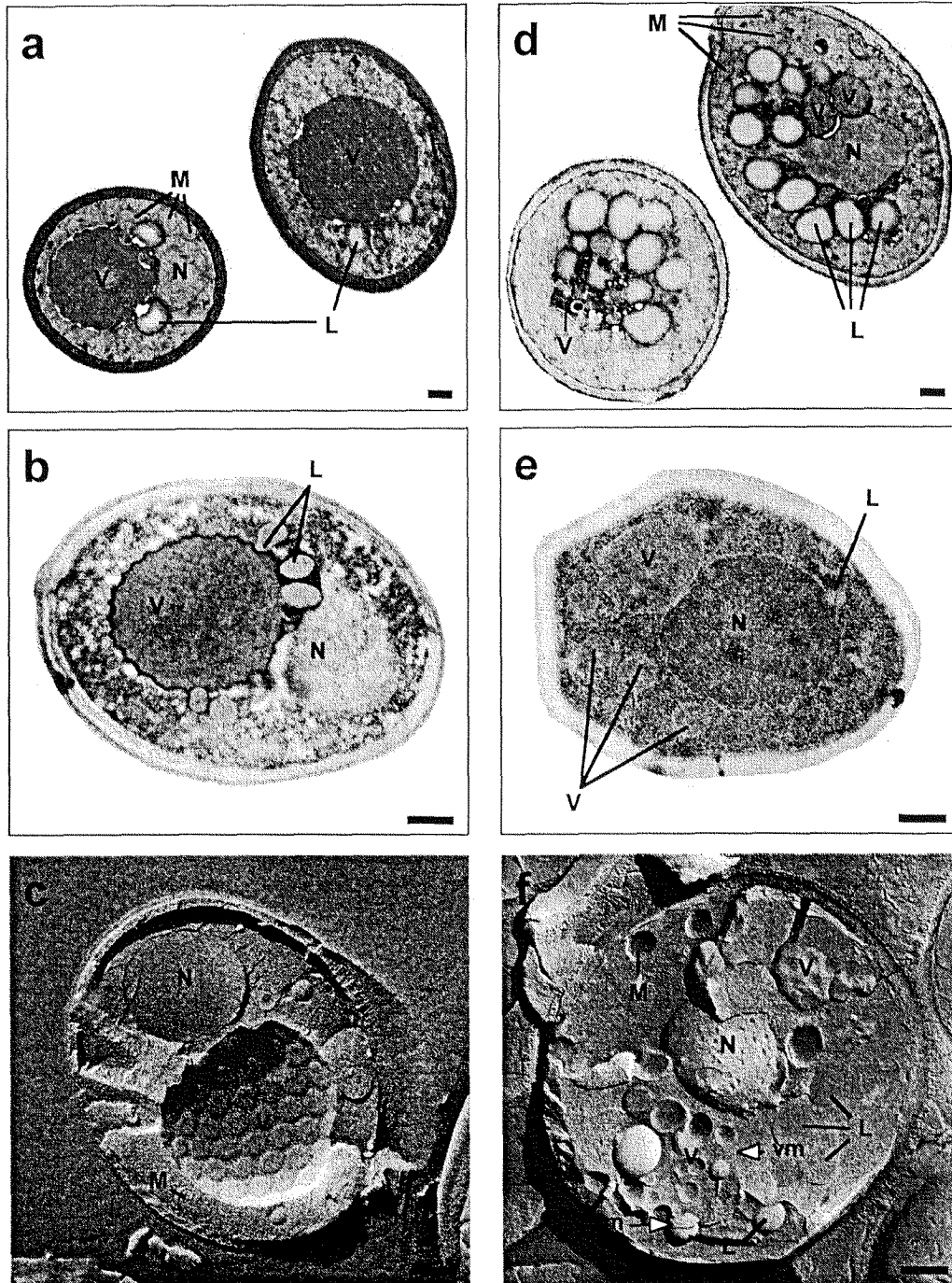


**Figure 6.** Cellular morphology of transformants of CBS7752 (a-c) and revertant CBS7752\* (d-f) grown on 0.5% glucose-YMM. Micrographs were taken at late stages of growth with TEM of chemically fixed, Epon-embedded cells (a,d) and high-pressure cryo-fixed cells (b,e) or with cryo-SEM of high-pressure frozen cells (c,f). Note the scalloped tonoplast membrane (a,b) corresponding to a hexagonal tonoplast pattern of aggregated intramembrane particles in leucine-limited CBS7752 (c), in contrast to the different vacuolar morphology and the accumulation of lipid droplets in CBS7752\* (d-f). Abbreviations: N, nucleus, M, mitochondrion, L, lipid droplet, vm, vacuolar membrane, lm, membrane of lipid droplets. Bars: 0.5  $\mu$ m.

Taken together, our results obtained with strains CEN.PK 113-6B and CBS7752 suggest that leucine limitation causes leucine-auxotrophic cells to accumulate at the G1-phase. This prevents cell growth and division and leads to the large, single vacuoles with a geometric tonoplast pattern typical for non-dividing cells and induction of stationary phase.



## DISCUSSION

### **Vacuolar Morphology and Cell Cycle Distribution of Leucine-auxotrophic *S. cerevisiae* Depend on Initial Leucine Supplementation**

In this paper, we demonstrate for the first time an interrelation of vacuolar morphology, cell cycle distribution and amino acid deprivation of auxotrophic *S. cerevisiae*. We also present TEM analysis of high pressure-frozen, freeze-substituted yeast samples, which preserve a maximum of their native structure. In contrast to freeze fracturing techniques for TEM and SEM (Studer et al., 1989; McDonald et al., 1996; Erk et al., 1997), this cryomethod has been only occasionally successful with yeast due to the quite impermeable cell wall.

Leucine limitation in two different strains of leucine-auxotrophic *S. cerevisiae* was found to dramatically change vacuolar morphology. Leucine-auxotrophic cells grown in batch culture with limiting extracellular leucine supplementation or insufficient leucine biosynthesis based on plasmid-based marker gene expression, had mostly single, large vacuoles with a tonoplast showing geometric patterns of intramembrane particles. This is characteristic of G1-phase in the cell cycle of synchronized cultures (Wiemken et al., 1970; Severs et al., 1976) and of a transition to stationary phase (Moeller and Thomson, 1979a), eventually leading to G0-arrest (reviewed in Werner-Washburne et al., 1996). Thus, vacuolar morphology is consistent with a leucine-limitation of these cells, leading to reduced growth and cell division. In contrast, growing batch cultures of auxotrophic mutants at sufficient leucine supply yielded cells with many small vacuoles and rather homogeneous tonoplast morphology, an indicator of budding and cell division. Consistently, the portion of cells in G1-phase was much more prominent in leucine-auxotrophic cells as compared to cells grown with sufficient leucine supplementation. This indicates a 'partial' G1-arrest (Pringle and Hartwell, 1981) under leucine-limitation and a close relationship between cell cycle and vacuolar morphology under batch growth conditions. Taken together, our results demonstrate that not only nitrogen, phosphate, or sulfate starvation (Williamson and Scopes, 1962; Johnston et al., 1977), but also subtle, often unrecognized amino acid limitations in auxotrophic *S. cerevisiae* strains drastically affect cell physiology, vacuolar morphology and cell cycle distribution.

### **Vacuolar Morphology is Cell Cycle-dependent Also Under Batch Growth Conditions**

The major morphological difference between leucine-limited and leucine-sufficient yeast cells were changes in the vacuole ultrastructure, which coincided with differences in cell cycle distribution. Indeed, it is known that yeast vacuoles are very flexible and dynamic compartments, sensitive to different physiological and genetic conditions (Weisman et al., 1987; Jones et al., 1993; Bryant and Stevens, 1998). We have found that fragmentation of a single, large vacuole into multiple, small vacuoles of variable size were characteristic

of rapidly growing, non-leucine-limited batch cultures of *S. cerevisiae*. Such a vacuole fragmentation in budding yeast has been described for strain A363A in synchronized cultures, undergoing cell division (Wiemken et al., 1970; Severs et al., 1976) and for several *vps* mutants (Bryant and Stevens, 1998). For strain CBS7752, we characterized the ultrastructure of the single, large vacuole of leucine-limited cells in more detail. The tonoplast showed hexagonal patterns, similar to those previously described for cells approaching stationary phase (Moeller and Thomson, 1979a,b) and for secretion mutant *sec1* (Necas and Svoboda, 1986). These patterns are due to the aggregation of intramembrane particles and were explained by phase separation of lipid molecules of the tonoplast membrane (Moeller et al., 1981).

More recent studies, however, could not relate such morphological changes to specific phases of cell division. Using asynchronous batch growth conditions, Weisman et al. (1987) found that vacuole fragmentation was cell cycle-independent in strain X2180-1A, and Willison and Johnson (1985) failed to observe geometric patterns at the tonoplast surface of strain AG1-7 during later growth phase. The authors concluded that changes in vacuolar morphology related to cell division were restricted to specific yeast strains or dependent on synchronized culture conditions. By contrast, our results demonstrate that vacuolar morphology also changes in asynchronous batch cultures as a consequence of slight amino acid limitations. In addition, an *ade2* mutant of strain X2180-1A also showed significant vacuole fragmentation when grown with high levels of adenine (Weisman et al., 1987). This is probably also due to an auxotrophic limitation, as we have found for W303-1A, another *ade* strain of *S. cerevisiae* (Çakar et al., 1999).

### **Cell Cycle Studies with Auxotrophic *S. cerevisiae* Can Be Misleading if the Supply of Auxotrophic Substrate Is Limited**

The significant influence of even subtle amino acid limitations on the cell cycle distribution of batch cultures presents a note of caution for cell cycle studies in yeast, in particular as 80-100 mg/L of leucine is not generally recognized as limiting and even recommended by laboratory manuals (Adams et al., 1998). In fact, there are several published reports that are likely to be affected by this correlation. For example, the cell cycle behavior of auxotrophic *S. cerevisiae* strains was studied by flow cytometry, using minimal media with an insufficient amino acid supplementation (Lew et al., 1992; Porro and Srienc, 1995). In addition, some of the constructs used in those studies were based on gene disruption via insertions of amino acid-encoding genes like *leu2* (Lew et al., 1992; Aon and Cortassa, 1998). It follows from our results that the comparisons made with the wild type could be misleading, since the amino acid supplied by a gene does not seem to have the same physiological effects as the externally supplied corresponding amino acid (see also Çakar et al., 1999). In order to minimize such complications, the amino acid concentrations that make auxotrophic strains comparable to their wild types

have to be determined carefully for each particular strain, before using them in cell cycle, as well as physiological or morphological studies.

#### **ACKNOWLEDGEMENTS**

We thank Eva Niederer, Wolfgang Minas, Paul Walther and Else Zanolla for technical assistance. This work was supported by the Swiss Bundesamt für Bildung und Wissenschaft (BBW) within the Framework IV Biotechnology Programme of the European Commission (to J.E.B.), the Swiss National Science Foundation (SNF grant No. 3100-5082.97 to T.W. and U. Schlattner), and the ETH Zürich (graduate training grant).

**REFERENCES**

- Adams, A., Gottschling, D. E., Kaiser, C. A., Stearns, T. 1998. *Methods in Yeast Genetics: a Cold Spring Harbor Laboratory Course Manual*, 1997 Edition. Cold Spring Harbor Laboratory Press, New York.
- Ammerer, G. 1983. Expression of genes in yeast using the *ADCI* promoter. *Meth. Enzymol.* **101**: 192-211.
- Aon, M. A., Cortassa, S. 1998. Catabolite repression mutants of *Saccharomyces cerevisiae* show altered fermentative metabolism as well as cell cycle behavior in glucose-limited chemostat cultures. *Biotechnol. Bioeng.* **59**: 203-213.
- Banta, L. M., Robinson, J. S., Klionsky, D. J., Emr, S. D. 1988. Organelle assembly in yeast: characterization of yeast mutants defective in vacuolar biogenesis and protein sorting. *J. Cell. Biol.* **107**: 1369-1383.
- Becker, D. M. , Guarante, L. 1990. High efficiency transformation of yeast by electroporation. *Meth. Enzymol.* **194**: 182.
- Botstein, D., Falco, S. C., Stewart, S. E., Breenan, M., Scherer, S., Stinchcomb, D. T., Struhl, K., Davis, R. W. 1979. Sterile host yeasts (shy): a eukaryotic system of biological containment for recombinant DNA experiments. *Gene* **8**: 17-24.
- Brown, A. J. P. 1997. Control of metabolic flux in yeasts and fungi. *Trends Biotechnol.* **15**: 445-447.
- Bryant, N. J., Stevens, T. H. 1998. Vacuole biogenesis in *Saccharomyces cerevisiae*: protein transport pathways to the yeast vacuole. *Microbiol. Mol. Biol. Rev.* **62**: 230-247.
- Çakar, Z. P., Sauer, U., Bailey, J. E. 1999. Metabolic engineering of yeast: the perils of auxotrophic hosts. *Biotechnol. Lett.* **21**: 611-616.
- Cooper, T. G., Britton, C., Brand, L., Sumrada, R. 1979. Addition of basic amino acids prevents G1-arrest of nitrogen-starved cultures of *Saccharomyces cerevisiae*. *J. Bacteriol.* **137**: 1447-1448.
- Deere, D., Shen, J., Vesey, G., Bell, P., Bissinger, P., Veal, D. 1998. Flow cytometry and cell sorting for yeast viability assessment and cell selection. *Yeast* **14**: 147-160.
- Erk, I., Nicolas, G., Caroff, A., Lepault, J. 1998. Electron microscopy of frozen biological objects: a study using cryosectioning and cryosubstitution. *J. Microscopy* **189**: 236-248.
- Gaits, F., Russell, P. 1999. Vacuole fusion regulated by protein phosphatase 2C in fission yeast. *Mol. Biol. Cell* **10**: 2647-2654.
- Guthrie, B. A., Wickner, W. 1988. Yeast vacuoles fragment when microtubules are disrupted. *J. Cell Biol.* **107**: 115-120.
- Hohenberg, H., Mannweiler, K., Müller, M. 1994. High-pressure freezing of cell suspensions in cellulose capillary tubes. *J. Microscopy* **175**: 34-43.

- Jones, H. D., Schliwa, M., Drubin, D. G. 1993. Video microscopy of organelle inheritance and mobility in budding yeast. *Cell Motil. Cytoskeleton* **25**: 129-142.
- Jones, E. W., Webb, G. C., Hiller, M. A. 1997. *Molecular Biology of the Yeast Saccharomyces cerevisiae* vol. III. Cold Spring Harbor Laboratory Press, New York.
- Johnston, G. C., Pringle, J. R., Hartwell, L. H. 1977. Coordination of growth with cell division in the yeast *Saccharomyces cerevisiae*. *Exp. Cell Res.* **105**: 79-98.
- Kiss, J. Z., Staehelin, L. A. 1995. High pressure freezing. In: N.J. Severs, D.M. Shotton (eds.): *Rapid Freezing, Freeze Fracture and Deep Etching*, Wiley-Liss Inc., pp. 89-104.
- Lew, D. J., Marini, N. J., Reed, S. I. 1992. Different G1 cyclins control the timing of cell cycle commitment in mother and daughter cells of the budding yeast *S. cerevisiae*. *Cell* **69**: 317-327.
- Luft, J. H. 1961. Improvements in epoxy resin embedding methods. *J. Biophys. Biochem. Cytol.* **9**: 409-414.
- McDonald, K., O'Toole, E. T., Mastronarde, D. N., Winey, M., McIntosh, J. R. 1996. Mapping the three-dimensional organization of microtubules in mitotic spindles of yeast. *Trends in Cell Biol.* **6**: 235-239.
- Moeller, C. H., Thomson, W. W. 1979a. An ultrastructural study of yeast tonoplast during the shift from exponential to stationary phase. *J. Ultrastruct. Res.* **68**: 28-37.
- Moeller, C. H., Thomson, W. W. 1979b. Uptake of lipid bodies by the yeast vacuole involving areas of the tonoplast depleted of intramembranous particles. *J. Ultrastruct. Res.* **68**: 38-45.
- Moeller, C. H., Mudd, J. B., Thomson, W. W. 1981. Lipid phase separations and intramembranous particle movements in the yeast vacuole. *Biochim. Biophys. Acta* **643**: 376-386.
- Müller, M., Moor, H. 1984. Cryofixation of thick specimens by high-pressure freezing. In: J. P. Revel, T. Barnard, G. H. Haggis (eds.): *The Science of Biological Specimen Preparation*, AMF O'Hare, Chicago, pp. 131-138.
- Necas, O., Svoboda, A. 1986. Ultrastructure of two secretory mutants of *Saccharomyces cerevisiae* as revealed by freeze-fracture techniques. *Eur. J. Cell Biol.* **41**: 165-173.
- Porro, D., Srienç, F. 1995. Tracking of individual cell cohorts in asynchronous *Saccharomyces cerevisiae* populations. *Biotechnol. Prog.* **11**: 342-347.
- Pringle, J. R., Hartwell, L. H. 1981. The *Saccharomyces cerevisiae* cell cycle. In: J.N. Strathern, E.W. Jones, J.R. Broach (eds.): *The Molecular Biology of the Yeast Saccharomyces, Life Cycle and Inheritance*, Cold Spring Harbor Laboratory Press, New York, pp. 45-55.

- Raymond, C. K., O'Hara, P. J., Eichinger, G., Rothman, J. H., Stevens, T. H. 1990. Molecular analysis of the yeast *vps3* gene and its role in vacuolar protein sorting and vacuolar segregation during the cell cycle. *J. Cell Biol.* **111**: 877-92.
- Reynolds, E. S. 1963. The use of lead citrate at high pH as an electron-opaque stain in electron microscopy. *J. Cell. Biol.* **17**: 208-212.
- Severs, N. J., Jordan, E. G., Williamson, D. H. 1976. Nuclear pore absence from areas of close association between nucleus and vacuole in synchronous yeast cultures. *J. Ultrastruct. Res.* **55**:374-387.
- Studer, D., Michel, M., Müller, M. 1989. High pressure freezing comes of age. *Scanning Microsc. Suppl.* **3**: 253-269.
- Takehige, K., Baba, M., Tsuboi, S., Noda, T., Ohsumi, Y. 1992. Autophagy in yeast demonstrated with proteinase-deficient mutants and conditions for its induction. *J. Cell Biol.* **119**: 301-311.
- van Harreveld, A., Crowell, J. 1974. Electron microscopy after rapid freezing on a metal surface and substitution fixation. *Anat. Rec.* **149**: 381-386.
- van Tuinen, E., Riezman, H. 1987. Immunolocalization of glyceraldehyde-3-phosphate dehydrogenase, hexokinase, and carboxypeptidase Y in yeast cells at the ultrastructural level. *J. Histochem. Cytochem.* **35**: 327-333.
- Walther, P., Wehrli, E., Hermann, R., Müller, M. 1995. Double layer coating for high resolution low temperature SEM. *J. Microscopy* **179**: 229-237.
- Walther, P., Müller, M. 1997. Double-layer coating for field-emission cryo-scanning electron microscopy -present state and applications. *Scanning* **19**: 343-348.
- Weisman, L. S., Bacallao, R., Wickner, W. 1987. Multiple methods of visualizing the yeast vacuole permit evaluation of its morphology and inheritance during the cell cycle. *J. Cell. Biol.* **105**: 1539-1547.
- Werner-Washburne, M., Braun, E. L., Crawford, M. E., Peck, V. M. 1996. Stationary phase in *Saccharomyces cerevisiae*. *Mol. Microbiol.* **19**: 1159-1166.
- Wiemken, A., Matile, P., Moor, H. 1970. Vacuolar dynamics in synchronously budding yeast. *Arch. Mikrobiol.* **70**: 89-103.
- Williamson, D. H., Scopes, A. W. 1962. A rapid method for synchronizing division in the yeast *Saccharomyces cerevisiae*. *Nature* **193**: 256-257.
- Willison, J. H. M., Johnson, G. C. 1985. Ultrastructure of *Saccharomyces cerevisiae* strain AG1-7 and its responses to changes in environment. *Can. J. Microbiol.* **31**: 109-118.

**Chapter 6**

**Directed Evolution of Multiple-Stress Resistant  
*Saccharomyces cerevisiae***

## SUMMARY

Various chemostat selection regimes and successive batch selection approaches were employed to elucidate their capability to select for multiple-stress resistant *Saccharomyces cerevisiae* strains. To increase genetic diversity prior to selection, all cultures were inoculated from the same pool of chemically mutagenized CEN.PK cells. Populations harvested at different time points during the selections as well as clones from selected populations were grown in batch cultures and exposed to oxidative, freezing, temperature and ethanol stresses, in order to determine the relative resistance levels. The results revealed that transient stress challenges in chemostat yield 'generalists', namely mutants with up to 10-fold improved oxidative, freezing, and ethanol stress survival, compared to the wild-type. Alternatively, subjecting a population to cycles of mutation and selection in batch culture yielded 'specialists', mutants with highly improved (up to 150-fold) resistances to two types of stresses (oxidative and freezing). Less successful were selection strategies with permanent stress challenge and without a direct stress challenge, although in the latter case freezing tolerance was improved up to 160-fold. It appears that the ideal selection strategy to obtain multiple-stress resistant *S. cerevisiae* would be a combination of batch selection and transient stress challenges in a chemostat, i. e. batch selection for oxidative stress resistance followed by extensive starvation in a glucose-limited chemostat.



## INTRODUCTION

In metabolic engineering, cellular activities are improved by directed manipulation of enzymatic, transport, and regulatory functions of the cell with the use of recombinant DNA technology (Bailey, 1991). This rational and deductive strategy is usually based on existing knowledge on the metabolic systems and a proposed, more or less defined, genetic manipulation towards a desired objective. However, selection of the effective targets is often hampered by our limited understanding of the complex cellular systems and by unanticipated secondary responses to genetic manipulation. As an alternative approach, inverse metabolic engineering attempts to reduce such problems by starting with the identification of a desired phenotype (Bailey et al., 1996). The genetic or environmental basis for this phenotype is then elucidated; and subsequently endowed on the organism of interest. This strategy has been successfully employed to increase the energetic efficiency of microaerobic bacterial respiration (Bailey et al., 1996).

However, many biotechnologically desirable phenotypes are not readily available in nature. One strategy to create such desired phenotypes for inverse metabolic engineering involves random mutation and selection of desired variants from the population. This has frequently been used in combination with selection on solid media to confer a specific phenotype to a strain, but may also be done by continuous selection of evolving populations in liquid culture, for example, in chemostat cultures (Dykhuisen and Hartl, 1983). Driven by spontaneous or induced mutagenesis, the initially monoclonal population segregates and fitter variants periodically take-over the culture. If an appropriate selection pressure towards a desired phenotype is applied, this procedure is referred to as directed evolution. Alternatively, selection for fitter variants may also be achieved by a person that periodically removes certain phenotypes from the population.

There are several successful selection studies reported. One example is evolution of phenol-degrading *Pseudomonas* strains (Masque et al., 1987). Another example is chemostat selection, at increasing chloramphenicol concentrations, of plasmids with increased segregational stability in *Bacillus subtilis* (Fleming et al., 1988). In a recent study, the evolution of *Escherichia coli* mutants was investigated in a glycerol-limited chemostat at a dilution rate of  $0.05 \text{ h}^{-1}$  over 126 days (Weikert et al., 1997). After this time, about 90% of the chemostat population consisted of mutant strains with altered colony morphology. Two particular isolates with this morphology had higher stress resistance, growth rates and biomass yields in batch cultures on various carbon sources, as compared to the parent strain.

To fully exploit such directed evolution strategies for inverse metabolic engineering, it is a prerequisite to identify the genetic basis of the evolved desired phenotype. While this is generally rather difficult to achieve, in particular in the absence of any information on the affected genes, there are several novel analytical methodologies

that may facilitate such endeavors. One example is two dimensional protein gel electrophoresis, which, in combination with mass spectroscopy and genomic sequence data, can identify differences in whole cell protein composition between mutants and parent (Wilkins et al., 1996). Another example are high-density oligonucleotide arrays that allow to monitor global mRNA levels. In this approach, mRNA levels are determined by hybridizing complete mRNA populations to sets of arrays which contain hundreds of thousand of chemically synthesized oligonucleotides (Wodicka et al., 1997). Both techniques are potentially capable of identifying the genetic basis of mutants with desirable characteristics.

Resistance to multiple stresses is a rather complex phenotype, which is very useful for applied purposes but would be difficult to achieve rationally. In all traditional yeast processes such as baking, brewing, distiller's fermentations, and wine making, the cells are exposed to various environmental stresses. There are several reported studies that investigate genetic factors that are involved in single stress resistances and how these factors may be improved. Typical examples are freeze- (Takagi et al., 1997) and salt-tolerant (Matsutani et al., 1992) *Saccharomyces cerevisiae* laboratory strains that were obtained by mutation and direct selection procedures. However, for improved process performance, a strain should acquire resistance to multiple stresses, because even the most common yeast bioprocess, aerobic fed-batch production of baker's yeast, causes a variety of stress conditions (Attfield, 1997). Firstly, the process is ultimately limited by the aeration capacity of the bioreactor system (Evans, 1990). Secondly, accumulation of metabolic byproducts like alcohols and organic acids poses additional challenges. Additionally, the fact that manufacturers grow baker's yeast at supraoptimal temperatures and often add salts causes further stress to yeasts (Reed and Nagodawithana, 1991). Moreover, molasses contain not only sugars, but also metabolizable and non-metabolizable inhibitors that can accumulate during the fed-batch process and damage yeast cells (Yokota and Fagerson, 1971). In addition to the production process, the storage of yeast in frozen dough introduces the additional stress of freezing/thawing (Attfield, 1997).

Here we compare the efficiency of different selection procedures for obtaining *S. cerevisiae* strains with multiple-stress resistance. These procedures can be categorized into five groups. First, glucose-limited chemostats under 'permanent stress challenge', where a growing population is challenged with increasing concentrations of the oxidative stress agent  $H_2O_2$  or temperature oscillations. Second, glucose-limited chemostats were subjected to 'transient stress challenges', including heat shock and starvation. Third and fourth, chemostats were operated under glucose or ethanol limitation in the absence of any other stress challenge. Fifth, successive cycles of mutation and selection were performed in batch cultures. To increase genetic diversity, the populations were subjected to

chemical mutagenesis prior to selection. The isolated mutant strains were characterized for their viability after exposure to four selected stresses. In order to access the genetic basis of the improved stress resistance phenotype, total mRNA was isolated and sent out for global transcript analysis.

## MATERIALS AND METHODS

### Strain, Media, and Chemical Mutagenesis

The *S. cerevisiae* wild-type strain CEN.PK 113.7D (*MATa*, *MAL2-8<sup>c</sup>*, *SUC2*), obtained from Dr. P. Kötter (Institute of Microbiology, Johann Wolfgang Goethe-University, Frankfurt, Germany) was used throughout this study. For cultivation prior to chemical mutagenesis, YPD medium (10 g/L yeast extract, 20 g/L peptone, and 20 g/L dextrose) was used. Yeast minimal medium (YMM), containing 0.5% (w/v) glucose and 6.7 g/L yeast nitrogen base without amino acids (Difco) was used in all other cultivations. For the ethanol-limited chemostat, 0.5% (v/v) ethanol was used as the sole carbon source. EMS (ethyl methane sulfonate) mutagenesis was performed as described elsewhere (Lawrence, 1991).

### Selection Cultures

Chemostat cultures were grown in a 1.5-L benchtop fermentor (Bioengineering) with 1 L working volume at a dilution rate of  $0.07 \text{ h}^{-1}$ . The pH was maintained at  $5.5 \pm 0.1$  by the addition of 3 M KOH. The cultivation temperature was  $30^\circ\text{C}$ , stirrer speed at 1200 rpm, and the aeration rate was 0.5 L air/min. Polypropylene glycol 2000 (1:10 (v/v) dilution in  $\text{dH}_2\text{O}$ ) (Fluka) was added at 200  $\mu\text{L/L}$  to prevent foaming. A mass-controlled pump was used to keep the culture volume constant. Temperature oscillations were achieved by sinusoidally varying the temperature between  $25^\circ\text{C}$  and  $35^\circ\text{C}$ . During the oscillations, one full sinusoidal cycle ( $2\pi$ ) was completed in 1 h. The oscillations were continued for 7 days (about 17 generations). Batch cultures were grown in test tubes under aerobic conditions at  $30^\circ\text{C}$  and 200 rpm in YMM containing 0.5% (w/v) glucose as the sole carbon source. Aliquots were taken from both chemostat and batch cultures at regular intervals and kept at  $-20^\circ\text{C}$  as frozen stocks in 30% (v/v) glycerol. Diluted aliquots were plated on solid YPD medium in order to verify the absence of contaminants.

### Estimation of Stress Resistance

Cell growth was monitored by determining the optical density at 600 nm ( $\text{OD}_{600}$ ). Resistance to oxidative stress, heat shock, rapid freezing, and ethanol was determined as described previously (Lewis et al., 1997). Briefly, cells were grown at  $30^\circ\text{C}$  and 200 rpm into late exponential growth phase ( $\text{OD}_{600}=1.2-1.8$ ) in YMM containing 2% (w/v) glucose as the sole carbon source. They were then harvested at 3000 rpm for 2 min in a benchtop centrifuge and resuspended in 5 mL of fresh medium without glucose. For each stress, 1 mL-aliquots of cells were used. Oxidative stress was applied by adding  $\text{H}_2\text{O}_2$  to the cultures at a final concentration of 0.3 M. Cells were then incubated at room temperature for 1 h, harvested as above, and resuspended in fresh medium. For heat shock, the cells were incubated at  $65^\circ\text{C}$  for 10 min in an Eppendorf heater-shaker, and then cooled on ice. For rapid freezing, aliquots of cells in 1.5 mL-microfuge tubes were immersed in liquid nitrogen for 20 min and then thawed in a water bath at  $24^\circ\text{C}$  for 2-3 min. Ethanol stress

was applied by adding absolute ethanol to a final concentration of 20% (v/v) and incubation for 30 min at room temperature, after which the cells were harvested as above and resuspended in fresh medium.

### **Analytical Methods**

A Synchron CX5CE automated enzyme analysis system (Beckman) was used to determine glucose and ethanol concentrations in the culture supernatant using kits supplied by the manufacturer. The concentrations of oxygen and carbon dioxide in the reactor off-gas were determined with a Fisons quadrupole mass spectrometer (Uxbridge). Viable cell numbers were determined by a **most-probable-number** (MPN) assay (Russek and Colwell, 1983), using serial dilutions in 96-well plates that contained 180  $\mu$ L YMM with 2% (w/v) glucose. For five parallel samples, dilutions were made in the range of  $10^1$ - $10^8$ . Based on the ability of aliquots to grow at higher dilutions, their MPN cell counts were estimated by using published tables for the case of 'five-tube MPN' (Lindquist, 1999).

### **Isolation of *S. cerevisiae* Total RNA and mRNA for Transcriptome Analysis**

Fifty mL yeast culture at an  $OD_{600}$  of 0.4 or 1.2 were either harvested directly (for stress-negative controls) or as quickly as possible after the stress challenge in a benchtop centrifuge at 3000 rpm for 1 min at room temperature. The pellets were frozen immediately in liquid nitrogen and stored at  $-80^\circ\text{C}$ . For RNA isolation, pellets were resuspended in 7 mL lysis buffer (10 mM Tris-HCl, pH 7.5; 10 mM EDTA, 0.5% (w/v) SDS) and 7 mL water-saturated acid phenol (C. Mei-Fang Kao, personal communication), vortexed vigorously, and incubated in a water bath at  $65^\circ\text{C}$  for 1 h with occasional vortexing. The samples were then placed on ice for 10 min and transferred to sterile 15-mL tubes for phase separation at 3000 rpm and 10 min at room temperature. The aqueous phase was transferred to a fresh centrifuge tube and reextracted with phenol as above at room temperature without incubation. After an additional extraction with chloroform, the aqueous phase was transferred to a fresh tube and incubated at  $-20^\circ\text{C}$  for 30 min after addition of sodium acetate to 0.3 M and two volumes of 100% ethanol. RNA pellets were then obtained by centrifugation as above, and dried overnight with loose caps. They were then resuspended in 100  $\mu$ L ddH<sub>2</sub>O and the RNA content and purity was determined by measuring  $OD_{260}$  and  $OD_{280}$  in a UV/Vis spectrophotometer. Furthermore, RNA was separated and visualized on a 2% agarose gel, to verify the absence of significant degradation.

Isolation of mRNA from total RNA was performed using a commercial mRNA isolation kit according to the instructions of the manufacturer (Oligotex mRNA Midi Kit, QIAGEN).

## RESULTS

Following chemical mutagenesis to increase genetic diversity, several batch and chemostat selection procedures were performed to compare their efficiency to enrich or evolve multiple-stress resistant yeast strains from the mutagenized population. Schematic representations of the employed directed evolution strategies are shown in Figure 1a and b. All selections were started with the same pool of EMS mutants. To minimize potentially interfering adaptations to different environmental conditions, all chemostats were performed at a dilution rate of  $0.07 \text{ h}^{-1}$ . To monitor the progress of selection, aliquots of the population were subjected to four different stresses and their capability for survival was determined by the MPN method. All samples for these analyses were taken from aliquots that were frozen at different time points of the cultivations, to assure identical pre-stress treatment.

### **Permanent Stress Challenge (PSC) in Chemostat Culture**

As a first selection approach, EMS-mutagenized CEN.PK was grown in a glucose-limited chemostat and exposed to a permanent but gradually increasing stress challenge after reaching a physiological steady state. Oxidative stress was chosen as the first stress, because a previous co-tolerance study reported a strong correlation of oxidative stress tolerance with several other stress tolerances (Lewis et al., 1997). For this purpose, the concentration of  $\text{H}_2\text{O}_2$  in the feed was increased from 0 to 100 mM in steps of 20 mM  $\text{H}_2\text{O}_2$  per day, which equals 2.4 generations. After this period, the  $\text{CO}_2$  concentration in the fermenter off-gas remained essentially unaltered. After 17 generations, at a final feed concentration of 100 mM  $\text{H}_2\text{O}_2$ , it was not possible to further increase the concentration without risking wash-out. The culture was then switched to a new medium without  $\text{H}_2\text{O}_2$  and was challenged with sinusoidally oscillating temperature between  $25^\circ\text{C}$  and  $35^\circ\text{C}$  for another 17 generations.

The relative resistance to each stress is given in Table 1, revealing that there was apparently no effective selection for improved resistance to any of the stresses investigated. The sole exception was a 30% improvement in temperature resistance of the PSC15 population, withdrawn after 17 generations of exposure to oscillating temperature. Because the performance of the population represents the average of different variants that may co-exist, we picked 24 randomly chosen clones from a plated aliquot of the PSC8 and PSC15 populations. The individual stress resistances of the 24 clones varied within 10% and the statistical average resembled the performance of the whole population, including the 30% increased temperature resistance (data not shown).

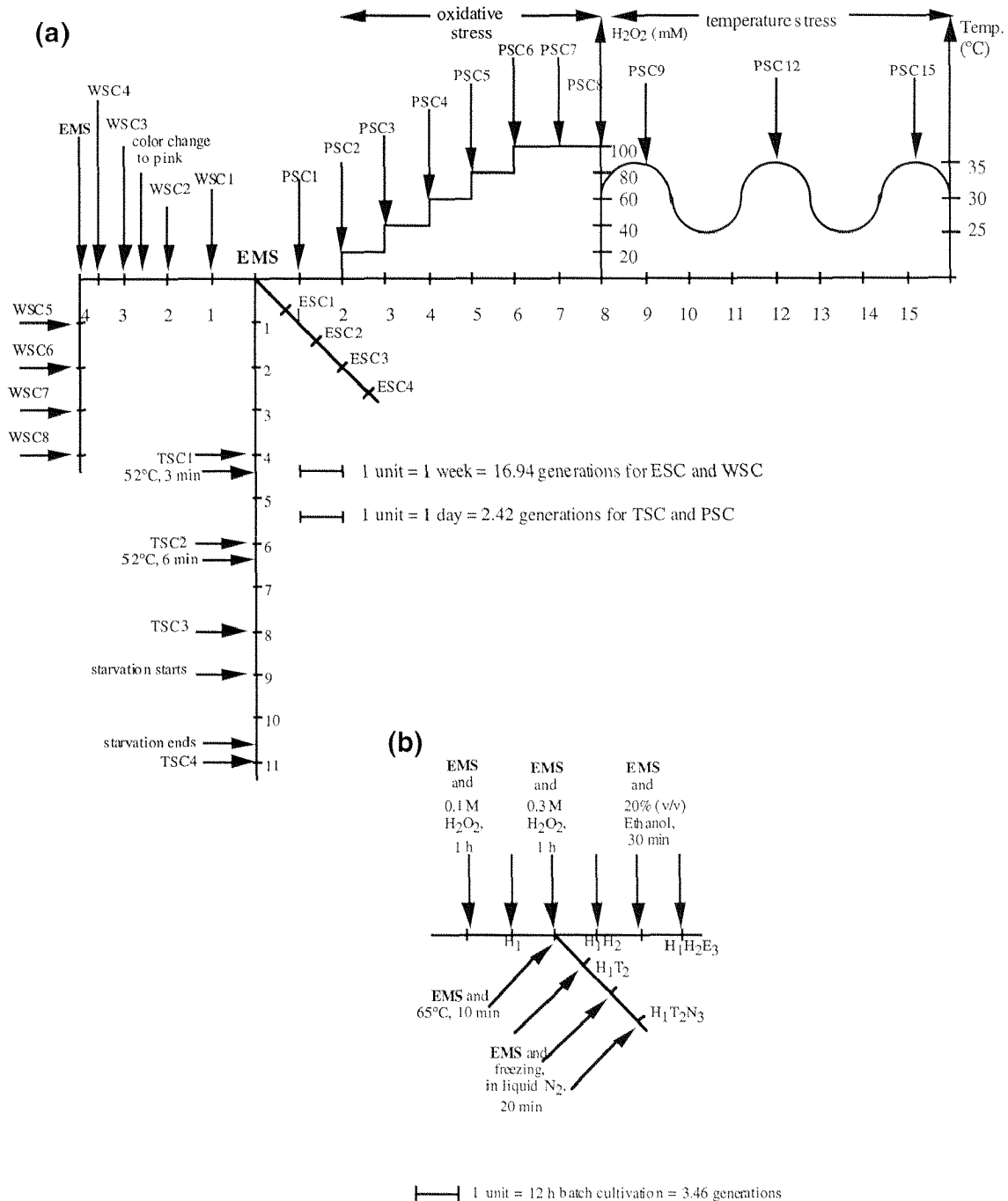


**Figure 1.** Schematic representation of chemostat (a) and batch (b) selection strategies used. PSC: permanent stress challenge; TSC: transient stress challenge; ESC: ethanol-limited chemostat without stress challenge; WSC: glucose-limited chemostat without stress challenge.  $H_1$ ,  $H_1H_2$ ,  $H_1T_2$ ,  $H_1H_2E_3$ , and  $H_1T_2N_3$  are the batch populations withdrawn at the indicated points. The numbers following the selection abbreviation refer to weekly (ESC and WSC) or daily (TSC and PSC) samples taken from the chemostats. The sinusoidal curve (PSC9-PSC15) is not drawn to scale, as 192 cycles were performed over the period of selection. The samples PSC2 to PSC6 were taken in steady state just before each stepwise increase in  $H_2O_2$  stress. In batch selection, stresses were applied immediately after EMS mutagenesis.

**Table 1.** Stress resistances of various mutant populations expressed as survival ratios normalized to the wild-type CEN.PK level. The absolute survival ratios for CEN.PK to each stress were between 0.5 and  $3 \times 10^{-3}$ . For abbreviations see the legend to Figure 1.

POPULATION	STRESS			
	oxidative	freezing	temperature	ethanol
<i>Permanent Stress Challenge (PSC)</i>				
PSC1	1.0±0.0	0.9±0.1	1.0±0.1	0.9±0.0
PSC2	0.9±0.1	0.9±0.0	0.9±0.1	1.0±0.1
PSC3	1.0±0.1	1.0±0.1	0.9±0.1	1.0±0.1
PSC4	1.0±0.0	0.9±0.1	1.0±0.1	0.9±0.1
PSC5	0.9±0.0	1.0±0.0	1.0±0.1	1.0±0.0
PSC6	0.9±0.1	0.9±0.0	0.9±0.1	1.0±0.1
PSC7	1.0±0.0	1.0±0.0	0.9±0.1	1.0±0.0
PSC8	1.0±0.1	1.0±0.1	0.9±0.0	0.9±0.1
PSC9	1.0±0.0	1.0±0.1	0.9±0.0	1.0±0.0
PSC12	0.9±0.1	1.0±0.1	1.0±0.0	1.0±0.1
PSC15	0.9±0.1	0.9±0.1	1.3±0.1	1.0±0.1
<i>Transient Stress Challenge (TSC)</i>				
TSC1	1.0±1.0	1.0±0.1	1.0±0.0	1.0±0.0
TSC2	1.0±1.0	1.0±0.0	1.0±0.0	1.0±0.0
TSC3	1.0±0.0	1.0±1.0	1.0±0.0	1.0±1.0
TSC4	5±1	8±2	1.0±0.0	5.0±1.0
<i>Without Stress Challenge (WSC)</i>				
WSC1	1.0±0.1	1.0±0.0	1.0±0.1	1.0±0.0
WSC2	1.0±0.0	1.0±0.1	1.0±0.0	1.0±0.1
WSC3	0.9±0.1	1.0±0.2	1.0±0.1	1.0±0.1
WSC4	0.9±0.1	1.0±0.1	1.0±0.0	1.0±0.0
WSC5	1.0±0.1	160±10	1.0±0.1	1.0±0.1
WSC6	1.0±0.0	155±8	1.0±0.1	1.0±0.0
WSC7	0.9±0.1	150±10	1.0±0.0	1.0±0.1
WSC8	1.0±0.0	153±9	1.0±0.1	1.0±0.1
<i>Ethanol Stress Challenge (ESC)</i>				
ESC1	1.0±0.1	0.9±0.1	1.0±0.0	1.0±0.0
ESC2	0.9±0.1	1.0±0.0	0.9±0.1	0.9±0.0
ESC3	1.0±0.0	0.9±0.1	0.9±0.1	1.0±0.1
ESC4	1.0±0.1	1.0±0.1	1.0±0.1	0.9±0.1
<i>Batch Stress Challenges</i>				
H <sub>1</sub>	1.0±0.0	0.9±0.1	1.0±0.1	1.0±0.0
H <sub>1</sub> H <sub>2</sub>	30±3	145±55	1.0±0.0	1.0±0.0
H <sub>1</sub> H <sub>2</sub> E <sub>3</sub>	9±4	87±32	1.0±0.1	1.0±0.0
H <sub>1</sub> T <sub>2</sub>	1.0±0.1	21±6	1.0±0.1	0.9±0.1
H <sub>1</sub> T <sub>2</sub> N <sub>3</sub>	65±38	25±8	1.0±0.0	0.9±0.1



### **Transient Stress Challenge (TSC) in Chemostat Results in Multiple-Stress Resistant Mutants**

In this approach, the EMS-mutagenized CEN.PK population was exposed to short-term 'stress shocks' in a glucose-limited chemostat. Once the cells reached a physiological steady-state after about 10 generations, they were exposed to a temperature shock at 52°C for 3 min. After another 5 generations, the culture attained again a steady state that was characterized by stable OD<sub>600</sub> and concentration of carbon dioxide in the off-gas. The values were identical to those prior to the stress challenge. The culture was then exposed to 52°C for 6 min. After an additional 7 generations, a physiological steady state was achieved and the population was subjected to 36 h of starvation by stopping the medium flow. Subsequently, the cells were allowed to grow for another 4 generations.

Analyzing the resistance of the population to various stresses revealed an improved performance only in the TSC4 population that was harvested after the starvation stress (Table 1). This population was characterized by a significantly improved resistance to oxidative, freezing, and ethanol stress, leading to 5-, 8-, and 5-fold increased viability, respectively, compared to the parent. This result was confirmed by the mean value obtained from the analysis of 24 randomly picked individual clones (Table 2). However, these data indicate a significant heterogeneity within the population. While several clones exhibited a behavior similar to the overall population, seven clones had a parent-like behavior (without any improvement) and three clones with the highest resistance to oxidative and freezing stress exhibited no improvement towards ethanol stress.

**Table 2.** Survival ratios (normalized to wild-type levels) of 24 individual mutants isolated from the TSC4 population. The error indicates the standard deviation between three independent repeats of stress tests for a given individual mutant. Mean values indicate the arithmetic means of 24 colonies.

STRAIN	STRESS			
	oxidative	freezing	temperature	ethanol
T1	8±3	7±4	1±0	16±6
T2	1±0	1±0	2±1	2±1
T3	1±0	1±0	2±1	7±3
T4	1±0	14±6	6±3	9±4
T5	1±0	4±1	1±1	1±0
T6	1±0	1±0	1±0	1±0
T7	20±7	23±7	1±0	1±1
T8	6±0	8±4	1±0	4±2
T9	3±1	5±2	1±1	2±1
T10	18±9	21±7	1±0	1±0
T11	1±0	1±0	1±0	1±0
T12	1±0	13±5	2±1	9±4
T13	1±1	5±3	1±0	1±0
T14	1±0	6±2	1±1	1±1
T15	1±0	1±0	2±0	2±1
T16	1±1	7±4	1±1	1±0
T17	1±0	1±1	1±0	1±0
T18	7±3	8±3	1±0	14±5
T19	1±0	5±2	1±1	5±2
T20	1±0	1±0	1±0	1±0
T21	19±9	17±7	1±0	1±0
T22	6±3	5±1	1±0	12±6
T23	1±0	1±1	1±1	1±0
T24	7±4	7±3	1±1	9±3
<i>Pool</i>	5±3	12±6	1±0	5±2
<i>Mean value</i>	4±6	7±6	1±1	4±5

### Glucose- and Ethanol-Limited Chemostats Without Stress Challenge (WSC and ESC)

To decipher selection due to nutrient limitation or stress, a glucose-limited chemostat without stress challenges was operated for 136 generations after inoculation with the EMS-mutagenized CEN.PK mutant pool (Figure 1a). After 68 generations, an aliquot was subjected to another round of EMS mutagenesis and used to inoculate an identical chemostat, which was operated for a further 68 generations. After about the 44<sup>th</sup> generation, cells changed their color from creamy white to pink. The second EMS mutagenesis during the 68<sup>th</sup> generation did not cause any reversion and the cells remained pink until the end of the cultivation. While there was no apparent improvement of resistance over the first 68 generations, there was a sudden increase in temperature

resistance in the WSC5 population that was harvested 13 generations after the second round of EMS mutagenesis (Table 1). This population was found to have a 160-fold higher survival ratio following a freezing stress. However, this value did not change in any direction during the following 50 generations. The individual clone data reveal a very homogeneous population and generally supported the population data (data not shown).

Additionally, a chemostat with 0.5% (v/v) ethanol as the sole carbon source was also operated with the EMS-mutagenized CEN.PK population for about 68 generations, without any stress challenge (Figure 1a). However, no improvement was detected in any of the stress resistances of interest (Table 1).

### **Batch Culture Selection for Improved Stress Resistance**

As an alternative to selection in chemostats, we used several cycles of mutagenesis and selection for improved resistance to different stresses in batch culture (Figure 1b). First, a CEN.PK population was mutagenized using EMS and exposed to 0.1 M H<sub>2</sub>O<sub>2</sub> for 1h. The survivors were then allowed to grow overnight in fresh YMM medium for about 4 generations. This population (H<sub>1</sub>) was indistinguishable from the parent (Table 1). An aliquot of this population was mutagenized again and split prior to exposure to temperature (H<sub>1</sub>T<sub>2</sub>) or oxidative (H<sub>1</sub>H<sub>2</sub>) stress. The temperature stress was applied by incubating the cells at 65°C for 10 min. In the case of oxidative stress, the selection pressure was increased by exposing the cells to 0.3 M H<sub>2</sub>O<sub>2</sub> for 1 h. The two resulting populations were each mutagenized a third time and subjected to freezing (20 min in liquid nitrogen and thawing at 24°C in a water bath) or ethanol (30 min in 20% ethanol) stress, to yield the populations H<sub>1</sub>T<sub>2</sub>N<sub>3</sub> and H<sub>1</sub>H<sub>2</sub>E<sub>3</sub>, respectively.

Upon increased oxidative selection pressure, the H<sub>1</sub>H<sub>2</sub> population was found to exhibit greatly increased resistance not only to oxidation stress but also to freezing (Table 1). This behavior of the total population was found to be remarkably conserved by almost all individual clones analyzed, indicating a very homogeneous population (Table 3). In no case did we see improved resistance to either ethanol or temperature stress. Another round of mutagenesis and selection for ethanol stress resistance (H<sub>1</sub>H<sub>2</sub>E<sub>3</sub>) caused a significant decrease in the population's resistance to oxidative stress (Table 1). Again, this pattern was conserved by the majority of the analyzed individual clones (Table 4). Surprisingly, we did not detect any improvement in ethanol tolerance.

**Table 3.** Survival ratios (normalized to wild-type levels) of 24 individual mutants isolated from the H<sub>1</sub>H<sub>2</sub> population. The error indicates the standard deviation between three independent repeats of stress tests for a given individual mutant. Mean values indicate the arithmetic means of 24 colonies.

STRAIN	STRESS			
	oxidative	freezing	temperature	ethanol
B <sub>1</sub> 1	14±3	45±8	0.9±0.1	1.0±0.0
B <sub>1</sub> 2	34±5	218±72	1.0±0.0	0.9±0.1
B <sub>1</sub> 3	36±3	18±5	1.0±0.0	0.9±0.1
B <sub>1</sub> 4	34±6	125±57	1.0±0.0	1.0±0.0
B <sub>1</sub> 5	33±5	128±63	0.9±0.1	0.9±0.1
B <sub>1</sub> 6	27±7	218±70	0.9±0.1	1.0±0.0
B <sub>1</sub> 7	26±4	165±70	1.0±0.1	1.0±0.0
B <sub>1</sub> 8	30±7	147±55	0.9±0.1	0.9±0.1
B <sub>1</sub> 9	26±3	208±75	1.0±0.0	1.0±0.0
B <sub>1</sub> 10	33±6	200±82	0.9±0.1	0.9±0.1
B <sub>1</sub> 11	32±5	163±63	0.9±0.0	0.9±0.1
B <sub>1</sub> 12	30±3	96±37	1.0±0.0	1.0±0.1
B <sub>1</sub> 13	27±6	185±53	0.9±0.0	1.0±0.1
B <sub>1</sub> 14	28±7	210±67	1.0±0.1	0.9±0.1
B <sub>1</sub> 15	30±3	175±62	0.9±0.0	1.0±0.0
B <sub>1</sub> 16	27±5	88±17	0.9±0.1	0.9±0.1
B <sub>1</sub> 17	33±3	73±14	1.0±0.1	0.9±0.1
B <sub>1</sub> 18	32±7	157±52	0.9±0.1	1.0±0.0
B <sub>1</sub> 19	27±7	203±77	1.0±0.0	1.0±0.0
B <sub>1</sub> 20	32±3	199±73	0.9±0.1	0.9±0.1
B <sub>1</sub> 21	33±6	93±28	1.0±0.0	0.9±0.0
B <sub>1</sub> 22	30±5	207±75	0.9±0.0	1.0±0.0
B <sub>1</sub> 23	32±3	99±32	1.0±0.1	1.0±0.0
B <sub>1</sub> 24	34±4	189±58	0.9±0.1	0.9±0.1
<i>Pool</i>	26±7	212±65	1±0.1	0.9±0.1
<i>Mean value</i>	30±5	150±59	1.0±0.1	1.0±0.1

When using selection for temperature resistance instead of increased oxidative stress, the H<sub>1</sub>T<sub>2</sub> population was found to exhibit a significant improvement in resistance to freezing but neither to oxidation nor temperature stress (Table 1). By another round of selection, this time for freezing tolerance (H<sub>1</sub>T<sub>2</sub>N<sub>3</sub>), it was possible to greatly increase resistance to oxidative stress, without affecting the achieved freezing tolerance (Table 1). At the individual clone level, however, the population appears to be heterogeneous, including some strains with very moderately improved resistance (Table 5).

**Table 4.** Survival ratios (normalized to wild-type levels) of 24 individual mutants isolated from the  $H_1H_2E_3$  population. The error indicates the standard deviation between three independent repeats of stress tests for a given individual mutant. Mean values indicate the arithmetic means of 24 colonies.

STRAIN	STRESS			
	oxidative	freezing	temperature	ethanol
B <sub>2</sub> 1	20±6	197±96	1.0±0.1	1.0±0.0
B <sub>2</sub> 2	6±2	21±12	0.9±0.1	0.8±0.2
B <sub>2</sub> 3	16±4	123±58	1.0±0.0	0.9±0.1
B <sub>2</sub> 4	3±1	9±4	0.9±0.1	0.9±0.0
B <sub>2</sub> 5	5±2	57±26	0.9±0.1	0.8±0.0
B <sub>2</sub> 6	12±3	103±51	1.1±0.0	0.9±0.1
B <sub>2</sub> 7	7±3	56±19	0.9±0.0	0.9±0.0
B <sub>2</sub> 8	11±4	117±54	0.9±0.1	0.8±0.1
B <sub>2</sub> 9	8±4	38±16	1.0±0.0	0.9±0.1
B <sub>2</sub> 10	7±5	62±30	1.0±0.1	1.0±0.0
B <sub>2</sub> 11	9±4	88±39	1.0±0.1	0.9±0.2
B <sub>2</sub> 12	10±3	49±21	0.9±0.1	1.0±0.1
B <sub>2</sub> 13	12±4	113±64	0.9±0.0	0.9±0.0
B <sub>2</sub> 14	16±6	155±82	0.9±0.0	1.0±0.1
B <sub>2</sub> 15	8±4	73±38	1.0±0.1	0.9±0.2
B <sub>2</sub> 16	14±5	77±30	1.0±0.0	0.8±0.1
B <sub>2</sub> 17	6±2	65±32	1.1±0.0	0.8±0.2
B <sub>2</sub> 18	9±3	79±41	0.9±0.1	1.0±0.0
B <sub>2</sub> 19	12±4	127±66	0.9±0.0	0.9±0.1
B <sub>2</sub> 20	8±3	105±51	1.0±0.0	0.9±0.1
B <sub>2</sub> 21	11±4	81±35	0.9±0.1	0.9±0.1
B <sub>2</sub> 22	13±4	161±88	0.9±0.1	1.0±0.1
B <sub>2</sub> 23	8±3	79±41	0.9±0.0	0.9±0.0
B <sub>2</sub> 24	9±4	72±30	1.0±0.0	0.9±0.1
<i>Pool</i>	8±3	70±20	1±0.0	0.9±0.1
<i>Mean value</i>	10±4	88±44	1.0±0.1	1.0±0.1

### Differences Between Stress Resistances During Early and Late Exponential Phases of Growth

In our stress tests, we mainly focused on the late exponential phase of growth, with  $OD_{600}$  values between 1.2-1.8. However, stress resistance is known to increase in stationary phase (Jenkins et al., 1990), thus, stationary phase-associated stress resistance may have interfered with our analysis. Industrially, it would be desirable to have multiple-stress resistant yeasts that retain their resistance throughout all growth phases. To verify improved resistance also during early exponential phase, we grew 24 individual clones from the TSC4 and  $H_1H_2$  populations to an  $OD_{600}$  of 0.4 and 1.2 and determined their resistance to four stresses (data not shown). These data reveal that while the resistance of

the H<sub>1</sub>H<sub>2</sub> clones was very similar at both OD<sub>600</sub> values, the TSC mutants did not exhibit any significantly improved stress resistance at an OD<sub>600</sub> of 0.4.

**Table 5.** Survival ratios (normalized to wild-type levels) of 24 individual mutants isolated from the H<sub>1</sub>T<sub>2</sub>N<sub>3</sub> population. The error indicates the standard deviation between three independent repeats of stress tests for a given individual mutant. Mean values indicate the arithmetic means of 24 colonies.

STRAIN	STRESS			
	oxidative	freezing	temperature	ethanol
B <sub>3</sub> 1	20±11	31±9	0.9±0.1	0.9±0.1
B <sub>3</sub> 2	1±3	3±1	1.0±0.1	1.0±0.0
B <sub>3</sub> 3	91±38	29±8	0.9±0.1	0.9±0.1
B <sub>3</sub> 4	132±80	45±17	1.0±0.0	1.0±0.0
B <sub>3</sub> 5	13±4	19±7	0.9±0.0	1.0±0.0
B <sub>3</sub> 6	98±27	33±12	0.9±0.1	0.9±0.0
B <sub>3</sub> 7	2±1	7±3	0.9±0.1	1.0±0.1
B <sub>3</sub> 8	73±22	30±12	1.0±0.0	0.9±0.0
B <sub>3</sub> 9	110±75	38±16	0.9±0.0	1.0±0.0
B <sub>3</sub> 10	17±9	23±6	1.0±0.1	1.0±0.0
B <sub>3</sub> 11	4±1	8±2	0.9±0.0	0.9±0.1
B <sub>3</sub> 12	116±77	43±11	1.0±0.0	0.9±0.0
B <sub>3</sub> 13	88±56	26±9	1.0±0.0	1.0±0.0
B <sub>3</sub> 14	105±73	33±13	0.9±0.1	0.9±0.0
B <sub>3</sub> 15	68±42	22±8	1.0±0.0	1.0±0.0
B <sub>3</sub> 16	64±44	24±9	1.0±0.0	0.9±0.1
B <sub>3</sub> 17	118±73	38±13	0.9±0.1	1.0±0.0
B <sub>3</sub> 18	85±53	33±10	0.9±0.0	0.9±0.1
B <sub>3</sub> 19	27±17	24±9	1.1±0.0	0.9±0.0
B <sub>3</sub> 20	15±9	26±11	1.0±0.1	1.0±0.1
B <sub>3</sub> 21	94±53	36±14	0.9±0.0	0.9±0.0
B <sub>3</sub> 22	58±37	21±6	1.0±0.1	1.0±0.0
B <sub>3</sub> 23	63±39	24±11	0.9±0.1	1.0±0.1
B <sub>3</sub> 24	17±10	21±7	0.9±0.0	1.0±0.0
<i>Pool</i>	53±38	18±6	1.0±0.0	1.0±0.0
<i>Mean value</i>	62±43	27±11	1.0±0.1	1.0±0.1

### Isolation of Total and mRNA from Stress-Exposed Mutants, the Wild-Type and Their Corresponding Stress Controls

To elucidate the genetic basis of the selected mutants, DNA array technology was chosen. From the TSC4 and H<sub>1</sub>H<sub>2</sub> populations the clones T1 and B<sub>1</sub>1 (Tables 2 and 3) and the wild-type CEN.PK were chosen for DNA array analysis. This technology requires the cDNA from the mutants to be hybridized to DNA arrays containing several oligonucleotides. For this purpose, we first isolated total RNA from the above cultures. Cultures at early and late phases of the exponential growth with OD<sub>600</sub> values of 0.4 and

1.2, respectively, were either harvested directly or as quickly as possible after the stress challenge.

The quality of the preparation was verified on a 2% agarose gel (Figure 2), and found to be sufficient for further preparation. From these samples we enriched mRNA by the use of a commercial kit (Figure 3). These samples are currently under investigation by our collaborators at Stanford University.

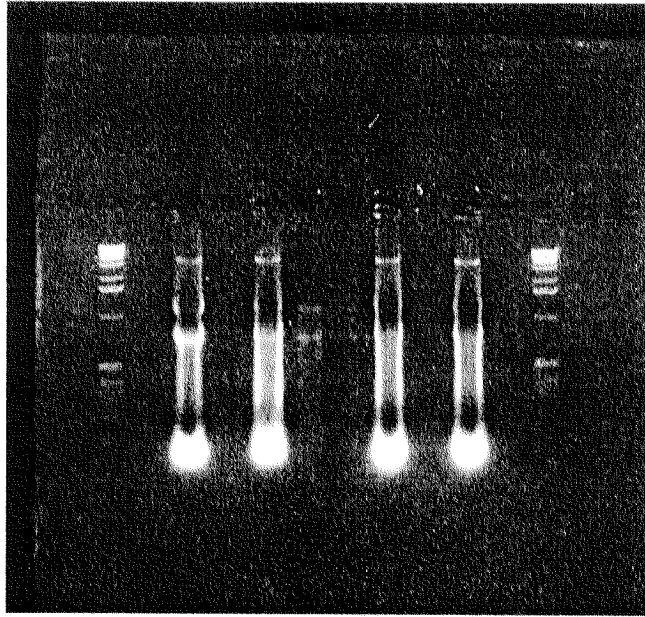


**Figure 2.** Total RNA isolated from the T1 clone of the TSC4 population after exposure to four stresses. From left to right: 1 kb-ladder DNA size marker; TSC4 T1 after oxidative; freezing; temperature; and ethanol stresses; 1 kb-ladder DNA size marker. Samples were run on 2% agarose gel.

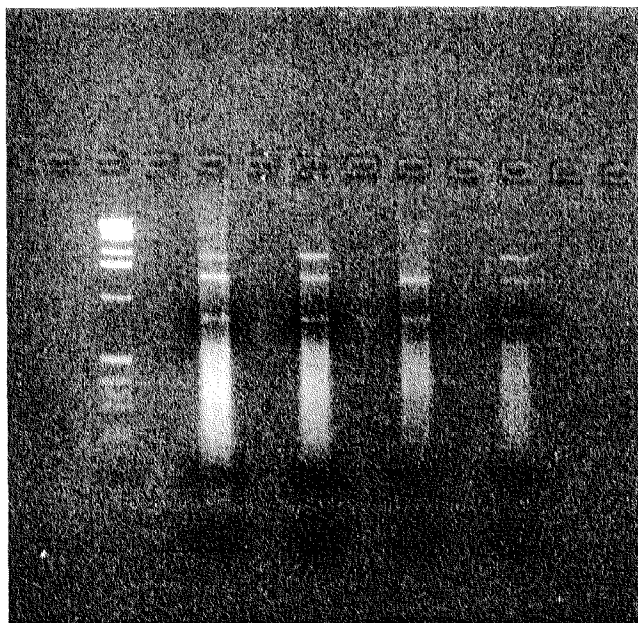


**Figure 3.** m-RNA isolated from total RNAs shown in Figure 2. From left to right: 1 kb-ladder DNA size marker; TSC4 T1 after oxidative; freezing; temperature; and ethanol stresses. Samples were run on 2% agarose gel.



## DISCUSSION

A priori it is not clear how much the relative resistance to multiple stresses can be improved and when a maximum level of resistance is attained. The primary goal of this study was to compare the efficiency of various selection procedures to enrich improved variants from a diverse (mutagenized) population. Although there are previous selection studies on yeast stress resistance, almost all of them focus on single stress resistances, such as freezing (Takagi et al., 1997) and salt tolerance (Matsutani et al., 1992), using successive mutation and direct selection procedures. Additionally, there are some studies on transient adaptation to stress in yeast. One such study focused on improvement of oxidative stress resistance upon preexposure to low  $H_2O_2$  levels (Davies et al., 1995). These results revealed that pretreated, adapted cells exhibited about 90% stress survival, whereas the non-treated cells could not survive the 0.8 M  $H_2O_2$  stress treatment. To our knowledge, however, there is only one study that investigates multiple-stress resistance in yeast. In this case, retrotransposon Ty insertion mutants exhibited significantly improved heat- (up to 1000-fold improvement), UV- (up to 10-fold improvement) and ethanol- (up to 2-fold improvement) resistance (Iida, 1988).

Transient stress challenges (TSC) in chemostat yielded 'generalists', which, in our case, had moderately (up to 10-fold) increased oxidative, freezing, and ethanol stress resistances, compared to their parent. However, the moderate improvement of those stress resistances appeared to be confined to the late exponential growth phase, and was not found in early exponential phase cells. Thus, the improved stress resistance of the TSC population might be related to an earlier induction of stationary phase responses that also encompasses a higher stress resistance, as was shown for bacteria (Jenkins et al., 1990). This might also explain why the ethanol stress resistance was improved by this approach, but not by any other selection, including ethanol stress. Thus, ethanol resistance is apparently different from other stress resistances, as was reported previously (Lewis et al., 1997), which may be related to its mechanism of toxicity; deterioration of the membrane. Hence, it can be expected that stationary phase cells are more resistant, because their membrane composition also changes.

The applied permanent oxidative and temperature stress challenges did not lead to any improved resistance of the four stresses analyzed. Likewise, the glucose- and ethanol-limited chemostat selections without any stress challenge were also not successful with respect to yielding multiple-stress resistant strains. Surprisingly, however, the glucose-limited chemostat that was basically intended as a control to the stress selection chemostats, yielded mutant strains with altered morphology (data not shown) and a highly improved freezing resistance. Although not ideal for multiple-stress resistance selection, this result indicates that individual stress tolerance may evolve without direct selection for this phenotype. The observed color change from creamy white to pink, is not directly

related to this high freezing resistance feature, because it occurred prior to the increase in freezing resistance. Pink color in *S. cerevisiae* fermentations is usually associated with amino acid auxotrophs that carry mutations in the *ade1* or *ade2* genes of the adenine synthesis pathway (Pearson et al., 1986). Although our mutants definitely had no adenine auxotrophy, they might still have a mutation in this pathway, which causes this color change without affecting biosynthesis. The results of this selection indicate that either two mutations are necessary for a freezing resistance phenotype or that a required single mutation was not present in the first population.

The first stress challenge in the permanent stress chemostat, oxidative stress was chosen, because a recent study with fourteen industrial strains of *S. cerevisiae* showed that tolerance to H<sub>2</sub>O<sub>2</sub> was correlated with the tolerance to several other stresses like slow and rapid freezing, salt, heat, but not ethanol stress (Lewis et al., 1997). It was claimed that H<sub>2</sub>O<sub>2</sub> tolerance might be an important marker for general stress tolerance in yeast. Aerobic organisms such as *S. cerevisiae* usually have multiple defense mechanisms to avoid the generation of highly reactive oxygen derivatives and to repair damages caused by oxidative stress, such as modifications of DNA, lipids, and proteins (Juhnke et al., 1996). The most important ones are superoxide dismutases, catalases, peroxidases, and DNA repair systems, which all exist in *S. cerevisiae* (Costa et al., 1997; Moradas-Ferreira et al., 1996). However, permanent oxidative stress challenge in chemostat did not select for multiple-stress resistant strains. This conclusion is supported by the fact that the PSC8 population did not grow in batch culture containing 100 mM H<sub>2</sub>O<sub>2</sub> (data not shown). However, using batch cultivations and successive cycles of mutation and selection for various stresses, the so-called batch stress challenge 'specialist' mutant strains were obtained with highly improved freezing (150-fold) and oxidative (30-fold) stress resistances. These results indicate that H<sub>2</sub>O<sub>2</sub> in the chemostat may have been degraded, either via physiological adaptation or evolution of subpopulations. Thus, the effective H<sub>2</sub>O<sub>2</sub> concentration in the reactor was probably very low, preventing an effective selection. Similar observations were made with *Bacillus subtilis* carrying a pUB110-derived plasmid encoding chloramphenicol resistance (Fleming et al., 1988). During chemostat selection for increased segregational plasmid stability, it was important to periodically increase the chloramphenicol concentration to avoid plasmid loss. Apparently, the chemostat population inactivated the supplemented chloramphenicol and only a small, plasmid-carrying subpopulation was sufficient for this purpose.

Generally, analysis at the population level was very informative about the progress of selection, because most populations were homogeneous. This indicates that we have enriched already existing mutants, rather than selected periodically evolving fitter variants (Dykhuizen and Hartl, 1983). Our finding that transient stress challenges in glucose-limited chemostat select for moderately improved resistance to multiple stress may be

exploited to further improve stress resistances by applying more frequent and harsher transient stresses, in particular starvation. Clearly, the improvements attained were not optimal (Table 1). The batch selection strategy should probably be improved by using harsher selection conditions for ethanol and temperature stresses, since this strategy did not yield any improvement in these two stresses. Alternatively, the batch ‘specialists’ of freezing and oxidative stress resistance may be grown in a chemostat with permanent temperature stress challenge for a longer period as in the present PSC case, to improve temperature stress resistance. To obtain stress resistance that persists throughout different growth phases, the use of the batch selection approach is recommended.

In general, our findings reveal that starvation is very useful to improve multiple-stress resistance in a transient challenge chemostat; and oxidative stress is very useful for batch selection. In light of these findings, the ideal selection strategy should be a combination of both approaches, e.g. starting with batch selection using oxidative stress and exposing the resulting mutant population to extensive starvation periods in a glucose-limited chemostat.

#### **ACKNOWLEDGEMENTS**

We thank Dr. Camilla Mei-Fang Kao for technical advice on RNA isolation.

**REFERENCES**

- Attfield, P. V. 1997. Stress tolerance: the key to effective yeast strains of industrial baker's yeast. *Nature Biotechnol.* **15**: 1351-1357.
- Bailey, J. E. 1991. Toward a science of metabolic engineering. *Science* **252**: 1668-1675.
- Bailey, J. E., Sburlati, A., Hatzimanikatis, V., Lee, K., Renner, W. A., Tsai, P. S. 1996. Inverse metabolic engineering: a strategy for directed genetic engineering of useful phenotypes. *Biotechnol. Bioeng.* **52**: 109-121.
- Costa, V., Amorim, M. A., Reis, E., Quintanilha, A., Moradas-Ferreira, P. 1997. Mitochondrial superoxide dismutase is essential for ethanol tolerance of *Saccharomyces cerevisiae* in the post-diauxic phase. *Microbiol.* **143**: 1649-1656.
- Davies, J. M. S., Lowry, C. V., Davies, K. J. A. 1995. Transient adaptation to oxidative stress in yeast. *Arch. Biochem. Biophys.* **317**: 1-6.
- Dykhuizen, D. E., Hartl, D. L. 1983. Selection in chemostats. *Microbiol. Rev.* **47**: 150-168.
- Evans, I. H. 1990. Yeast strains for baking, pp. 13-45 in *Yeast Technology*, Spencer, J. F. T., and Spencer, D. M. (eds.). Springer-Verlag, Berlin, Germany.
- Fleming, G., Dawson, M. T., Patching, J. W. 1988. The isolation of strains of *Bacillus subtilis* showing improved plasmid stability characteristics by means of selective chemostat culture. *J. Gen. Microbiol.* **134**: 2095-2101.
- Iida, H. 1988. Multistress resistance of *Saccharomyces cerevisiae* is generated by insertion of retrotransposon Ty into the 5' coding region of the adenylate cyclase gene. *Mol. Cell. Biol.* **8**: 5555-5560.
- Jenkins, D. E., Chaisson, S. A., Matin, A. 1990. Starvation induced cross protection against osmotic challenge in *Escherichia coli*. *J. Bacteriol.* **172**: 2779-2781.
- Juhnke, H., Krems, B., Kötter, P., Entian, K.-D. 1996. Mutants that show increased sensitivity to hydrogen peroxide reveal an important role for the pentose phosphate pathway in protection of yeast against oxidative stress. *Mol. Gen. Genet.* **252**: 456-464.
- Lawrence, C. W. 1991. Classical mutagenesis techniques. *Meth. Enzymol.* **194**: 277-278.
- Lewis, J. G., Learmonth, R. P., Attfield, P. V., Watson, K. 1997. Stress co-tolerance and trehalose content in baking strains of *Saccharomyces cerevisiae*. *J. Indust. Microbiol. Biotechnol.* **18**: 30-36.
- Lindquist, J. 26 August 1999, revision date. A five-tube MPN table (online). <http://www.bact.wisc.edu/bact102/102dil3a.html>. (27 August 1999, last date accessed).
- Masque, C., Nolla, M., Bordons, A. 1987. Selection and adaptation of a phenol-degrading strain of *Pseudomonas*. *Biotechnol. Lett.* **9**: 655-660.

- Matsutani, K., Fukuda, Y., Murata, K., Kimura, A., Yajima, N. 1992. Adaptation mechanism of yeast to extreme environments: construction of salt-tolerance mutants of the yeast *Saccharomyces cerevisiae*. J. Ferment. Bioengin. **73**: 228-229.
- Moradas-Ferreira, P., Costa, V., Piper, P., Mager, M. 1996. The molecular defense against reactive oxygen species in yeast. Mol. Microbiol. **19**: 651-658.
- Palasova, E., Stejskalova, E., Sikyta, B. 1983. Strains of *Escherichia coli* with simultaneous elevated synthesis of three catabolic enzymes. Biotechnol. Lett. **6**: 19-24.
- Pearson, B. M., Fuller, L. J., Mackenzie, D. A., Keenan, M. H. J. 1986. A red/white selection for *Saccharomyces cerevisiae* auxotrophs. Lett. Appl. Microbiol. **3**: 89-91.
- Piper, P. W. 1995. The heat shock and ethanol stress responses of yeast exhibit extensive similarity and functional overlap. FEMS Microbiol. Lett. **134**: 121-127.
- Reed, G., Nagodawithana, T. W. 1991. Yeast technology. 2<sup>nd</sup> edition, Van Nostrand Reinhold, New York.
- Russek, E., Colwell, R. R. 1983. Computation of most probable numbers. Appl. Environ. Microbiol. **45**: 1646-1650.
- Takagi, H., Iwamoto, F., Nakamori, S. 1997. Isolation of freeze-tolerant laboratory strains of *Saccharomyces cerevisiae* from proline-analogue-resistant mutants. Appl. Microbiol. Biotechnol. **47**: 405-411.
- Weikert, C., Sauer, U., Bailey, J. E. 1997. Use of a glycerol-limited, long-term chemostat for isolation of *Escherichia coli* mutants with improved physiological properties. Microbiol. **143**: 1567-1574.
- Wilkins, M. R., Pasquall, C., Appel, R. D., Ou, K., Golaz, O., Sanchez, J. C., Yan, J. X., Gooley, A. A., Hughes, G., Smith, I. H., Williams, K. L., Hochstrasser, D. F. 1996. From proteins to proteomes: large scale protein identification by two-dimensional electrophoresis and amino acid analysis. Nature Biotechnol. **14**: 61-65.
- Wodicka, L., Dong, H., Mittmann, M., Ho, M.-H., Lockhart, D. J. 1997. Genome-wide expression monitoring in *Saccharomyces cerevisiae*. Nature Biotechnol. **15**: 1359-1367.
- Yokota, M., Fagerson, I. S. 1971. The major volatile components of cane molasses. J. Food Sci. **26**: 1091-1094.

**Chapter 7**

**General Conclusions**

In this thesis, one of the most important industrial microorganisms, the yeast *Saccharomyces cerevisiae*, was chosen as the target organism for metabolic engineering and the establishment of a method for metabolic flux analysis. The purpose of installing the creatine kinase-phosphocreatine (CK-PCr) circuit in yeast, described in **Chapter 2**, was to improve yeast energy metabolism, because CK is known to be a key enzyme in energy metabolism of excitable cells and tissues of vertebrate species (Wallimann et al., 1992). Our work was based on the premise that creatine could be taken up by yeast, for which strong evidence came from a previous study (Brindle et al., 1990). Although we successfully installed a CK system in yeast, consisting of a cytoplasmic and a mitochondrial CK, we could not identify any distinct phenotype. Furthermore,  $^{31}\text{P}$ -NMR and CK inhibitor studies provided data that strongly suggest the absence of creatine uptake as the primary problem of a *functional* CK system.

Metabolic engineering mostly concerns in one way or another central carbon metabolism, either as the primary target or as a responsive element. Therefore, it is desirable to have an analytical tool, which would allow to monitor intracellular flux responses. The aim of our work presented in **Chapter 3** was to establish a reliable state-of-the-art procedure for metabolic flux analysis in yeast by combining stoichiometric flux balancing and metabolic flux ratio (METAFor) analysis. The developed metabolic model also considered the previously neglected compartmentalization. By comparing the estimated flux distributions between *Pichia stipitis* and *S. cerevisiae*, we identified several significant differences between these two yeasts. Most prominently, our analyses revealed a smaller contribution of the pentose phosphate pathway to glucose catabolism in aerobic *S. cerevisiae*, compared to *P. stipitis*. This conclusion is based on the higher fraction of PEP molecules originating from pentoses, identified by METAFor analysis and our net flux estimates. These results further suggest that the pentose phosphate pathway of *S. cerevisiae* is not optimally suited for catabolic function, which may explain the problems of engineering this organism for efficient pentose utilization (van Zyl et al., 1999), which *P. stipitis* is naturally capable of.

The so-called secondary responses to metabolic engineering (Bailey et al., 1996) have been the main focus in the work summarized in **Chapters 4** and **5**. These secondary responses are metabolic consequences of the genetic change introduced, which are much different from the expected ones (Bailey, 1991). Our results clearly show previously neglected physiological sensitivities of auxotrophic yeasts and complementing vectors that are frequently used in yeast research and applications. Thus, metabolic changes that occur upon expression of cloned genes in such host-vector systems may well arise from peculiarities of the auxotrophic host, rather than from activity of the cloned proteins. Moreover, we have shown that the exogeneous supplementation of leucine for auxotrophic strains should be much higher than suggested by common laboratory

manuals to allow for optimal growth. These often unnoticed limitations in availability of leucine have not only physiological implications, but also effects on vacuolar morphology and cell cycle distribution of leucine-auxotrophic *S. cerevisiae*. Both chapters present a note of caution for all physiological and cell cycle studies with auxotrophic yeasts.

Inverse metabolic engineering may help overcome some of the above-mentioned problems of rational metabolic engineering (Bailey et al., 1996). It requires, however, first the availability of a desired phenotype. In **Chapter 6**, we used directed evolution to improve multiple-stress resistance of *S. cerevisiae*, an industrially relevant property for food applications and large-scale fermentations (Singer and Lindquist, 1998). The primary goal was to compare the efficiency of different selection procedures to enrich improved variants from a mutagenized population, in order to provide guidance for further selection. From the currently used strategies, we found transient starvation challenge chemostats and oxidative stress in batch selection most appropriate for obtaining multiple-stress resistant yeast. These results allow us to devise more efficient selection procedures to obtain further improved mutants. To identify the relevant mutations, successfully selected mutants are currently subjected to global transcript analysis.



**REFERENCES**

- Bailey, J. E. 1991. Toward a science of metabolic engineering. *Science* **252**: 1668-1675.
- Bailey, J. E., Sburlati, A., Hatzimanikatis, V., Lee, K., Renner, W. A., Tsai, P. S. 1996. Inverse metabolic engineering: a strategy for directed genetic engineering of useful phenotypes. *Biotechnol. Bioeng.* **52**: 109-121.
- Brindle, K., Braddock, P., Fulton, S. 1990. <sup>31</sup>P NMR measurements of the ADP concentration in yeast cells genetically modified to express creatine kinase. *Biochemistry* **29**: 3295-3302.
- Singer, M. A., Lindquist, S. 1998. Thermotolerance in *Saccharomyces cerevisiae*: the Yin and Yang of trehalose. *Trends Biotechnol.* **16**: 460-468.
- van Zyl, W. H., Eliasson, A., Hobley, T., Hahn-Hagerdal, B. 1999. Xylose utilization by recombinant strains of *Saccharomyces cerevisiae* on different carbon sources. *Appl. Microbiol. Biotechnol.* **52**: 829-833.
- Wallimann, T., Wyss, M., Brdiczka, D., Nicolay, K., Eppenberger, H. M. 1992. Intracellular compartmentation, structure and function of creatine kinase isoenzymes in tissues with high and fluctuating energy demands: the 'phosphocreatine circuit' for cellular energy homeostasis. *Biochem. J.* **281**: 21-40.

## Curriculum Vitae

### Personal Details

Last Name: Çakar  
 First Name(s): Zeynep Petek  
 Place and Date of Birth: Istanbul, 23.08.1972  
 Nationality: Turkish

### Education

Jan. 2000-present: Post-doctoral training on transcytosis and endocytosis in endothelial cell lines, Dept. of Biochemistry, Biocenter, University of Basle, Switzerland.  
 1996-2000: Ph.D. studies on metabolic engineering of yeast, supervisors: Prof. James E. Bailey and Dr. Uwe Sauer, Institute of Biotechnology, ETH-Zurich, Switzerland.  
 1994-1996: M.Sc. in Chemical Engineering, Thesis title: Cloning and expression of *TaqI* endonuclease in *E. coli* by using the cloning vector pUC18, Bogaziçi (Bosphorus) University, Istanbul, Turkey.  
 1992-1995: B.Sc. in Molecular Biology and Genetics, Double Major Program, Bogaziçi University.  
 1990-1994: B.Sc. in Chemical Engineering, Bogaziçi University.  
 1983-1990: High School Education, Istanbul Lisesi, Istanbul, Turkey.

### Work Experience

Jan. 2000-present: Research and teaching assistantship, Dept. of Biochemistry, Biocenter, University of Basle.  
 1997-present: Proof-reading (Eng.) and technical translation (Ger.->Eng.) for the biotechnology journal BioWorld, Kusnacht, Switzerland.  
 1996-1999: Research and teaching assistantship, Institute of Biotechnology, ETH-Zurich.  
 1994-1996: Research and teaching assistantship, Dept. of Chemical Engineering, Bogaziçi University.  
 July-Sept. 1993: Summer internship, Procter & Gamble, Eur. Technical Center, Egham, U.K..  
 July-Sept. 1992: Summer internship, Turk-Hoechst, Istanbul, Turkey.

### Languages

English: Fluent  
 German: Fluent (with 'Sprachdiplom')  
 Turkish: Native language